Puszkiewicz, Caleb (2024) ***Underground and over-looked: groundwater assessment of coastal aquifers in the Townsville Region, Queensland, Australia..*** **Masters (Research) Thesis, James Cook University.**

Underground and Over-looked: Groundwater Assessment of Coastal Aquifers in the Townsville Region, Queensland, Australia.

By

Caleb Puszkiewicz, BGeo (Hons first-class)

A thesis submitted to the College of Science and Engineering, James Cook University, in partial fulfilment of the requirements for Master of Philosophy.

James Cook University

Australia

November 2024

Acknowledgements

I respectfully acknowledge the Wulgurukaba and Bindal People as the Traditional Custodians of the land on which my study area resides. I express my gratitude for their custodianship and pay my respects to their Elders, past and present.

I extend my deepest gratitude to James Cook University for providing me with the invaluable opportunity to pursue my master's degree. Special thanks are due to the Graduate Research School for their unwavering support throughout my academic journey.

I am indebted to my thesis panel members for their guidance, feedback, and encouragement. I am especially grateful to Dr. Christa Placzek for her steadfast support and mentorship from the inception of this project to its completion. Her insights and dedication were instrumental in shaping the direction of my research.

I would also like to express my heartfelt appreciation to Dr. Mohan Jacob for his invaluable assistance during challenging moments, where his support was unparalleled and indispensable. His expertise and unwavering commitment helped navigate through obstacles that seemed insurmountable.

Additionally, I extend my sincere appreciation to Dr. Paul Nelson for entrusting me with the opportunity to assist in his soils class, and to Dr. Han She Lim for providing me with the privilege to aide in her hydrology class. Assisting in both classes enriched my understanding of soil science and hydrological processes, while also refining my skills as an educator and researcher. These opportunities have been pivotal in my academic and professional development, allowing me to expand my knowledge base and refine my scientific abilities.

I owe an immeasurable debt of gratitude to my wife, Carina. Her unwavering love, support, and understanding have sustained me through the highs and lows of this journey. Her encouragement and belief in my abilities have been the cornerstone of my perseverance. The journey has been long, and I wouldn't have been able to make it this far without her untiring love and support.

Finally, I acknowledge the contributions of all those whose names may not be mentioned but who have played a role, big or small, in the realization of this thesis. Your support has been deeply appreciated.

Statement of the Contribution of Others

Nature of Assistance	Contribution	Name/Affiliation
Intellectual support	-Editorial assistance	-Dr. Christa Placzek/ AGE Consultants -Dr. Mohan Jacob/ JCU -Dr. Mahmood Sadat Noori/ JCU
Financial Support	- PhD Postgraduate Research stipend and scholarship-JCUPRS (2018) -Research costs -Research costs -CSE Research Training Grant (2021)	-JCU Graduate Research School -Townsville City Council -Estate Directorates Office, JCU -James Cook University
Data Collection	-Groundwater sampling November 2019	-Danica Brice, JCU undergraduate -Brodhie Slavin, JCU undergraduate

Statement of the use of Generative A.I.

During the preparation of this thesis, I acknowledge the use of ChatGPT 3.5 [https://chat.openai.com] for editorial assistance. The prompts used include: *rephrase, review, rewrite, compile, check punctuation/spelling, check references to master list*. The output from these prompts was used to review, edit, and revise this thesis to final draft form.

Abstract

This study investigates the hydrogeochemical processes influencing groundwater chemistry, recharge dynamics, and suitability for irrigation in the coastal plain of Townsville, Queensland, Australia. A total of 125 groundwater samples were collected from 74 bore between April 2018 and November 2019, analysing physicochemical parameters such as pH, electrical conductivity, major cations (Ca^{2+}, Mg^{2+}, Na^{+}, K^{+}), and anions (HCO_3^-, Cl^-, SO_4^{2-}). Isotopic signatures (^{18}O, ^{2}H) were examined to understand groundwater recharge sources, while chloride mass balance analysis provided recharge estimates for distinct groundwater systems. Principal component analysis (PCA) identified key variables influencing groundwater hydrogeochemistry, while hierarchical clustering analysis (HCA) grouped samples and revealed distinctions between aquifer systems. The groundwater exhibits slightly acidic to neutral characteristics, with Na-Cl and Na-HCO_3 facies predominating, alongside Ca-Cl, Mg-Cl, and Ca-HCO_3 water types. Electrical conductivity values varied widely, from 137 to 7060 μS/cm, indicating diverse origins including silicate, carbonate, and evaporite mineral weathering, or high degree of evapotranspiration. Chloro-alkali indices suggest that cation exchange, specifically the replacement of Ca^{2+} and Mg^{2+} with K^{+} and Na^{+}, influences groundwater chemistry in 57.0% of samples. PCA revealed two principal components explaining 88.0% of the variance, with PC1 (53.3%) dominated by Ca^{2+}, Mg^{2+}, and HCO_3^- and PC2 (34.7%) by K^{+} and SO_4^{2-}. HCA identified four distinct water groups, further divided into subgroups A and B. Recharge estimates, derived from the chloride mass balance method, ranged from 3 to 160 mm/year, with the freshest water group showing the highest recharge rates, which declined as salinity increased. Seasonal variation analysis conducted on a subset of samples (n=57) indicated no significant differences between sampling sessions ($p < 0.05$, 95% confidence). Assessment of irrigation water quality utilized the sodium adsorption ratio (SAR), residual sodium carbonate (RSC) indices, and the Wilcox diagram. SAR analysis categorized 57.3% of samples as posing ‘slight to moderate’ issues, while RSC showed minimal concern for most samples. Wilcox classification identified water Groups 3 and 4 as having the highest risk due to SAR and salinity, with Group 3B exhibiting excessive values, limiting its suitability for irrigation in areas where there is a prevalence of alkali soils. These findings provide baseline data that can inform sustainable groundwater management strategies in the Townsville coastal plain, particularly in areas where domestic irrigation is reliant on groundwater. The comprehensive analysis of groundwater recharge and quality enhances the understanding of aquifer vulnerability and supports decision-making to mitigate risks associated with salinization, seawater intrusion, and alkali soil profiles. This research contributes valuable insights into the hydrogeochemical and hydrogeological processes of the Townsville, Australia, coastal plain and similar coastal aquifers in dry tropical environments, facilitating better-informed resource management practices for environmental sustainability.

THIS PAGE INTENTIONALLY LEFT BLANK

Table of Contents

List of Tables

List of Figures

List of Equations

THIS PAGE INTENTIONALLY LEFT BLANK

Chapter 1: Introduction

1.1 Background and Study Area

The Townsville coastal plain (TCP) area (fig. 1.1.1) is in far north Queensland, Australia, and includes eight sub-basins of the (Lower) Ross and Black Rivers basins. The TCP encompasses the most populated suburbs of Townsville. Apart from two sampling sites, located in the adjacent basin (Upper Ross River basin), all sites in this study are within the TCP. The Ross and Black River catchments drain into the Great Barrier Reef Marine Park waters, with Townsville being the largest urban area adjacent to the Great Barrier Reef (GBR) (Gunn and Manning 2010 pp. 7).

The area is characterized by a tropical savanna climate (Köppen climate classification Aw/As) and experiences most of its average 1143 mm of rain from November to April. The TCP experiences subhumid to seasonally semi-arid climate, with frequent, prolonged droughts but also periods of intense rainfall. The periodic droughts are sometimes severe and commonly correspond with the El Niño phase of the (El Niño-Southern Oscillation) ENSO climate phenomenon; conversely, severe rainfall and flooding events are more frequent during La Niña events.

The study area is situated at the base of the hills constituting the Mount Stuart complex. Rising up to 584 meters above the coastal plain, the Mount Stuart complex has a steep topography gradient. Composed primarily of Permian-aged granitoids and a blend of mafic and felsic volcanics, the complex also includes late Carboniferous felsic rocks, such as rhyolite, rhyodacite, dacite, lava, and tuff. This complex and its associated escarpment comprises the western boundary of the study area, adjoining the colluvium and alluvium that define the coastal plain. Detailed surface geology (The State of Queensland 2019) of the Townsville coastal plain is shown in figure 1.1.2, highlighting the distribution of alluvial, colluvial, and igneous units that influence groundwater occurrence and movement.

Ross Lake is a manmade reservoir, designed to alleviate flooding events from the upper Ross River basin. The dam is located at the natural drainage outlet from the Upper Ross River basin to the Lower Ross River basin. Ross Lake is within the larger, upper catchment. Ross Lake generally feeds the Ross River, which flows north along the flanks of Mount Stuart before turning east and flowing to the marshes and estuaries of Cleavland Bay.

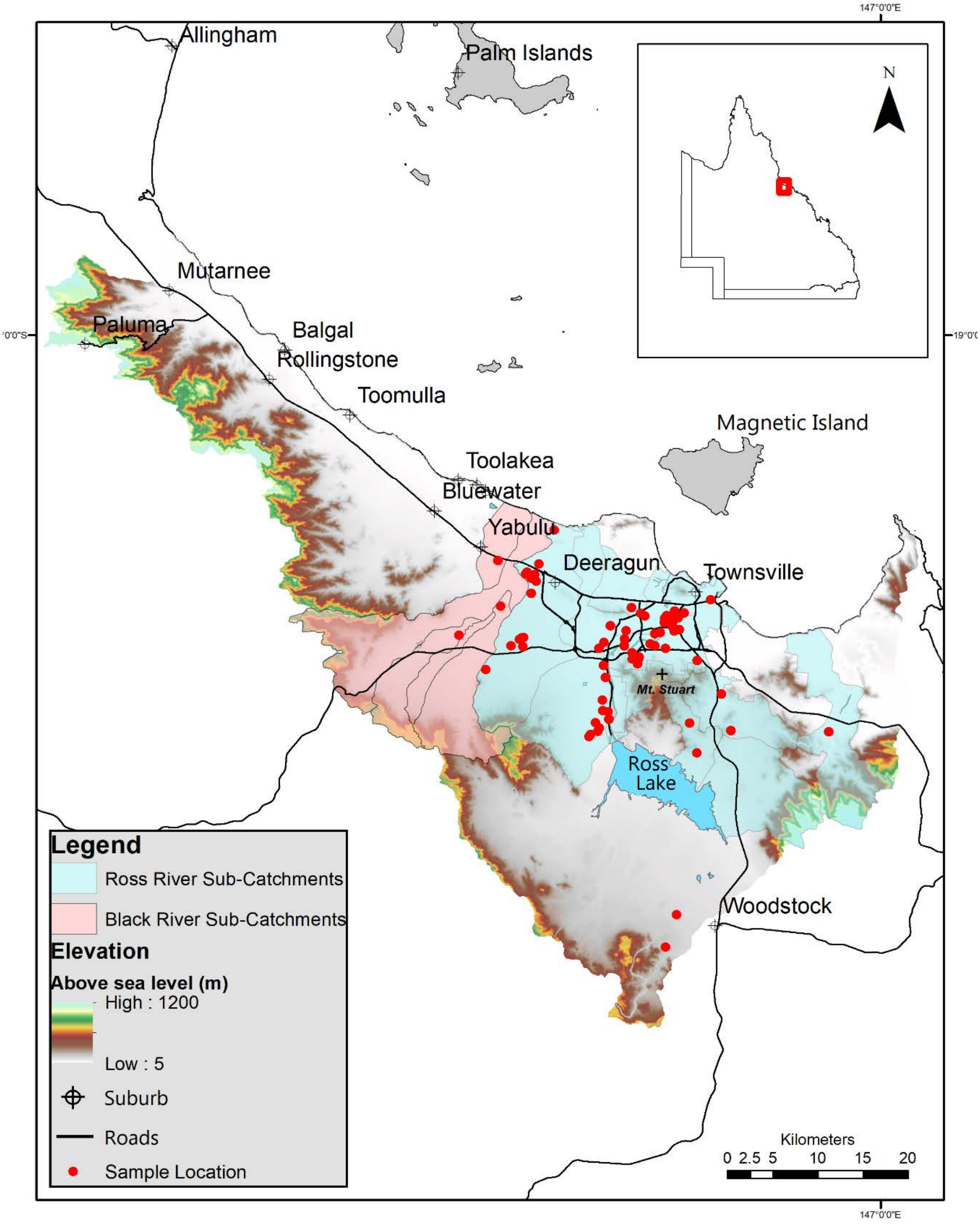

Figure 1.1.1: Townsville, Queensland. The Townsville coastal plain (TCP) study area includes subbasins of the Lower Ross River (blue) and Black River (pink) basins with bore sample locations (red) and prominent elevation features.

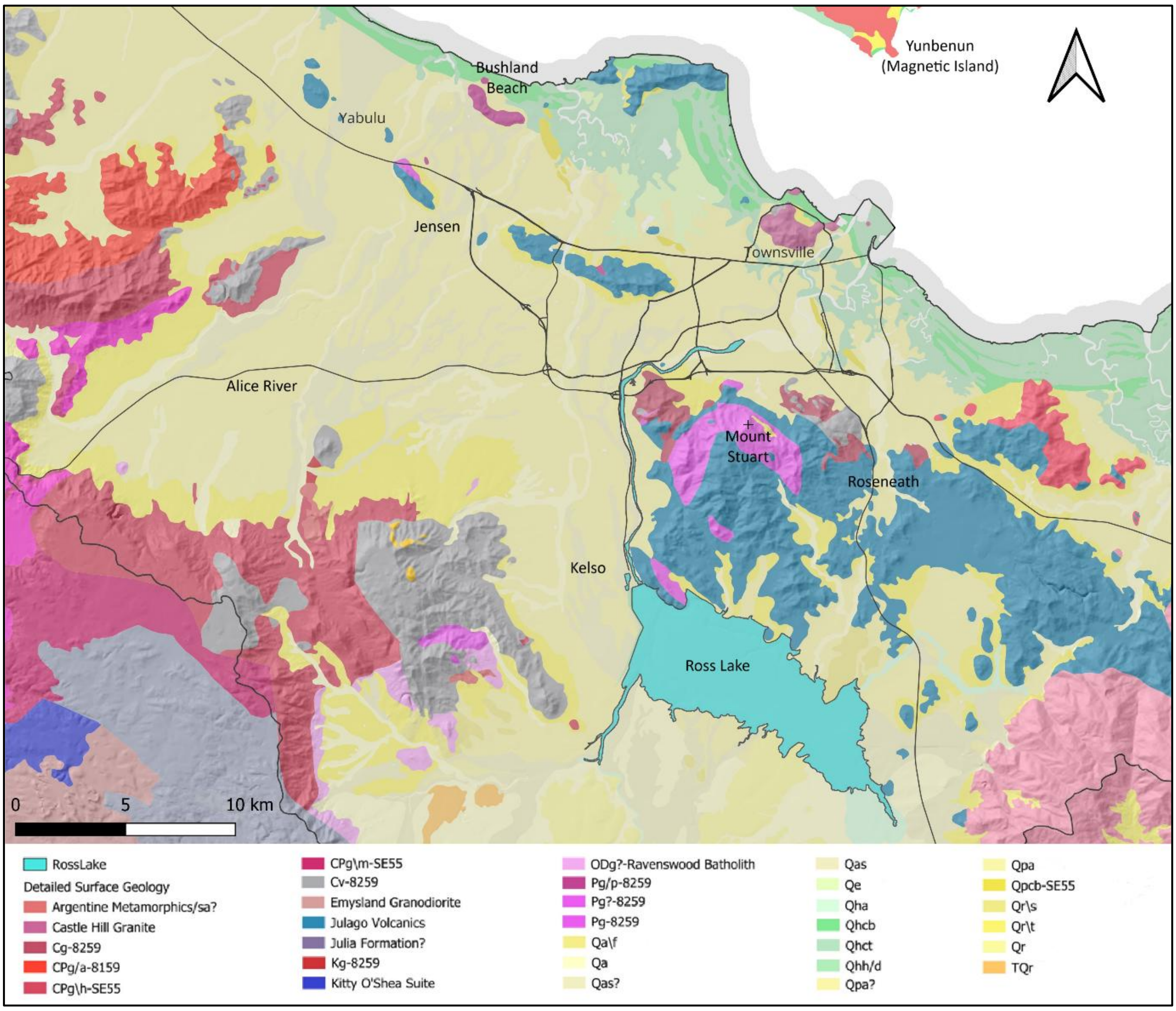

Figure 1.1.2: Townsville, Queensland. Detailed surface geology of the Townsville coastal plain (TCP) study area, with detailed descriptions for geological units are given in Table 1.1.1

Table 1.1.1: Townsville, Queensland. Detailed lithology descriptions of surface geology of the Townsville coastal plain (TCP) study area (State of Queensland 2025) displayed in Figure 1.1.2.

Map Symbol	Lithology Description
Cg	Biotite granite, microgranite
CPg/a	Pink, buff or grey microgranite, aplite, alkali granite
CPg\h	Unassigned biotite granite, biotite-hornblende to biotite granodiorite and tonalite, minor microgranite to microgranodiorite; moderate to high magnetic domain
CPg\m	Unassigned, generally pink, fine to medium-grained biotite granite, leucogranite, and porphyritic microgranite; low to mderate magnetic domain

Map Symbol	Table 1.1.1 (continued): Lithology Description
CPge	White and pink to grey, slightly porphyritic, hornblende-biotite and biotite granodiorite and biotite granite
CPik	Microdiorite, dolerite, gabbro and intrusive andesite and basalt
Cv	Rhyolite, rhyodacite, dacite, lava, tuff, agglomerate, some andesite
Ddj/q	Medium to coarse-grained feldspathic to quartzose sandstone
Kg	Hornblende-biotite granodiorite, biotite granite
ODg?	Unassigned equigranular to porphyritic, locally foliated biotite-hornblende to biotite granite, granodiorite, microgranite, microgranodiorite and leucogranite
Pgs	Biotite granite, some microgranite, granodiorite, diorite, gabbro
Pj	Rhyolitic to andesitic lava, tuff, volcanic breccia, agglomerate, some conglomerate, sandstone, siltstone, shale, coal seams
Qa	Clay, silt, sand and gravel; flood-plain alluvium
Qa\f	Clay, silt, sand and gravel; alluvial fans
Qas	Sand and silt; abandoned levee, channel and outwash deposits; sandy rises in alluvial planes
Qe	Clay, silt, sand; estuarine and deltaic deposits
Qha	Sand, gravel, silt and clay; active stream channels and low terraces
Qhcb	Moderately well-sorted, fine to coarse-grained quartzose to shelly sand and some gravel: beach ridges and cheniers
Qhct	Silt, mud, sand and minor salt; coastal tidal flats, mangrove flats, supratidal flats, saltpans and grasslands
Qhh/d	Rock-fill, sand and clay; man-made deposits - dam wall or embankment
Qpa	Clay, silt, sand and gravel; flood-plain alluvium on high terraces
Qpcb	Sand and minor gravel; some carbonate nodules: older beach ridges
Qr	Clay, silt, sand, gravel and soil; colluvial and residual deposits
Qr\s	Sand and subordinate silt and clay; residual soil and colluvium
Qr\t	Boulders and cobbles with interstitial sand and clay; talus deposits
Qr>Dfb,PLEa	Clay, silt, sand, gravel and soil; colluvial and residual deposits
TQr	Clay, silt, sand, gravel and soil; colluvial and residual deposits (generally on older land surfaces)

1.2 Research Problem

This study focuses on groundwater systems in and around the TCP. Groundwater of the Townsville region is at risk of environmental degradation due to insufficient understanding and over extraction groundwater. The extraction of groundwater for residential use in the most populated areas of the Ross and Black River Basins is currently unregulated despite averaging an annual increase of 11.7% from 2000 – 2019 for domestic users (fig. 1.2.1).

The TCP experiences periodic drought in sync with the ENSO global climate cycle; this cyclical drought is compounded by changing climate patterns and extreme events. El Niño conditions result in below average annual precipitation, which stresses both the main source for the municipal water supply (Ross Lake) and local groundwater recharge. When drought conditions persist, residents install groundwater bores to meet domestic irrigation needs (Fernbach 2016); this is because municipal water restrictions implemented by The Townsville City Council during drought do not apply to users of groundwater.

Groundwater use is regulated by the Queensland Government through a Water Plan. In Queensland, water plans have been developed under Environmental Protection (Water and Wetland Biodiversity) Policy 2019 (EPP Water). EPP Water aims to protect Queensland's water environment while allowing for development that is ecologically sustainable. A critical component of EPP Water is progressively developing water plans to manage Queensland's waters. The Ross and Black River Basins do not have a Water Plan under EPP Water (Business Queensland 2024) (i.e. they are not included in Schedule 1 of EPP Water), which means that generic conditions of EPP Water apply. These generic conditions largely relate to management of surface water and definitions of the environmental value of surface and ground waters. However, EPP Water states that groundwater and coastal waters are included, which is also the case for the Queensland Water Quality Guidelines 2009 (The State of Queensland 2013).

An Underground Water Management Area was established in 1972 (Queensland Government 2024) for the Black River basin (Black River Underground Water Management Area), to ensure groundwater supply to the Yabulu Nickle Refinery. This management area does place constraints on the extraction of groundwater, but this area is outside of the major urban areas of the TCP.

The lack of constraints on groundwater extraction is not isolated to the TCP, as 9 out of the 78 basins in Queensland are not covered by a Water Plan (discussed in Chapter 2). These non-regulated basins are scattered along an approximately 800-kilometer stretch of the east

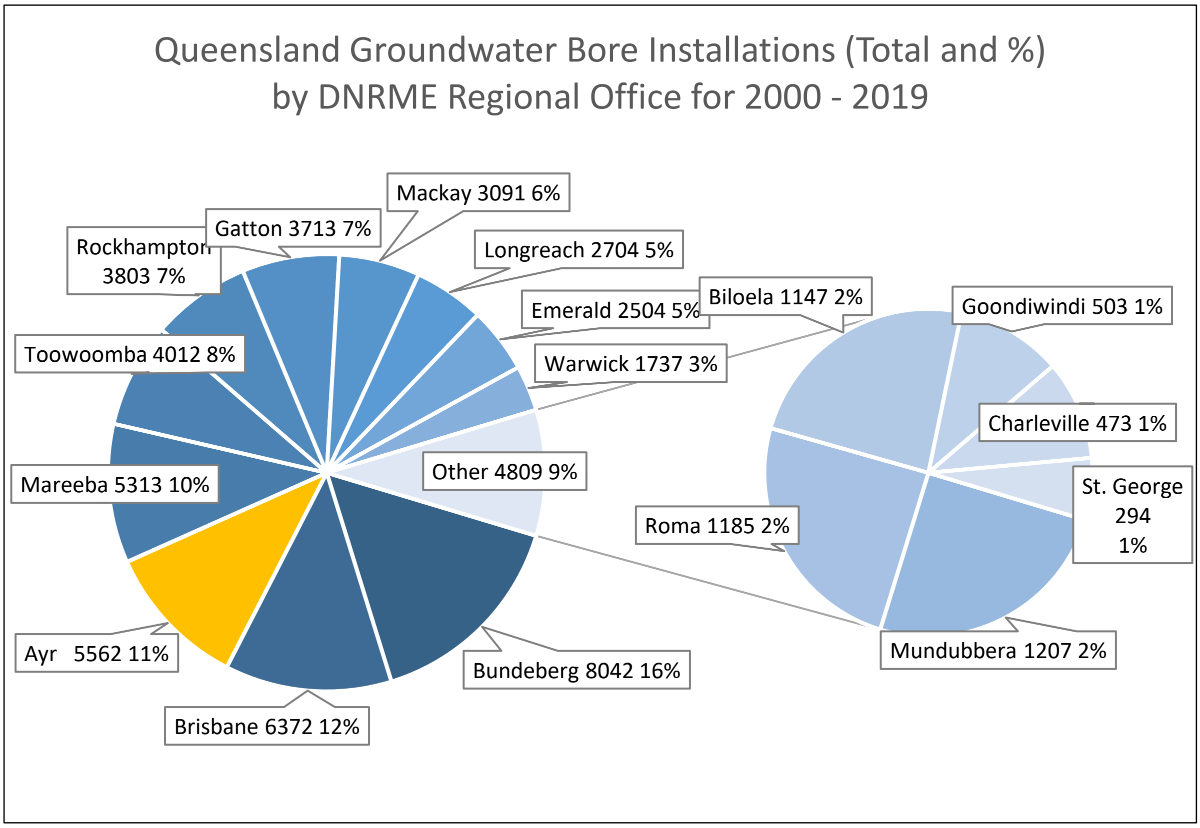

Figure 1.2.1: Pie chart showing the 17 regional offices comprising Queensland and the relative number (and percentage) of new, existing groundwater bores installed in Queensland from 2000-2019. The Ayr regional office (yellow) ranks third highest and represents 11% of total (51,662) bores installed in the state.

Australian coastline, extending from Gladstone in the south to Townsville in the north (see Ch. 2, fig 2.1.1 – red inset).

The rate of new groundwater bore installations in the Townsville region has increased in the last two decades as conditions have become drier, and residents turn to groundwater for their irrigation needs (Fernbach 2016). The Queensland Department of Natural Resources and Mines (DNRM) maintains a groundwater database (Qspatial) (The State of Queensland 2019) that lists bore status and installation data. Bores installed in the TCP are registered in the Ayr Regional Office. The DNRM records indicate that the number of new groundwater bores registered as 'existing' status (EX) across the state annually for the years 2000 to 2019, totalling 51,662 (fig. 1.2.1). Of the 17 regional offices covering Queensland, the Ayr Regional Office ranks third highest with 5,562 (10.8%) for the period, averaging 278 installations per year.

Examining the top four regional offices (Bundaberg, Brisbane, Ayr, and Mareeba) more recently (fig. 1.2.2), from 2010-2019, the Ayr regional office ranks second highest averaging 11.7% of the total percentage of bores installed in Queensland for the decade, with the Bundaberg regional office ranked highest at 14.8%. From 2015-2019, the Ayr office ranked second again, however, the gap between Bundaberg and the Ayr regional office was less than a tenth of a percent, averaging 14.7% and 14.6% total percentages of bore installations, respectively. This pattern of increased bore installations is despite a 44% decrease in annual bore installations in the Ayr region in 2011, when Cyclone Yasi struck the region. A similar drop is noted between 2018 and 2019 and is attributed to the record rainfall and flooding events that occurred in the region in early 2019.

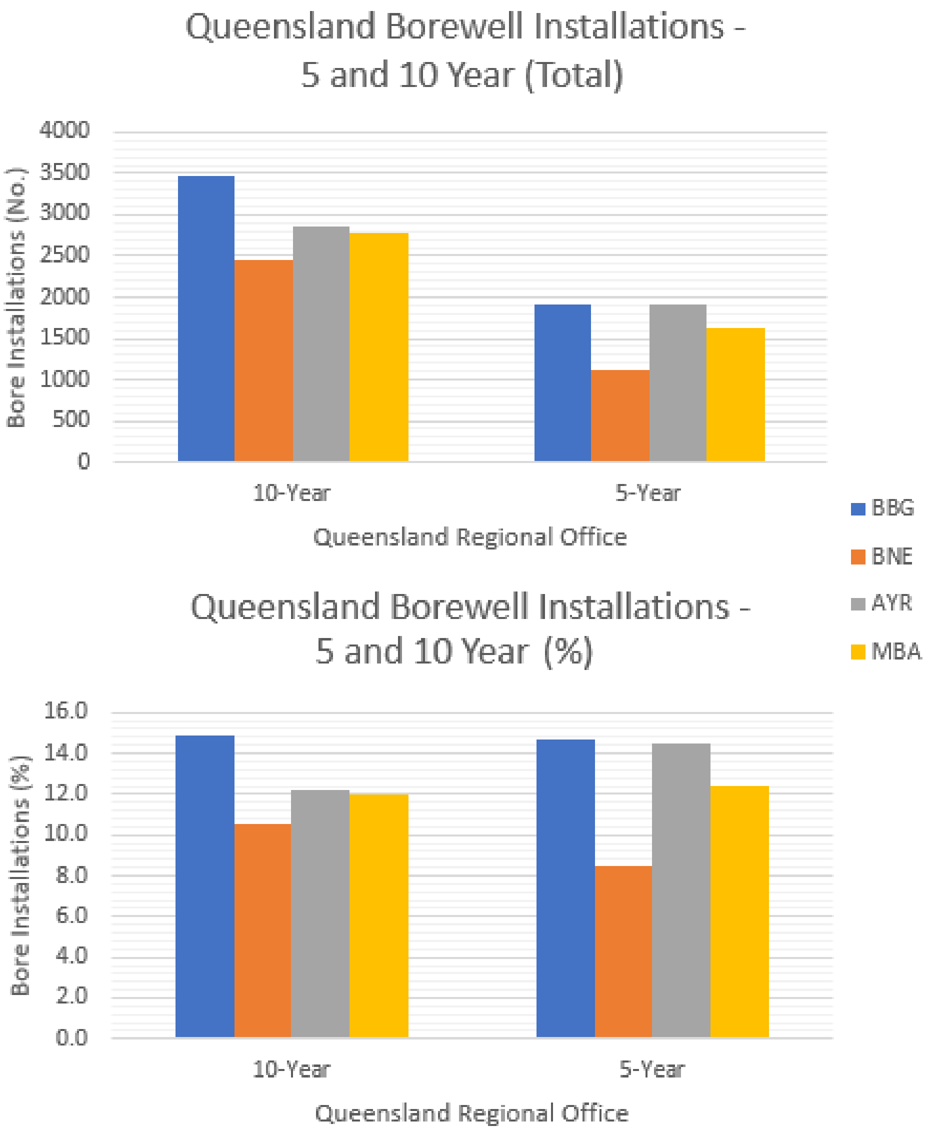

Figure 1.2.2: Bar graph showing bore installations (total and percentage) for the top four DNRM regional offices (BBG:Bundaberg, BNE:Brisbane, AYR:Ayr, MBA:Mareeba) for time periods shown (10 year = 2010-2019, 5 year = 2015-2019). In both time periods, Bundaberg (BBG) has had the highest installations with the Ayr office ranking second.

In figure 1.2.2, the number of new users accessing the groundwater system in the Ayr (Townsville) region is almost equivalent to that of highly populated areas like Brisbane, as well as one of the largest agricultural regions in the state, Bundaberg. The increased relative proportion of groundwater bores installed in the Ayr office region demonstrates a growing number of groundwater users and, by proxy, an increase in extraction of groundwater. Thus, excessive groundwater extraction, or overextraction, may occur.

Abstracting groundwater from aquifers hydraulically connected to the sea disrupts established natural hydraulic gradients, prompting the migration of saltwater from the ocean towards the bore (Freeze and Cherry 1979, pp. 375; Todd and Mays 2005, pp. 589). This phenomenon, where seawater infiltrates freshwater aquifers due to groundwater extraction, is known as seawater intrusion. This intrusion can occur horizontally and vertically, guided by hydraulic gradients, eventually compromising groundwater quality (Todd and Mays 2005 pp. 589, Han *et al*. 2013 pp. 13) as a result of the salinity of sea water. The complex processes involved encompass geochemical interactions like water source mixing, the release of concentrated brines, interactions with geological formations, and the introduction of anthropogenic pollutants (Han *et al*. 2014 pp. 13, Todd and Mays 2005 pp. 589). The potential risks of extraction induced seawater intrusion in the TCP are further compounded by projected sea level rise and reduced seasonal rainfall in the region spanning from 2000 to the present (CSIRO 2020, pp. 7).

In addition to aquifer impacts due to overextraction and/or sea water intrusion, the prevalence of alkali clays in coastal catchments, including the TCP, create an additional risk to soil degradation. This can occur due to the use of high-sodium waters for irrigation. The sodium displaces calcium and magnesium in the soil structure of alkali soils, thus changing the chemistry of the clays and negatively impacting soil structure and permeability (Zaman *et al*. 2018 pp. 117).

The investigation of groundwater in the TCP has been limited, relying on extrapolated data, and residents have been granted unrestricted access to, and utilization of, groundwater. In contrast, the groundwater systems of Brisbane (Queensland Government 2020) and Bundaberg (Queensland Government 2017) are better understood and have limits on the groundwater extraction. The continued increase in residential groundwater users in the TCP poses a substantial risk to groundwater quantity and quality.

Sufficient understanding of groundwater quality and characteristics is essential to successful sustainable management (van der Gun 2018) and there is an urgent need for effective management strategies to safeguard the long-term viability of the groundwater resources, prevent further seawater intrusion, and preserve the water quality of the GBR Marine Park.

To manage the groundwater system and mitigate the effects of climate change and the increasing number of users, a relatively in-depth understanding is needed of system characteristics and interactions, flow paths, and recharge processes (Villholth and Conti 2018).

The facts outlined above hold significance, as the understanding of groundwater systems in the area is limited, lacking clear and well-substantiated information on groundwater and recharge processes. With the predicted changes to Townsville's climate, including a decrease in rainfall and increases in temperature, potential evapotranspiration, wind-speed, drought frequency/spatial extent (Hennessy *et al*. 2008 pp. 4), this uncertainty poses challenges in effectively managing and safeguarding the system for all users.

As such, a clear understanding of TCP groundwater systems is the requisite starting point to sustainable groundwater management in the TCP because it enables development of appropriate monitoring programs.

1.3 Research Questions

The effective management of coastal plain groundwater systems is crucial for ensuring water availability, sustaining ecosystems, and meeting the growing water demands of urban and rural communities. In the case of Townsville, Australia, understanding the hierarchical clustering of water groups, the principal components driving mineral assemblages, and the geochemical processes influencing water chemistry—such as weathering, dissolution, ion exchange, and evapotranspiration—is crucial for interpreting groundwater system dynamics. Additionally, the assessment of water quality through stable isotope analysis, recharge estimation, irrigation water quality, and seasonal variations provides a comprehensive foundation for developing sustainable water resource management strategies. This study aims to address these existing knowledge gaps through a comprehensive investigation of the TCP. To achieve the overall objective, several research questions have been formulated, each focusing on a specific aspect of the groundwater system.

Research Questions:

1. To what extent do geographic and geological features influence the hydrogeochemical characteristics of coastal plain groundwater systems in Townsville, Australia?
2. How do the hydrogeochemical composition, recharge dynamics, and water quality of coastal plain groundwater systems in Townsville, Australia, vary across different urban areas.
3. How can an understanding of geographical and hydrogeological factors contribute to effective decision-making regarding sustainable use of groundwater resources?

1.4 Research Methods

The methodology used to address the research questions is outlined below; how these methods relate to the research questions is summarised in table 1.4.1.

1. Investigating the hydrogeochemistry of TCP groundwater systems, including:
   - Collection of groundwater samples from representative bores in the TCP.
   - Analysing the concentrations of major ions, such as calcium, magnesium, sodium, potassium, chloride, sulphate, and bicarbonate, in the groundwater samples.
   - Determining the stable isotopic composition of deuterium (^{2}H) and 18-oxygen (^{18}O) in the groundwater samples.
2. Applying a chloride mass balance analysis to estimate recharge to the coastal plain aquifers, involving:
   - Measuring the chloride concentrations in the groundwater samples.
   - Calculating the net chloride mass balance to estimate the recharge to the coastal plain aquifers.
   - Assessing the reliability and accuracy of the chloride mass balance method for estimating recharge in the study area.
3. Applying multivariate statistical techniques, including hierarchical clustering analysis (HCA) and principal component analysis (PCA), to identify patterns and relationships within the groundwater data, including:
   - Performing HCA on the hydrogeochemical dataset to identify distinct clusters or groups of groundwater samples.
   - Applying PCA to the hydrogeochemical dataset to identify dominant factors controlling the groundwater chemistry.
   - Determining the key variables contributing to the observed variations in the groundwater chemistry.
   - Exploring the relationships between groundwater chemistry and potential hydrogeological or environmental factors.
   - Assessing the similarities and dissimilarities among the groundwater samples based on their hydrogeochemical characteristics.

Table 1.4.1: Research questions with applicable method and defined purpose.

Research Question	Method	Purpose
1: How does hydrochemistry, recharge dynamics, and water quality vary across the TCP?	Hierarchical Cluster Analysis (HCA)	Groups samples together of similar hydrochemistry.
	Stable Water Isotopes	Elucidates recharge dynamics for each sample
	Residual Sodium Carbonate (RSC)	Assesses water quality for irrigation purposes.
	Sodium Adsorption Ratio (SAR)	Assesses water quality for irrigation purposes.
	Chloride Mass Balance (CMB)	Provides assessment of recharge to groundwater system of each sample.
	Wilcox Diagram	Classifies irrigation water based on sodium and salinity hazards
2: How do geological features influence hydrochemistry, recharge, and water quality in the TCP?	Piper Diagram	Indicates processes (freshening, seawater intrusion, mixing) occurring in groundwater system.
	Gibbs Diagram	Indicates processes (rock-water interaction, seawater, precipitation, evaporation) occurring in groundwater chemistry.
	Calc-Alkaline Index (CAI)	Indicates cation exchange or reverse ion exchange processes.
	Ionic Ratios	Indicates calcite, dolomite, gypsum, silicate, halite weathering and dissolution, and cation exchange, rock weathering, evaporation, and reverse ion exchange reactions.
3: What are the dominant factors controlling the variability and distribution of hydrochemistry in the TCP?	Principal Component Analysis (PCA)	Determines principal ions controlling hydrochemistry within samples.
	Graphical/Bi-variate Plots	Classifies water and indicates processes affecting hydrochemistry.

   - Examining the spatial distribution of the identified clusters and their potential correlation with geological features or hydrological processes.
4. Assessing water quality using standard indices and evaluating its suitability for irrigation purposes, involving:
   - Calculate the residual sodium carbonate (RSC) and sodium adsorption ratio (SAR) for the collected groundwater samples using appropriate parameters.
   - Classifying the water quality based on the Wilcox diagram and evaluate its suitability for irrigation purposes.
   - Identifying specific parameters contributing to any deviations from the desired water quality standards for irrigation.

1.5 Significance of the Study

The outcomes of this research have implications for sustainable management of coastal plain groundwater systems, both within the Townsville area and across Queensland's coastal plains. The research questions and applied methodology (table 1.4.1) have focused on key factors influencing groundwater and its chemistry, as these are critical for understanding the groundwater system. Without a thorough understanding of these systems, effective management and sustainable resource use cannot be achieved. Quantification of recharge using chloride mass balance analysis provides valuable information about the replenishment rates of the aquifers, enabling more accurate assessments of groundwater availability. The integrated hydrogeochemical analyses, multivariate statistical techniques (PCA and HCA), and water quality assessment furthers understanding of the factors controlling groundwater chemistry, the spatial variations in water quality, and the suitability of groundwater for irrigation purposes.

This research has practical significance for water resource managers, policymakers, and stakeholders involved in coastal plain groundwater management. The improved understanding of recharge processes and groundwater chemistry supports informed decision-making, facilitating the development of effective strategies for the sustainable utilization of local groundwater resources. Additionally, assessment of the suitability of water quality for irrigation purposes ensures the responsible and efficient use of groundwater, minimizing potential impacts on soil health and the environment.

1.6 Organization of the Thesis

This thesis is organized into six chapters as follows:

- **Chapter 1** introduces the study area, establishes the research problem, and delineates the significance of the study.
- **Chapter 2** delves into a thorough literature review encompassing the geological history, hydrogeological setting, existing water plans, and previous studies related to coastal plain aquifers' hydrogeochemistry.
- **Chapter 3** describes the methodology, elucidating data collection, hydrogeochemical analysis, chloride mass balance, and various analytical techniques used in this research.
- **Chapter 4** presents results from the hierarchical cluster and principal component analyses, focusing on hydrogeochemical results and groundwater processes including Piper diagram, bi-variate plots, chloro-alkaline indices, and the Gibbs diagram.
- **Chapter 5** presents detailed results on stable water isotopes, recharge, and water quality, including the residual sodium carbonate, sodium adsorption ratio, and Wilcox diagram, and the results of the assessment of seasonal change.
- **Chapter 6** offers a conclusion summarizing research outcomes and their implications for groundwater management, sustainability, along with recommendations for future studies.

The chapter-specific reference lists in Chapters 1-5 ensure clarity, complemented by a master reference list at the end of Chapter 6. Appendices provide additional supportive materials.

1.7 References – Chapter 1

Business Queensland 2024, *Water plan areas*, Business Queensland, Queensland Government, viewed 09 January 2024 from <https://www.business.qld.gov.au/industries/mining-energy-water/water/catchments-planning/water-plan-areas>.

CSIRO (Commonwealth Scientific and Industrial Research Organisation) 2020, *State of the Climate 2020*, Bureau of Meteorology, Australian Government, viewed 04 July 2021, <https://www.csiro.au/en/research/environmental-impacts/climate-change>.

Fernbach, N 2016, *Townsville residents turn to bores as water restrictions and dry spell continue*, ABC News North Queensland, viewed 19 April 2019, <https://www.abc.net.au/news/2016-12-07/boring-solution-to-drought-in-townsville/8096130>.

Freeze, RA, and Cheery, JA 1979, Groundwater: Englewood Cliffs, NJ, Prentice-Hall, pp. 604.

Gunn, J. and Manning, C. 2010, Black Ross (Townsville) Water Quality Improvement Plan: Improving Water Quality from Creek to Coral, Townsville City Council – Creek to Coral, Townsville, viewed 19 April 2019, <http://www.creektocoral.org/wqip/plandocs_final.html>.

Han, DM, Song, XF, Currell, MJ, Yang, JL, and Xiao, GQ 2014, ‘Chemical and isotopic constraints on the evolution of groundwater salinization in the coastal plain aquifer of Laizhou Bay, China’, *Journal of Hydrology*, vol. 508, pp. 12-27, DOI: 10.1016/j.jhydrol.2013.10.040.

Hennessy K, Webb L, Ricketts J, Macadam I 2008, ‘Climate Change Projections for the Townsville Region’, CSIRO, Townsville City Council, viewed 19 April 2019, <http://www.creektocoral.org/draftwqip/climatechange/csiro/>.

Queensland Government 2017, *Water Plan (Burnett Basin) 2014*, Office of the Queensland Parliamentary Counsel, Queensland Government, Brisbane, <https://www.legislation.qld.gov.au/view/html/inforce/current/sl-2014-0184>.

Queensland Government 2020, *Water Plan (Moreton) 2020*, Office of the Queensland Parliamentary Counsel, Queensland Government, Brisbane, <https://www.legislation.qld.gov.au/view/html/inforce/current/sl-2007-0031>.

Queensland Government 2024, ‘Black Catchment Story’, Department of Environment, Science and Innovation, Brisbane, <https://wetlandinfo.des.qld.gov.au/wetlands/ecology/processes-systems/water/catchment-stories/transcript-black.html>.

The State of Queensland 2013, ‘Environmental Protection (Water) Policy 2009: Black River Basin Environmental Values and Water Quality Objectives Basin No. 117, including all waters of the Black River Basin and adjacent coastal waters’, Department of Environment and Heritage Protection, Brisbane, available at <https://trove.nla.gov.au/work/188532431>.

***The State of Queensland 2019, Queensland Spatial Catalogue – Qspatial, Department of Nautral Resources, Mines and Energy, viewed 05 May 2019, <http://qldspatial.information.qld.gov.au/catalogue/custom/index.page>.

Todd, D, and Mays, L 2005, *Groundwater Hydrology*, 3rd Edition, John Wiley and Sons, Inc., Hoboken, 652 p., ISBN: 978-0471059370.

Van der Gun, J 2018, ‘Data, information, knowledge and diagnostics on groundwater’, in Villhoth, López_Gunn, Conti, Garrido & van der Gun (eds), *Advances in Groundwater Governance*, CRC Press, Taylor & Francis Group, pp. 193-213. Available from www.un-igrac.org.

Villholth, KG and Conti, KI 2018, ‘Groundwater governance: rationale, definition, current state and heuristic framework’, in Villholth, López_Gunn, Conti, Garrido & van der Gun (eds), *Advances in Groundwater Governance*, CRC Press, Taylor & Francis Group, pp. 3-31. Available from www.un-igrac.org.

Zaman, M, Shahid, SA, and Heng, L 2018 ‘Irrigation Water Quality’, In: Guideline for Salinity Assessment, Mitigation and Adaptation Using Nuclear and Related Techniques, Springer, Cham, DOI: 10.1007/978-3-319-96190-3_5.

Chapter 2: Literature Review

2.1 Overview of the Coastal Plain Groundwater System

2.1.1 Geological Setting

Generalized geological information relative to the Townsville regional area is available from Trezise and Stephenson (1990) and detailed geographical and geological maps were examined from The State of Queensland's Department of Natural Resource and Mines geospatial database (Qspatial) (The State of Queensland 2019).

Prior to the Cretaceous (145-66 Ma), the Australian coast extended much further east then its present position and was comprised of mainly sedimentary lithologies and volcanic sequences (Trezise & Stephenson 1990 pp. 12). These sequences, which were formed during the Cambrian (541-485 Ma) and Ordovician (485-419 Ma), were subsequently folded and metamorphosed into gneiss, quartzite, schist and metavolcanics (Trezise & Stephenson 1990).

Towards the end of the Cretaceous, the Coral Sea Basin began to open, leading to subsidence of the Precambrian landmass (Trezise & Stephenson 1990). The subsidence, in combination with eustasy as a result of cyclic sea level changes, led to the westward erosion of the continental landmass creating what is presently known as Hervey's Range escarpment (Trezise & Stephenson 1990). The escarpment, which borders the study area to the southwest, runs nearly parallel to the coastline and is the coastal highlands drainage divide.

Eustatic uplift and associated erosion played a critical part in creating the current landscape. The erosion of Hervey's Range created voluminous amounts of terrigenous sediment. This sediment was deposited both onshore and offshore, forming a new coastal plain that generally pro-graded toward the sea (Trezise & Stephenson 1990). The coastal plain extends from the escarpment to the northwest and is dominated by several prominent inselbergs and topographical highs of the erosion resistant plutonic intrusions.

Sea level changes shaped the coastal plain. During sea-level regression, the coastline moved eastward, exposing more of the coastal plain to weathering and erosion. During these events, much of the coastal area was dominated by flood plains, with fluvial networks of braided streams and rivers that, through time, down-cut channels into the landscape (Trezise & Stephenson 1990, Creek to Coral 2007, Gunn *et al*. 2009). Transgression periods, or rises in sea level, resulted in sediment infilling the incised river channels, and a change of deposition on the seaward side of the plain to shallow marine sediments (Trezise & Stephenson 1990).

As the surrounding landmass was eroded away, more resistant rocks were left behind as topographical features, such as Castle Hill, Mount Louisa, and Mount Stuart. These features are composed of intrusive (crystalline) rock. The higher resistance to weathering and erosion of Mount Stuart is due to its composition, which includes several Permian Period (299-252 Ma) micro-granitoid intrusions (Trezise & Stephenson 1990). These micro-granitoids are frequently cross-cut by mafic dykes and swarms.

The base and lower slopes of the escarpment consist of Quaternary (2.6 Ma – present) alluvial fans and colluvial deposits (Trezise & Stephenson 1990 and The State of Queensland 2019).

This colluvial sediment is immature and unconsolidated, deposited on slopes, primarily by non-fluvial processes (Boggs 2014). Processes that deposit colluvium include mass-wasting and slope-wash (Kearey 2001), and the immature and unconsolidated nature of the sediments provides an ingress area for groundwater recharge.

The geology of the TCP is summarized in table 2.1.1, with detailed surface geology and lithological descriptions are shown in Chapter 1, Figure 1.1.2 and Table 1.1.1, respectively.

Table 2.1.1: List of geology present in the TCP, with description and age.

Geology	Description	Age
Gneiss	Metamorphosed igneous or sedimentary rock; bedrock	Cambrian (541-485 Ma) and Ordovician (485-419 Ma)
Quartzite	Metamorphosed sandstone rock; bedrock	Cambrian (541-485 Ma) and Ordovician (485-419 Ma)
Schist	Medium grained metamorphic rock with foliations; bedrock	Cambrian (541-485 Ma) and Ordovician (485-419 Ma)
Metavolcanics	Metamorphosed volcanic rock; bedrock	Cambrian (541-485 Ma) and Ordovician (485-419 Ma)
Micro-granitoid	Fine grained igneous rock	Permian Period (299-252 Ma)
Colluvium	Poorly sorted, angular sediments deposited by mass wasting or sheet wash	Quaternary (2.6 Ma – present)
Alluvium	Clay, silt, sand, gravel deposited by flowing water	Quaternary (2.6 Ma – present)

2.1.2 Hydrogeology

Morton (1973) showed groundwater flow is likely to flow north from Kelso toward Mount Louise, a small inselberg of Permian granite, which acts as a barrier and diverts groundwater flow to the east and toward the outlet at Cleveland Bay.

The report by Creek to Coral (2007, pp. 4) delineates three primary sources of groundwater, which include: fractured rock, alluvial sediments and beach ridge systems.

The groundwater system across each of the basins is broadly considered a dual-layered (shallow/deep) aquifer system within Quaternary sediments, with highly variable water quality and salinity concentrations generally increasing with depth. These two systems are separated by clay aquitards of varying thickness and spatial extent.

The following is a list and description of the hydrostratigraphic units and recharge in the TCP.

1. Basement (fractured rock)

Morton (1973) and Creek to Coral (2007, pp. 4) have independently identified a fractured rock aquifer, emphasizing its presence in basement rocks, with specific mentions of spatially confined limestone/dolomite regions noted in the Townsville-Thuringowa Strategic Plan 1996 by the Natural Resources Working Group, although the original report could not be independently reviewed and verified.

Composed of gneiss, quartzite, schist, and metavolcanics, the basement rocks are fractured. Given the age and composition of these units, it is assumed that primary porosity is not preserved and that they constitute fractured rock aquifers. The fractured rock was shown by Morton (1973) to be one of the best yielding aquifers in Black River basin, along with other layers located below 33m.

2. Shallow sedimentary

The shallow system unconfined groundwater resides within surficial alluvial and colluvial sediments, which exhibit characteristics influenced by the composition of source rocks, weathering processes, transport mechanisms, and depositional conditions. These deposits consist of variably sorted clay, silt, sand, and gravel

The report by Morton (1973) summarized the geological structure of the Bohle River sub-catchment area, based on geophysical and aerial surveys, with descriptions of drilling data and geophysical (seismic depth probing), showing paleochannels of river gravel and bedrock at 39-45m in the Upper Ross area; subsequently, this indicates that bedrock levels are significantly lower in the valley areas (compared to underneath the Ross River). The results of Morton (1973) suggest that the Bohle River closely follows an abandoned path of the Ross River and that ancient paleochannels of gravel sediments provide a groundwater flow path.

3. Deep sedimentary

The lower system is indicated as semi-confined, with varying thicknesses to the confining layers (aquitards). Drilling records in the current study area generally indicate thick (3-10+ m) argillaceous deposits, some with interbeds of coarse sand and gravel. Generally, the clay layers act as impermeable boundaries and are prevalent in drilling logs across most subbasins of the coastal plain. The presence of coarser sediments beneath the clay or within the interbeds of paleochannels allows for the possibility of a preferential flow path (conduit channels) allowing groundwater to travel greater distances, based on hydraulic head and transmissivities (Mazor 2004). This is consistent with Morton (1973 pp. 3), in that it's noted that the aquifer systems were channels of gravel and permeable sand lying within sediments of less permeable material. Groundwater is usually encountered beneath the clay, sometimes at the interbeds, or within the weathered profile of existing bedrock.

4. Recharge

The source of recharge for groundwater in the Bohle River area is stated to be primarily from rainfall and runoff from the Bohle and Ross River catchments (Morton 1973 pp. 3) and has been estimated to be 9% of annual rainfall (Brashears 1971 pp. 11). It should be noted that Morton (1973 pp. 3) indicates that recharge occurs from underflow from the current Ross River but does not elaborate any on the basis for this statement.

2.1.3 Water Plans

Water Plans are developed under the framework of the Water Act 2000 (Business Queensland 2020, State of Queensland 2018) and are designed to sustainably manage and allocate Queensland water resources across the state, including groundwater. The coastal catchments of Black and Ross River basins are located just outside of the Burdekin Water Plan.

The Black River Underground Water Management Area is the only Water Plan regulated groundwater area in the study region (fig. 2.1.1 – blue inset). It was implemented to protect the water resources for the Queensland's Nickel refinery at Yabulu, and this 239 km^2 area covers the south end of the Black River basin and its sub-catchments; the TCP is located entirely within the Ross River basin, adjacent to the south.

To effectively regulate the system for all users, the Queensland government relies on the Groundwater Ambient Network (GWAN) bores installed across Water Plan areas to oversee, manage, and regulate groundwater and surface water systems (Department of Environment and Science 2020).

In total, 44 GWAN bores are located in the Black River and Ross River basins and of these, 36 are within or at the edge of the Black River Underground Water Management Area (fig. 2.1.1 – blue inset). The GWAN bores in the Ross River basin are grouped locally near the northeast border of the Black River basin and water management area.

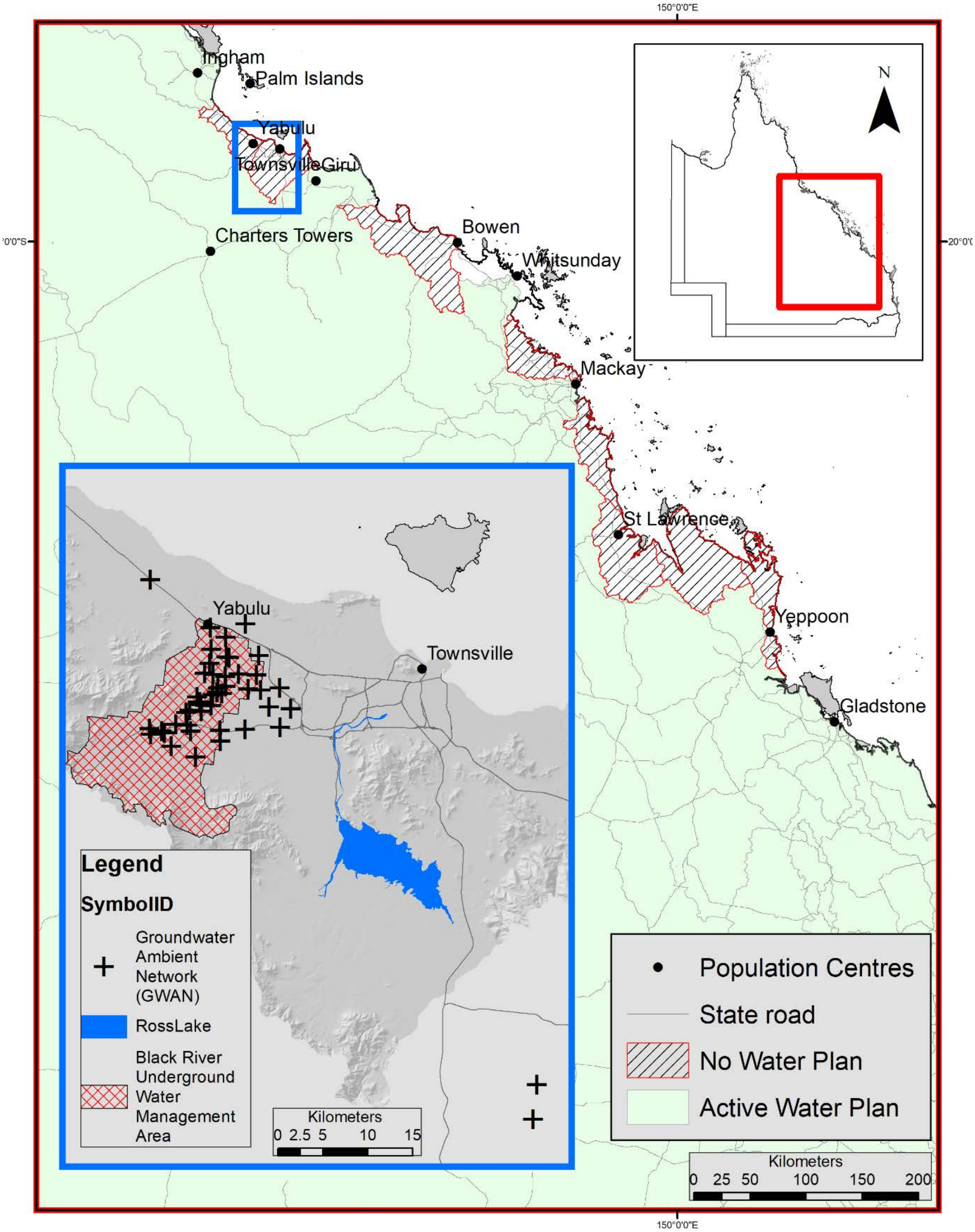

Figure 2.1.1: (Red inset) Map displaying central Queensland coastline from Gladstone to Townsville, highlighting (simple hatch, red outline) areas where Water Plans are not present. (Blue inset) Map displaying the TCP study area and the Black River Underground Water Management Area with GWAN bores (black plus).

2.1.4 Groundwater Background

Published hydrogeological investigations of the TCP are limited geographically to areas of industry interest and assessment and these investigations are mainly from the 1970's.

Though Townsville is part of the Dry Tropics Region with significantly different climate regimes compared to neighbouring regions (Gunn and Manning 2010 pp. 41), the regional hydrogeochemistry (fig. 2.1.2) has been inferred from a Wet Tropics desktop study (Raymond and McNeil 2013). Interestingly, this study asserts both the abundance of data for shallow, moderate, and deep-water levels, but acknowledges that only data from the 'moderate' depth is adequately distributed (Raymond and McNeil 2013 pp. 78) and designates 'ost of t'e tcp study area as 'limited data' for the Ross River and Black River basins (Raymond and McNeil 2013 pp. 37).

This study's objective was to explore areas with insufficient data, thus assisting in clarifying and characterizing regions with less certainty. Discrepancies are illustrated in the classification of Zone 9 – Low salinity coastal flood plain, which is stated to show consistent B-Type water across all depth zones (B-Type water is defined by sodium-dominated cations and chlorine or carbonate dominated anions, with very low salinity), however current results from this zone indicate Mg-Cl and Na- HCO_3^- groundwaters, in addition to Na-Cl type waters. All TCP study area samples from Zone 9 exceeded the 80th percentile management value for water quality objectives (WQO) set by the State of Queensland (2013). In addition, 64% and 70% of samples from Zone 10 (Granitic uplands and slopes) and Zone 20 (Tropical alluvial) exceeded the 80% percentile WQO, respectively. Another example includes the Townsville-Thuringowa Strategy Plan (Townsville Regional Council 2016) section on groundwater (section 4.4, p. 10) stating "Groundwater quality is variable on a seasonal basis" and references a document from 2007 indicating that a development area (Rocky Creek) showed the highest conductivity during the late Dry season and lowest at the end of the Wet season.

The document is referenced as "(C&R, 2007)" in text and is not listed within the references of the Townville Regional Council (2016) report. Subsequent research failed to locate the document. As this is listed under section 4.4: Groundwater, it is assumed that water samples were obtained using standard procedures from groundwater sampling points. It is here reported that this information is erroneous and not representative of the general region, as current data for this research shows very limited variability between seasons – based on 19 locations sampled during each sample collection period (discussed in Chapter 5).

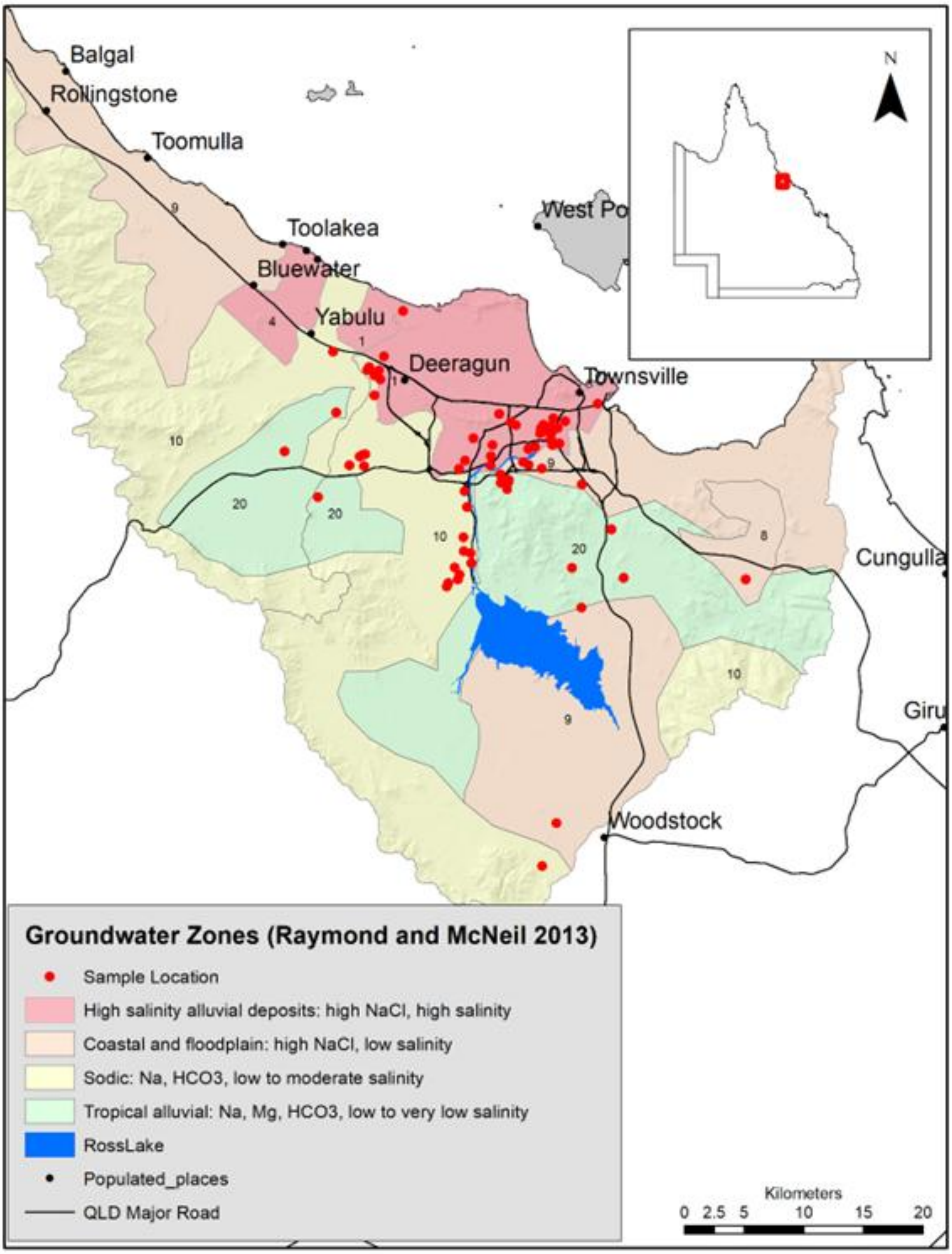

Figure 2.1.2: Groundwater zones as defined by Raymond and McNeil (2013) including high salinity alluvial deposits (Zone 1 - red), coastal floodplain (Zone 9 - orange), Sodic (Zone 10 - yellow), and tropical alluvial (Zone 20 - green); Sample locations (red circle) are shown within each zone.

A report by Creek to Coral (2007) summarized the then-current understanding and extent of knowledge of the Ross and Black Rivers catchments, to assist the Coastal Catchment Initiative and Water Quality Improvement Plan (Gunn and Manning 2010), to protect marine sensitive areas from pollution and sediment runoff into the GBR Marine Park waters. This desktop report identified knowledge gaps related to the identification of groundwater dependent ecosystems (GDEs) and the lack of groundwater mapping/hydrogeochemistry. GDEs play a crucial role in supporting the environment. When groundwater levels decline, flow patterns are altered, impacting the movement of groundwater (van Engelenburg *et al*. 2018). This shift can lead to changes in the availability of groundwater to specific areas, potentially cutting off previously sustained regions. Understanding and managing the unique hydrological needs of GDEs are essential for their sustainability and, by extension, the ecosystems they support. As current at the time of writing, the location and extent of any GDEs within the two basins remains unknown (Department of Environment and Science 2020).

Coastal plain aquifers are vital sources of freshwater supply in coastal regions, characterized by unique hydrogeochemical signatures shaped by the dynamic interaction between freshwater and seawater. These aquifers exhibit distinct characteristics that play a crucial role in supplying residents with domestic irrigation in the Townsville region. One of the key attributes of coastal plain aquifers is their heterogeneity, resulting from complex geological formations and depositional processes over geological time scales. Heterogeneity gives rise to variations in hydraulic conductivity and porosity, influencing groundwater flow patterns and distribution of solutes (Todd and Mays 2005). Coastal plain aquifers often exhibit high mineral dissolution and ion exchange rates due to the presence of reactive minerals in the geological formations. As groundwater interacts with these minerals, it can acquire a unique hydrogeochemical composition characterized by elevated concentrations of certain elements, such as sodium, potassium, calcium, magnesium, bicarbonate, and sulphate (Todd and Mays 2005). Furthermore, organic matter from vegetation and organic-rich sediments can influence the hydrogeochemistry of coastal plain aquifers, the decomposition of which generates dissolved organic carbon and reduces conditions, facilitating redox reactions that affect the mobility of trace elements and nutrients (Todd and Mays 2005).

The Queensland Government has set the environmental values (EVs) and water WQO of groundwaters based on a depth classification of shallow (0-15m), moderate (15-40m), deep (40-65m) and very deep (>65m) (State of Queensland 2013). The Evs and WQOs were developed to protect the natural chemistry of surface waters and runoff to the Coral Sea in efforts to defend the GBR from anthropogenic impacts. The depth categories were defined across a diverse and extensive region, encompassing various groundwater systems and might not always be entirely representative at a local scale and to enhance precision, further monitoring and analysis would be essential to refine zonal boundaries and increase confidence in scenarios with limited data (Raymond and McNeil 2013 pp. 47). Anticipated changes to local and regional evapotranspiration, rainfall, and weather patterns could exacerbate the potential for groundwater over-extraction by unlimited growth in the population of groundwater users; rainfall is predicted to decline in volume but increase in frequency and evapotranspiration is predicted to increase (SEAO2 2008). As climate change continues and more people turn to groundwater for irrigation, the risks associated with over-extraction of groundwater increases exponentially (Werner 2010). The most recent Townsville State of Environment (SOE) Report (2003) noted that groundwater extraction rates in some areas exceeded recharge rates. The resulting decrease in groundwater volumes (from lack of recharge/rainfall or anthropogenic extraction) can have adverse effects on groundwater quality, including saltwater intrusion (Klassen and Allen 2017), degradational changes to water chemistry, such as increasing salinity and precipitation of minerals within pore space (Freeze and Cherry 1979, Todd and Mays 2005), and soil (Xian *et al.* 2019). Most importantly, decreasing groundwater levels alter groundwater flow patterns and reduce groundwater-dependent ecosystem areas (Havril *et al.* 2018).

2.2 References – Chapter 2

Brashears, ML 1971, ‘Review of Ground-Water Investigations made by the Australian Groundwater Consultants PTY. Limited in the Townsville Region, Queensland, Australia’, Leggette, Brashears & Graham Consulting Ground-Water Geologists (New York), Irrigation & Water Supply Commission, QLD DNR Library I29952.

Boggs, S 2014, *Principles of sedimentology and stratigraphy*, 5th ed., Pearson, St. Ives, England.

Business Queensland 2020, *Developing Water Plans*, Business Queensland, Queensland Government viewed 09 January 2024, <https://www.business.qld.gov.au/industries/mining-energy-water/water/catchments-planning/planning>.

Creek to Coral 2007, *A Summary Review of Groundwater Research and Knowledge for the Black River and Ross River Basins*, Townsville City Council – Creek to Coral, Townsville.

Department of Environment and Science 2020, *Groundwater Ambient Network (GWAN) – Water quality*, WetlandInfo, Queensland Government, viewed 21 January 2020, <https://wetlandinfo.des.qld.gov.au/wetlands/assessment/monitoring/current-and-future-monitoring/groundwater-ambient-network.html>.

Freeze, RA, and Cheery, JA 1979, Groundwater: Englewood Cliffs, NJ, Prentice-Hall, pp. 604.

Gunn, J, Manning, C, and Connolly, N 2009, *Basins, Catchments and Receiving Waters of the Black and Ross River Basins Water Quality Improvement Plan Area*, Townsville City Council – Creek to Coral, Townsville.

Gunn, J. and Manning, C. 2010, Black Ross (Townsville) Water Quality Improvement Plan: Improving Water Quality from Creek to Coral, Townsville City Council – Creek to Coral, Townsville, viewed 19 April 2019, <http://www.creektocoral.org/wqip/plandocs_final.html>.

Havril T, Toth T, Molson JW, Galsa A, Mádl-Szőnyi J 2018, ‘Impacts of predicted climate change on groundwater flow systems: Can wetlands disappear due to recharge reduction?’, Journal of Hydrology, 563, pp. 1169-1180, DOI: 10.1016/j.jhydrol.2017.09.020

Kearey P 2001, *The New Penguin Dictionary of Geology*, 2nd ed., Penguin Group, England.

Klassen J, Allen, DM 2017, ‘Assessing the risk of saltwater intrusion in coastal aquifers’, Journal of Hydrology, 551, pp. 730-735, DOI: 10.1016/j.jhydrol.2017.02.044.

Mazor, E 2004, *Chemical and Isotopic Groundwater Hydrology*, 3 ed., Marcel Dekker Inc., Halsted Press (John Wiley & Sons), United States of America, ISBN: 0-8247-4704-6.

Morton, WH 1973 “Groundwater in the Bohle-Ross Rivers Area, Townsville, QLD”, Australian Groundwater Consultants PTY. LTD, Department of Environment & Resource Management, catalogue 551.49 GRO 1973, QLD DNR Library: I42148, available from <https://trove.nla.gov.au/version/192977949>.

Raymond, MAA, McNeil, VH 2013, ‘Queensland wet tropics and Black and Ross catchments: Regional chemistry of the groundwater’, Department of Science, Information Technology, Innovation and the Arts, Brisbane, v. 2, Libraries Australia ID 50859873, viewed March 23, 2021, <http://hdl.handle.net/10462/pdf/833>.

SEAO2 2008, *Climate change in Townsville and potential impacts on water quality*, Townsville City Council – Creek to Coral, Townsville.

State of Queensland 2013, *Environmental Protection (Water) Policy 2009: Black River Basin Environmental Values and Water Quality Objectives, Basin No. 117, including all waters of the Black River Basin and adjacent coastal waters*, Department of Environment and Heritage Protection, Queensland Government, Brisbane, <https://environment.des.qld.gov.au/__data/assets/pdf_file/0023/88106/black-river-basin-ev-wqo.pdf>.

State of Queensland 2018, Water Act 2000, Department of Natural Resources, Mines, and Energy viewed 20 April 2019, <https://www.legislation.qld.gov.au/view/pdf/inforce/current/act-2000-034>.

***The State of Queensland 2019, Queensland Spatial Catalogue – Qspatial, Department of Natural Resources, Mines and Energy, viewed 05 May 2019, <http://qldspatial.information.qld.gov.au/catalogue/custom/index.page>.

Todd, D, and Mays, L 2005, *Groundwater Hydrology*, 3rd Edition, John Wiley and Sons, Inc., Hoboken, 652 p., ISBN: 978-1-118-00177-6.

Townsville Regional Council 2016, 'Townsville Regional Stormwater Strategy', Bligh Tanner Pty Ltd Job No. 2015.025.600, Townsville Regional Council, retrieved 20 March 2022 from: <https://www.townsville.qld.gov.au/__data/assets/pdf_file/0015/30048/2016-06-28-Regional-Stormwater-Strategy-Part-2-Analysis-Report.pdf>.

Townsville State of Environment Report 2003, Inland Waters, Townsville City Council, viewed 17 April 2019, <http://www.soe-townsville.org/inlandwaters.html>.

Trezise, DL and Stephenson, PJ 1990, *Rocks and Landscapes of the Townsville District*, Department of Resource Industries, Queensland Government, ISBN 0 7242 33 81.

Van Engelenburg, J, Hueting, R, Rijpkema, S, Teuling, AJ, Uijlenhoet, R, and Ludwig, F 2018, 'Impact of Changes in Groundwater Extractions and Climate Change on Groundwater-Dependent Ecosystems in a Complex Hydrogeological Setting', Water Resource Management, vol. 32, pp. 259-272, DOI: 10.1007/s11269-017-1808-1.

Werner, AD 2010, 'A review of seawater intrusion and its management in Australia', Hydrogeology Journal, vol. 18(1), viewed 15 February 2018, DOI: 10.1007/s10040-009-0465-8.

Xian, X, Pang, M, Zhang, J, Zhu, M, Kong, F, Xi, M 2019, 'Assessing the effect of potential water and salt intrusion on coastal wetland soil quality: simulation study', Journal of Soils and Sediments, Preprint, viewed 31 March 2019, DOI: 0.1007/s11368-018-02225-y.

THIS PAGE INTENTIONALLY LEFT BLANK

Chapter 3: Methodology

3.1 Data Collection and Treatment

Seventy-four groundwater bores were sampled between April 2018 and November 2019 (fig. 3.1.1). These bores are distributed across the TCPs most populated areas and are representative of the shallow (<15m), moderate (15-40m) and deep (40-65m) depth profiles set by the Queensland Government (2013); no bore exceeding 65m was sampled. The location of each bore was cross-referenced with Queensland Government records (The State of Queensland 2019) to ascertain bore depth; records do not exist for n=27 (22%) and could not be classified by depth (unknown – UNK).

A total of 124 (n=124) samples were obtained during sample collection in April 2018 (n=21), November 2018 (n=32), and November 2019 (n=71) and submitted for analysis of the major-ions, including sodium (Na^+), potassium (K^+), calcium (Ca^{2+}), magnesium (Mg^{2+}), chloride (Cl^-), sulphate (SO_4^{2-}), and bicarbonate (HCO_3^-) as alkalinity ($CaCO_3$), and stable water isotopes deuterium (δD) and 18-oxygen (δO).

Major ion samples were submitted to ALS Laboratories, a NATA certified laboratory. Cl^- and SO_4^{2-} were measured by Discreet Analyser while carbonate alkalinity (as $CaCO_3$) was measured by PC titrator. Ca^{2+}, Mg^{2+}, Na^+, and K^+ were measured by ICP-AES and ICP-MS. Below detection limit (DL) values from laboratory analyses can present issues in the application of HCA and PCA. Laboratories usually report non detected elements as the value of the DL or 0, referred to as 'censored' data.

Of the 74 sites sampled, 19 of these sites were sampled during each of the three collection periods. Based on the results of the seasonal analysis, which indicated that the variation between concentrations in the sample collection periods was not significant, the data points (variables) from these 19 sites were combined and averaged (see Appendix 1). This resulted in a total of 86 (n=86) data points being used in subsequent analyses (see Appendix 2), which reduced the overall noise within the data set.

The April 2019 and April 2020 sampling rounds were cancelled due to record flooding in the study area (2019) and the COVID global pandemic (2020), respectively. As such, the data and analyses are heavily weighted toward the low-flow (dry) conditions of the groundwater system.

Groundwater samples were collected in accordance with Australian Standards (AS/NZs 5667.11:1998) for bore sampling and each bore was flushed for 15 minutes prior to sampling, or until Ph and electrical conductivity (EC) stabilized. Field parameters of EC, Ph, and temperature (T in °C) were measured with Hannah Instruments T/Ph (model HI98127) and T/EC (model HI98311) meters. Both devices were calibrated each day of use, using procedures included with each device and standardized solutions. EC results above 4000 μs/cm (upper limit of model HI98311) were calculated by AQQA (Rockware) software.

Samples for major ion hydrogeochemistry were collected in 250ml polyethylene bottles with no head space and kept cool (~5°C) until submission to the laboratory. Stable isotope samples were filtered to 22 micrometre (μm) and collected in 50ml polyethylene bottles with no head space, with the screw lid secured by parafilm and kept cool until lab submission.

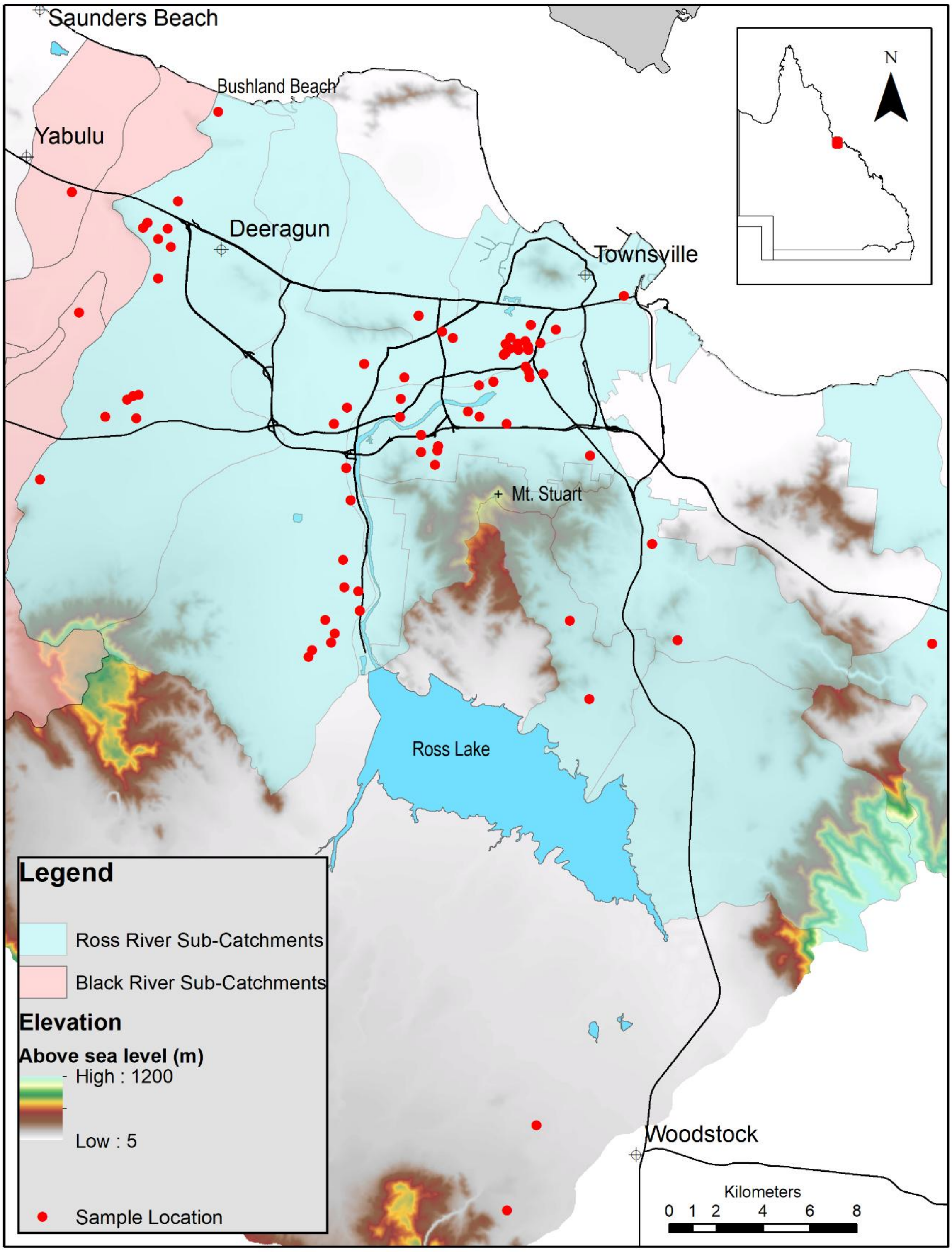

Figure 3.1.1: Map of TCP showing topography and sampling locations (red circle) within the Ross River basin (blue area) and Black River basin (pink area).

3.2 Multivariate Analyses (PCA/HCA)

The characterization of groundwater systems and processes holds significant value in regional-scale groundwater management (Gosselin *et al*. 2001). Within the literature, multivariate statistical analyses are recognized for their effectiveness in simplifying the complexities of these factors. Alongside conventional techniques such as the Piper diagram, multivariate statistical methods like principal component analysis (PCA) and hierarchical clustering analysis (HCA) have been successfully employed across various hydrogeological contexts. These methods reveal and elucidate underlying processes, spanning diverse environments from coastal plains (Güler *et al*. 2012; Kumar *et al*. 2014) to mountain streams for groundwater-surface water interactions (Menció and Mas-Pla, 2008), and encompassing intricate scenarios like the interplay between shallow and deep aquifer systems (Carucci *et al*. 2012), anthropogenic impacts in complex alluvial systems (Singh *et al*. 2017), as well as the origins and processes of groundwater salinization in urban coastal aquifers (Cary *et al*. 2015), among others. In this study, Q-mode HCA, using Ward's Linkage, was used to group groundwater samples based on their hydrogeochemistry. PCA was performed to identify major groundwater processes contributing to groundwater chemistry in the region.

Farnham *et al*. (2002) showed the effectiveness of HCA and PCA was highest by halving the DL (DL/2) and was preferred to substitution by 0 or DL. When censored values were >30% of total values, the HCA and PCA were also shown to be less effective; only K^+ values (48.4%) were greater than threshold (correlation matrix) but was kept within the analyses as correlation was noted (discussed later).

The data was log transformed (except pH) to attain a more normal distribution, as most naturally occurring elemental concentrations tend to be skewed positively (Güler *et al*. 2002, pp. 461). The standard scores (*z*-scores) were calculated as follows:

$$z_i = \frac{x_i - \bar{x}}{s} \tag{1}$$

Where z_i = standard score of the sample *I*; x_i = value of sample *I*; $\bar{x}$ = mean; s = standard deviation.

This standardization of the log transformed data allows equal weight to each variable, thus avoiding stronger influences by higher value data points, and homogenises the distribution's variance (Güler *et al*. 2002 pp. 462). PCA analysis reduces the dimensions (variables) to linear combinations (covariance) of the original variables, which explain the maximum variance within the data and are represented by eigenvalues. Eigenvalues of >1 were accepted as significant. This is based on the Kaiser criterion, in which a factor (variable) should have variance that is at least one standardized variable to be accepted (Belkhiri, Boudoukha, and Mouni 2011 p.542). The Ward's linkage method, in conjunction with Euclidean distance, was used as these two in combination produce the most distinctive groups such that similarity within groups and dissimilarity between groups is maximized (Güler *et al*. 2002 p.465).

The initial PCA results were evaluated for communalities, also known as the r-square value. Communalities indicate the proportion of variance in the variables explained by the extracted factors. Typically, a variable with communalities exceeding 0.5 is considered for further analysis. For temperature and Ph, the communalities were found to be 0.257 and 0.300, respectively. Consistent with Guler *et al*.'s (2012 pp. 441) groundwater research, which employed a threshold of 0.7, temperature and Ph were excluded from the analysis. This refinement led to eight variables being used in the final PCA analysis.

The statistical package IBM SPSS Statistic' for Windows, version 26 (IBM Corp., Armonk, N.Y., USA) was used for the statistical analyses. The Bartlett chi-squared statistic was used to indicate if the data has a structure and is correlated (not orthogonal), thereby validating the application of PCA (Chander *et al*. 2017 pp. 62).

The standardization and transformation of the data fulfils the data assumptions of 1) independent observations 2) normality, and 3) homogenous variance, of the paired t-test. The parametric paired t-test was used to assess seasonal variation in water quality by performing paired t-tests for each of the major ions and physiochemical parameters and compared between each sampling season (April 2018, November 2018, and November 2019), resulting in 30 paired tests with 95% confidence ($p < 0.05$ at 95% confidence).

In the preliminary stages of factor analysis, it is crucial to evaluate the sampling adequacy, and the Kaiser–Meyer–Olkin (KMO) measure serves this purpose, assessing whether the responses from the sample are adequate (Güler *et al*. 2012). According to Kaiser (1960), a KMO value around 0.5 is minimally acceptable, while values between 0.7 and 0.8 are considered satisfactory, and those above 0.9 are excellent. This aligns with the confirmation that variables are correlated, not orthogonal (Menció and Mas-Pla 2008) and signifying acceptable intercorrelation among variables and the suitability for PCA (Belkhiri, Boudoukha, and Mouni 2011). Concurrently, Bartlett's test examines whether the correlation matrix is an identity matrix, and the obtained chi-square statistic of 976.5 with 28 degrees of freedom and a significance level below 0.001 further confirms the correlation among variables (Chander *et al* 2017 pp. 62).

The Kaiser criterion, as proposed by Kaiser (1960), was applied to determine the appropriate number of factors for each dataset in the analysis. Factors with eigenvalues equal to or exceeding 1 were considered as potential contributors to variance, with a focus on the factor possessing the greatest sum of eigenvectors. The threshold of 1 was chosen based on the requirement that a factor should exhibit variance equal to or surpassing that of an individual standardized original variable to be considered significant (Belkhiri, Boudoukha, and Mouni 2011). Integrating these approaches, HCA and PCA were conducted on groundwater hydrogeochemistry data from N=86 samples, considering major ion parameters. The initial dataset comprised 10 physio-chemical variables. However, the refined PCA model incorporates only 8 variables (Na^+, K^+, Ca^{2+}, Mg^{2+}, Cl^-, SO_4^{2-}, HCO_3^-, EC).

3.3 Hydrogeochemical Analysis

The charge-balance equation (Freeze and Cherry 1979, pp. 97) was calculated to assess analytical results with most results <5% and all results <10%.

Data analysis was conducted using SPSS (IBM Corp. 2020, version 26.0) statistical software for multivariate analyses and paired-t testing of the data and ArcMap GIS (ESRI 1996) software version 10.6.1 was used with Spatial Analyst toolset.

The Piper (1944) diagram (fig. 3.3.1 and 3.3.2) is a multifaceted plot that uses milliequivalents percentage concentrations of major cations to classify water types for groundwater. The major ions include the cations Ca^{2+}, Mg^{2+}, Na^+, and K^+, and the anions HCO_3^{--}, SO_4^{2-}, and Cl^-, and are plotted in two triangular fields, which are then projected further into the central diamond field. The data plotted on the subdivisions of the diamond-shaped field decides the water type or hydro-chemical facies in a water sample (Hem 1985 pp. 178).

The Piper diagram visually portrays the categorization of water types, an arrangement established upon major ion concentrations (Bartos and Ogle 2002). This framework relies on the dominance of either a cation or anion, with determination based on a relative percentage surpassing 50%. These predominant ions plot toward the apexes of the cation and anion triangles, situated at the lower left and right corners respectively. Instances where ions with relative concentrations below 50% aggregate at the central field as ‘no dominant type’, while maintaining classification rooted in the ion exhibiting the highest relative concentration.

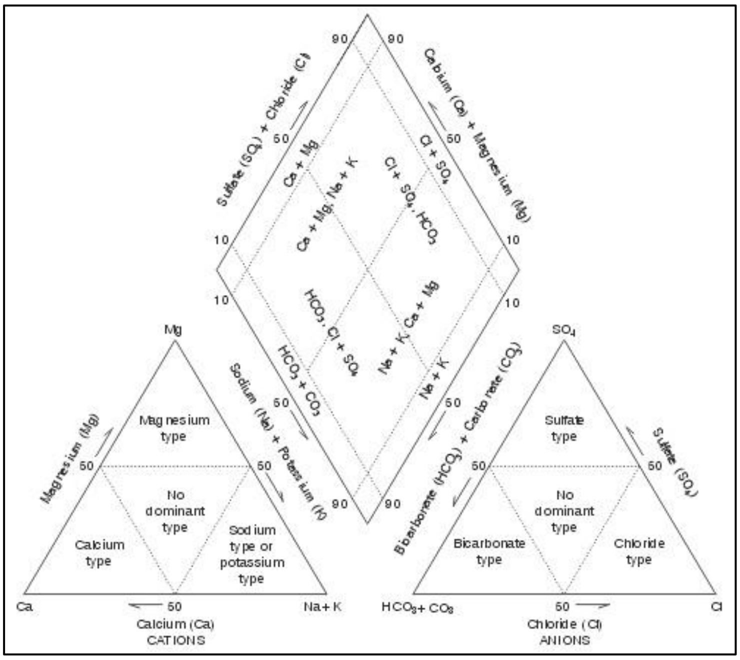

Figure 3.3.1: Water type classification in the Piper diagram is based on major ion concentrations (modified from* Bartos and Ogle 2002*, figure 13).

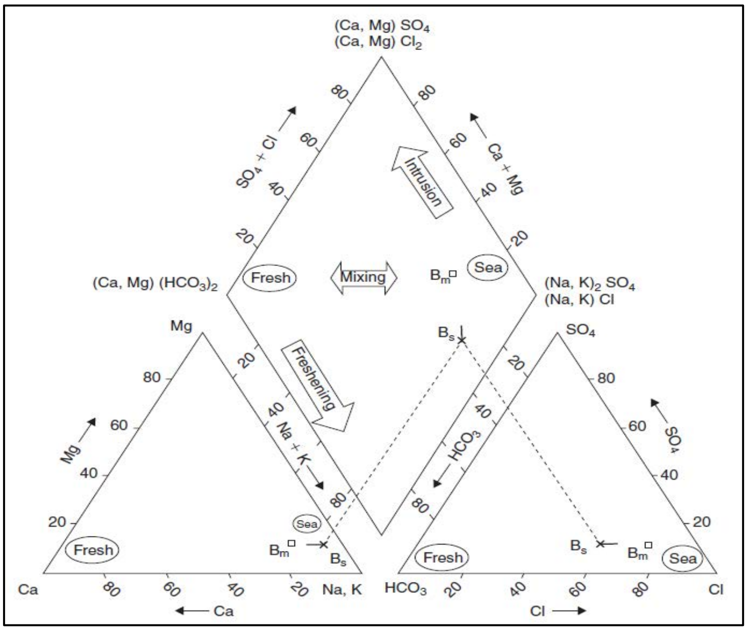

Figure 3.3.2: Diagram depicting processes shown in the Piper diagram, including mixing, freshening, and saline intrusion (modified from Appelo and Postma 2005, figure 6.4).

The diagrams typically present relationships that provide supplementary evidence for conclusions about water sources, which are often corroborated by other supporting factors (Appelo and Postma 2005 pp. 244).

Groundwater processes, including silicate weathering, carbonate weathering, and evaporite dissolution, can be effectively identified and understood through the analysis of certain ion ratios plotted in graphs. Combining specific ions and ratios, such as the Na^+ normalized Ca^{2+} to HCO_3^- and Mg^{2+} ratio plots, which can show distribution differences among samples and offer insight to processes influencing the chemistry, to include silicate weathering, evaporite dissolution, and carbonate dissolution (Singh *et al*. 2017 pp. 68, Li, He, and Gu 2019 pp. 10).

The evaluation of the proportional occurrence of ionic species within the groundwater has been conducted using several bivariate plots. These plots effectively demonstrate the connection between dissolved constituents in the groundwater, offering valuable insights into the potential hydro-chemical processes that influence groundwater chemistry (Ansari and Umar 2019 pp. 39).

This study also examined the Gibbs (1970) diagram, a tool that assesses the chemical signature of groundwater, discerning whether the water composition is influenced by rock-water interaction, seawater intrusion, or precipitation. The Gibbs diagram serves as a practical tool in hydrogeochemistry, offering key insights into the dominant processes influencing groundwater samples. Originating from Gibbs's foundational work in 1970, this graphical representation allows us to visually grasp the compositions of intricate multi-component systems, including aqueous solutions. Over time, the Gibbs diagram was tailored to hydrogeochemical studies, aiming to untangle the chemical transformation of groundwater by aligning major ions against total dissolved salts.

The diagram complements the Ca^{2+}/ Na^{+} plots, which focus on examining the weathering and dissolution patterns within the groundwater of the TCP.

3.3.1 Stable Isotopes

Stable isotopes offer a unique perspective on water sources, recharge processes, and hydrogeochemical interactions, providing invaluable information for effective water resource management (Hem 1985 pp161, Mook 2000 pp. 17). Stable isotope analysis was performed on all samples by a custom process (Munksgaard, Wurster & Bird 2011) Diffusion Sampling – Cavity Ring-Down Spectrometry (DS-CRDS) at the JCU Centre for Tropical Environmental and Sustainability Science (TESS) laboratory in Cairns, QLD.

The most used isotope ratios in hydrology are deuterium (D) and oxygen-18 (^{18}O). These nuclides are found in average proportions of 0.01 percent and 0.2 percent of hydrogen and oxygen, respectively. The reference standard composition of the isotope ratio is based on average seawater composition as determined by VSMOW (Vienna Standard Mean Ocean Water) where deviations of isotope ratios in water samples are expressed as delta-deuterium (δD) or delta-18-oxygen ($\delta^{18}O$) value in parts per thousand (‰) (Clark and Fritz 1997 pp. 7).

The deviation from VSMOW is calculated by (Clark and Fritz 1997 pp. 6):

$$\delta D‰ = \left(\frac{\left(\frac{D}{H}\right)_{Sample} - \left(\frac{D}{H}\right)_{VSMOW}}{\frac{D}{H}_{VSMOW}} - 1\right) \times 1000 \tag{2}$$

and

$$\delta^{18}O‰ = \left(\frac{\left(\frac{^{18}O}{^{16}O}\right)_{Sample} - \left(\frac{^{18}O}{^{16}O}\right)_{VSMOW}}{\frac{^{18}O}{^{16}O}_{VSMOW}} - 1\right) \times 1000 \tag{3}$$

The stable isotope ratios of the water molecule, specifically the ratios of $^{18}O/^{16}O$ and D/1H, hold significant value in hydrology due to their ability to provide insights into condensation and evaporation processes. These isotopic ratios are influenced by slight differences in reactivity caused by mass differences, with lighter isotopes exhibiting higher reactivity compared to heavier isotopes (Mazor 2004 pp. 182). Variations in D/1H and $^{18}O/^{16}O$ ratios in natural waters predominantly arise from isotopic fractionation during evaporation and condensation processes, where the heavy isotopes preferentially remain in the liquid phase during evaporation or pass into the liquid phase during condensation (Hem 1985 pp. 162, Mazor 2004 pp. 182).

Rainfall, found across the globe, is depleted in heavy isotopes of water relative to seawater through a phenomenon known as Rayleigh fractionation (Clark 2015 pp. 109). On the VSMOW scale, the isotopic composition of rainfall is heavier than that of clouds but lighter than the seawater that originally served as the source of water vapor forming the clouds (Mazor 2004 pp. 183). Due to the similar behaviour of D and ^{18}O isotopes, δD and $\delta^{18}O$ values in precipitation exhibit a high correlation (Clark and Fritz 1997 pp. 7). Craig (1961) made a significant observation, noting a strong correlation between the δD and $\delta^{18}O$ values in freshwaters worldwide (Clark 2015 pp. 129). The regression line derived from this correlation is referred to as the GMWL and is expressed as (Clark 2015 pp. 129):

$$\delta D = 8 * \delta^{18}O + 10‰ \quad (4)$$

Thus, the GMWL represents the average relationship between δD and $\delta^{18}O$ in precipitation, enabling its use as a benchmark for assessing the isotopic composition of both surface and groundwater (Clark 2015 pp. 129, Mook 2000 pp. 194). The stable isotopic composition of local rainfall often differs from the global mean, leading to the definition of a local meteoric water line (LMWL) and has been established for the study area by Liu *et al.* (2010).

In many cases, the mean δD and $\delta^{18}O$ composition of groundwater will resemble the mean amount-weighted δD and $\delta^{18}O$ composition of precipitation within its recharge area (Clark and Fritz 1997). The stable isotope signatures of groundwater are dependent on multiple factors, which include the stable isotope signature of the precipitation leading to recharge and potential evaporative effects through the unsaturated zone, but these signatures are generally preserved (Mook 2000 pp. 194). Water infiltration into the unsaturated zone happens through the porous matrix of surface sediments and potentially via open fissures and other rapid pathways like losing-streams. The configuration of this porous network and the saturation level of water offer a spectrum of pathways, ranging from slow to fast, facilitating water movement and mixing. These varied flow paths are significant for the isotopic makeup of water as it enters the saturated zone, as they contribute to the attenuation of seasonal fluctuations in precipitation (Clark and Fritz 1997, pp. 80-81). Fractionation processes give rise to variations in the isotopic composition of precipitation, and these variations can be used to identify the conditions under which groundwater recharge occurred (Mook 2000 pp. 194). By analysing the stable isotopic composition of groundwater, valuable insights can be gained regarding the source and history of the water, providing a deeper understanding of the hydrological processes within the study area.

3.3.2 Chloro-Alkaline Indices (CAI)

Schoeller (1977) introduced the chloro-alkaline indices (CAI) to mathematically elucidate the ionic exchange between groundwater and the aquifer's host rock material. This approach quantitatively analyses both the direct and reverse ion exchange processes, thereby revealing insights into groundwater chemistry (Chowdhury *et al*. 2022). CAI (I) and CAI (II) are computed using ion concentrations and the following equations (5, 6) (Schoeller 1977 pp. 10), expressed in meq/l:

$$CAI(I) = \frac{Cl-(Na+K)}{Cl} \tag{5}$$

and

$$CAI(II) = \frac{Cl-(Na+K)}{SO_4 + HCO_3 + CO_3} \tag{6}$$

The CAI (I) and CAI (II) indices hold a key to understanding the dynamics of ion exchange between groundwater and the aquifer host rock (Zaidi *et al*. 2015 pp. 606). A positive reading of these indices signifies a reverse ion exchange, denoting the interchange of (Na^+ + K^+) ions from the groundwater with (Ca^{2+} + Mg^{2+}) ions present in the aquifer material (Chowdhury *et al*. 2022 pp. 11338). On the contrary, in cases of direct ion exchange, both the CAI (I) and CAI (II) indices take on negative values, indicating the interaction of (Na^+ + K^+) cations from the aquifer material with (Ca^{2+} + Mg^{2+}) ions within the groundwater (Chowdhury *et al*. 2022 pp. 11338). When Na^+ and K^+ ions found in the groundwater engage in an exchange with Ca^{2+} and Mg^{2+} ions residing in the aquifer material, leading to a positive index, it indicates a reverse ion exchange reaction (Chowdhury *et al*. 2022).

3.4 Chloride Mass Balance Analysis

Accurate determination of groundwater recharge is essential in regional hydrogeological studies and groundwater resource assessments to facilitate water balance analyses and evaluate the potential of groundwater resources (Mensah *et al*. 2014).

Groundwater recharge can be generally defined as the downward movement of water from the unsaturated zone to the saturated zone. Recharge stands as a critical, uncertain parameter in any groundwater model calibration, holding significant influence over the accuracy and dependability of predictive groundwater models and is regarded as a major factor shaping the reliability of such models (Mensah *et al*. 2014). The scientific literature presents a variety of tracer techniques, encompassing various isotope applications to natural conservative tracers to estimate recharge rates. Chloride is one such ion and is the focus of this study.

Extensively tested and highly regarded, the chloride mass balance (CMB) methodology is one of the techniques used for estimating groundwater recharge in regional hydrogeological studies and basin-wide groundwater resource assessments (Mensah *et al*. 2014).

CMB is a widely recognized and applied technique in hydrogeology for estimating recharge to groundwater aquifers (Marei *et al*. 2010 pp. 781). The basis of the CMB technique relies on the conservative behaviour of the chloride ion, remaining largely unaffected by reactions as it moves through the unsaturated and saturated zones. This assumption, if valid, allows the ion to effectively trace groundwater recharge processes, leading to reasonable estimates of groundwater recharge (Wood and Sanford 1995 pp. 460).

Ting, Kerh, and Liao (1998) successfully used this method in the subtropical area of Taiwan to assess agricultural areas. In a more recent study, Mensah *et al*. (2014) successfully utilized the CMB method to evaluate recharge in a tropical, sedimentary basin located in Ghana. The study demonstrated that the approach performed effectively in a tropical setting, yielding accurate estimations of groundwater recharge (Mensah *et al*. 2014 pp. 7).

The Pioneering work on the development of the CMB method was conducted by Eriksson and Khunakasem (1969), who successfully applied this technique to a coastal plain in northern Israel, and since that time have been augmented by authors adjusting variables to suit conditions and account for uncertainties.

To apply the CMB method successfully, four critical assumptions must be addressed (Wood 1999 pp. 2, Marei *et al*. 2014 pp. 784). These assumptions are:

1) CMB assumes that chloride in the groundwater solely originates from precipitation and that no other sources contribute to the chloride content in groundwater. This relates the steadiness of chloride deposition rate and precipitation rate during the residence time of the groundwater being sampled, essentially assuming steady-state conditions and is considered nearly impossible to meet (Marei *et al*. 2010). In the study area, recharge is designated to occur by rainfall and ponding in upper catchment areas (Creek to Coral 2007, pp. 2). Connate water and halite may be present in coastal areas and cannot be excluded from consideration, nor is contamination from leaking swimming pools. Additional isotopic sampling and analysis would be required to

determine the origin, location, depth, and boundary conditions to quantify, and this is beyond the scope of this project.

2) CMB relies on the conservative nature of chloride in the hydrological system, implying that chloride does not undergo significant chemical reactions within the soil, rocks, and pore water. This second assumption revolves around the stability of the chloride mass flux over time, ensuring no significant changes have occurred meaning that the chloride concentration in groundwater is only from recharge by precipitation. In this study, a steady-state approach was adopted due to the disparity in time scales between hydrologic and climate systems, and the substantial uncertainty in precipitation patterns and annual amounts. The changes in the annual chloride content are influenced more by the intensity and duration of rainfall events rather than the total precipitation for the hydrological year and, therefore, variations in the amount of rainfall from one year to another have only a minor impact on the average chloride content (Marei *et al*. 2010 pp. 783). Chloride uptake by plants occurs but, on the long-term average, returns to the soil as biomass (Marei *et al*. 2010 pp. 787; Cooper *et al*. 2013 pp. 5). As such, it is assumed that nonlinear processes and feedbacks, such as daily evaporation and condensation in the unsaturated zone, are attenuated and averaged over the recharge timescale. Additional chloride, picked up during the infiltration process, can be accounted for using the chloride/bromine molar ratio (Marei *et al*. 2014 pp 787), but bromine was not included in this study.
3) The third assumption is that the rate of chloride deposition and the precipitation rate have remained consistent during the residence time of the groundwater. Enrichment of chloride by evaporation cannot be ruled out in the study area as recharge mechanisms are unclear. Rainfall in the study area is highly spatially and temporally variable, with clay soils very common. As such, intense surface pooling and runoff are also common. In this sense, the estimation of recharge using the method may be underestimated, if a significant portion of groundwater chloride originates from mineral dissolution processes (Mensah *et al*. 2014 pp. 2). For this study, it is assumed that the chloride concentrations and precipitation rates have remained consistent over time, enabling the use of current chloride measurements in precipitation as representative of the recharge conditions for the aquifer being tested. This is based on the last significant climate shift occurring around 12,000 years ago at the end of the Pleistocene (Cooper *et al*. 2013, pp.7). Because of the shallow nature of the sediments (<65 m), it is assumed that the age of local groundwaters falls within this time period and that chloride concentrations in precipitation are representative and valid for the calculation.

4) Lastly, the CMB method assumes that the measured chloride concentration in groundwater accurately represents the chloride concentration from recharge. This relates to a uniform chloride concentration in the groundwater. With few exceptions, sampled bores were located within 10km of the coast, and the majority of those <5km, and therefore it is assumed that chloride deposition is uniform over the study area.

After carefully addressing these assumptions, the CMB method provides a means to calculate the spatially averaged recharge flux to the aquifer, offering valuable insights into the groundwater recharge processes in the region (Mensah *et al*. 2014).

While numerous assumptions are involved in applying the CMB method, it is believed that they are adequately valid for providing an initial estimate for the Townsville region.

The conservative nature of chloride is assumed in this study, as is commonly done in chloride mass balance analysis, based on the premise that it behaves conservatively in groundwater systems (Marei *et al*. 2014 pp 787). While this assumption provides a practical starting point for estimating recharge rates, it is essential to recognize that deviations from conservative behaviour can occur under specific geological conditions (such as connate water) or due to the presence of contaminants. Given the lack of comprehensive testing of various geological formations in the area for chloride concentrations, this study assumes that all chloride originates from precipitation and aerosols. This assumption simplifies the analysis by focusing solely on atmospheric inputs without considering other potential sources of chloride.

Recharge can be estimated by (Wood and Sanford 1995 pp. 460; Marei *et al.* 2014 pp 787):

$$R = P \times \frac{Cl_P^-}{Cl_{gw}^-} \tag{7}$$

where *R* is recharge (mm/yr), *P* is the average rainfall (mm/year), Cl^-(*P*) is the average chloride concentration in rainfall (mg/L), and Cl^-(gw) is the average chloride concentration in groundwater (mg/L).

The average annual rainfall for the Townsville region, calculated by the Australian Bureau of Meteorology (BOM), is 1143 mm/yr. This value was chosen for *P*, considering the notable spatial-temporal variations in rainfall for the region and the variable intensity and duration of rainfall events across the coastal plain. An average chloride concentration in rainfall, Cl^-(*P*) of 2.52 mg/L was used, derived from research conducted by the CSIRO (Crosbie *et al*. 2012 pp. 5). Crosbie *et al*. (2012) highlight that rainfall in coastal areas, including Townsville, is primarily influenced by marine-origin moisture. Laboratory results for chloride concentration in groundwater, Cl^-(gw), were utilized for each sample to estimate recharge.

3.5 Water Quality

Coastal plain groundwater systems play a crucial role in supporting both human and ecological needs, serving as vital sources of freshwater in these low-lying regions. The hydrogeochemical characteristics of coastal plain groundwater are influenced by a complex interplay of factors, including geological formations, hydrological processes, and anthropogenic activities (Boyd 2000 pp. xiii; Hem 1985 pp. 10). Coastal aquifers face the dual challenges of sea-level rise and excessive groundwater extraction (An *et al*. 2023; Villholth and Conti 2018). Understanding the composition and quality of coastal plain groundwater is essential for assessing water resources, managing sustainable development, and safeguarding human and environmental health (Appelo and Postma 2005; Villholth and Conti 2018). Research has been conducted all over the world relating to groundwater quality and there are established indices and metrics. This study has focused on irrigation water quality, utilizing the residual sodium carbonate (RSC), the sodium adsorption ratio (SAR), and the Wilcox diagram (Wilcox 1955) classification.

Chemical parameters, encompassing major and minor ions, are frequently employed to determine the source and associated water quality issues in regions impacted by salinity along the coastal belt. The assessment of water quality in coastal aquifers involves various methodologies, which include hydrogeochemical techniques, geophysics, and remote sensing, with the hydrogeochemical approach being widely utilized among them (Kumar *et al*. 2014).

The evaluation process requires consideration of key parameters that significantly influence the appropriateness of water for irrigation. Salinity is probably the most widely used basic measure of the quality of water for irrigation and is commonly measured by EC and reported as micro-Siemens per centimetre (µs/cm) (Zaman *et al*. 2018 pp. 115). As excess salt in the soil solution elevates the osmotic pressure, this hinders the uptake of soil-water by plant roots (Zaman *et al*. 2018 pp. 15) and, consequently, wilting results from the loss of water through transpiration that cannot be replaced (Zaman *et al*. 2018 pp. 115).

Due to the significant presence of alkali soils across the coastal plain (Murtha 1975a, Murtha 1975b), the levels of specific cations that impact permeability, induce deflocculation, and contribute to the deterioration of soil structure in alkali soils requires examination. Specifically, the relative proportion of sodium Na^+ to Ca^{2+} and Mg^{2+} and the concentration of carbonate species as it relates to Ca^{2+} and Mg^{2+} ions, which is discussed below.

3.5.1 Residual Sodium Carbonate (RSC)

The presence of carbonate ions ($HCO_3^- + CO_3^{2-}$) in water can exert a significant influence on water quality by facilitating the precipitation of alkaline earths ($Ca^{2+} + Mg^{2+}$), consequently elevating the percentage of sodium ions (Na^+) (Eaton 1950). Increased concentrations of carbonates can combine with Na^+ ions, leading to the formation of NaHCO3, which can have adverse effects on soil structure (Hem 1985 pp 216). The concept of Residual Sodium Carbonate (RSC) is employed to assess the carbonate content of water, as described in Equation (8) (Eaton 1950):

$$RSC = [HCO_3- + (CO_3^2-/2)] – [Ca^{2+} + Mg^{2+}] \quad (8)$$

Based on the RSC values provided by Eaton (1950), water can be classified into three categories: suitable (RSC < 1.25 meq/L), marginally suitable (RSC between 1.25 and 2.50 meq/L), and unsuitable (RSC > 2.50 meq/L). Higher RSC values result in enhanced Na^+ adsorption in soil, leading to reduced soil permeability (Zaman *et al*. 2018 pp. 123).

The RSC parameter, calculated by AQQA (Rockware) software, serves as a crucial criterion for distinguishing between various water classes for irrigation purposes, as increasing RSC levels lead to the precipitation of Ca^{2+} and Mg^{2+} when water is applied to the soil.

3.5.2 Sodium Adsorption Ratio (SAR)

The suitability of groundwater for irrigation relies on the impact of mineral constituents present in the water on both plants and soil. Sodium concentration plays a crucial role in the classification of irrigation water due to its influence on soil behaviour (Zaman *et al*. 2018 pp. 117). When Na^+ ions replace Ca^{2+} and Mg^{2+} in the soil, it can lead to the deflocculation of clay particles and reduce permeability (Zaman *et al*. 2018 pp. 117). To assess the potential soil adsorption, the sodium adsorption ratio (SAR, measured in meq/L) is used. The SAR is directly related to soil adsorption, as expressed in Equation (9):

$$SAR = \frac{Na^+}{\sqrt{\frac{Ca^{2+}+Mg^{2+}}{2}}} \quad (9)$$

High SAR waters can negatively impact soil physical properties, leading to soil structure degradation and is not recommended for prolonged irrigation (Zaman *et al*. 2018 pp. 117). Continued use of water with a high SAR value results in soil structure breakdown, causing compact and hardened soil when dry and reduced water penetration when wet and soils with high clay content are especially vulnerable to this effect (Zaman *et al*. 2018 pp. 117).

When Na^+ content exceeds Ca^{2+} and Mg^{2+} proportions, the soil is termed sodic, while a predominance of calcium and magnesium cations yields a more permeable granular structure (Zaman *et al*. 2018 pp. 117). According to Halliwell *et al*. (2001, pp. 1263), the guidelines of assessing SAR values in water quality is used in conjunction with EC and classifies as ‘no problem’, ‘slight to moderate’, and ‘severe problem’ based on the measured and calculated values (table 3.5.1). SAR values were calculated by AQQA (Rockware) software.

Table 3.5.1: Classification of water quality based on SAR and EC values of water samples (modified from Halliwell et al 2002, Table 2).

SAR	EC (Ds/m)		
	No problem	Slight to moderate	Severe problem
0-3	>0.9	0.9-0.2	<0.2
3-6	>1.3	1.3-0.25	<0.25
6-12	>2.0	2.0-0.35	<0.35
12-20	>3.1	3.1-0.9	<0.9
20+	>5.6	5.6-1.8	<1.8

3.5.3 Wilcox Diagram

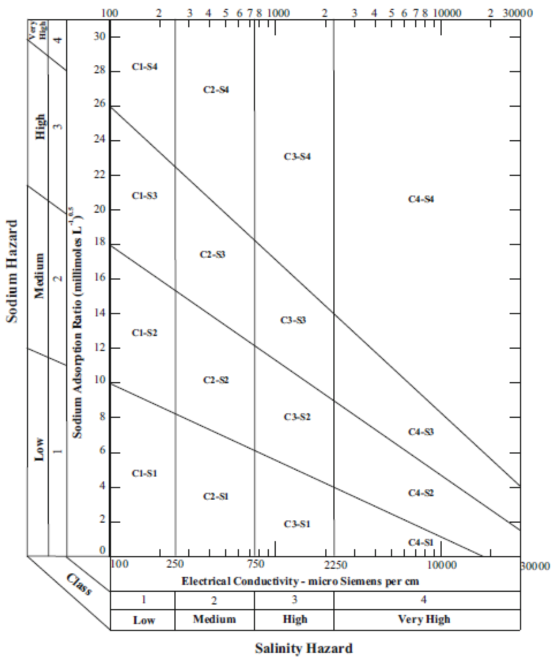

Figure 3.5.1: Wilcox and USSL diagram depicting irrigation hazard rating based on salinity (conductivity) and sodium concentrations in groundwater.

The Wilcox (1955) diagram, in conjunction with the Unites States Salinity Laboratory (USSL) (1954) is commonly utilized for irrigation waters to visualize the “sodium hazard” relationship that exists between salinity, as measured by EC, and excess sodium. The diagram (fig. 3.5.1) is divided into 16 zones based on the sodium hazard classification and is widely used to assess groundwater’s suitability for irrigation (Kumar *et al*. 2014). The semi-log scatter plot measures the salinity, using EC (in micro-mhos/cm at 25 °C), in log scale on the x-axis against SAR on the y-axis.

3.6 References – Chapter 3

An, G, Kang, H, Fu, R, Xu, D and Li, J 2023, 'Investigation on the Hydrogeochemical Characteristics and Controlling Mechanisms of Groundwater in the Coastal Aquifer', *Water*, MDPI, vol. 15(9), DOI: 10.3390/w15091710.

Ansari, AA and Umar R 2019, 'Evaluation of hydrogeochemical characteristics and groundwater quality in the quaternary aquifers of Unnao District, Uttar Pradesh, India', *HydroResearch*, vol. 1, pp. 36-47, DOI: 10.1016/j.hydres.2019.01.001.

Appelo, CAJ and Postma, D 2005, *Geochemistry, groundwater and pollution*, 2 ed., Taylor and Francis, A.A. Balkema Publishers, Great Britain.

Bartos, TT and Ogle KM 2002, 'Water Quality and Environmental Isotopic Analyses of Ground-Water Samples Collected from the Wasatch and Fort Union Formations in Areas of Coalbed Methane Development – Implications to Recharge and Ground-Water Flow, Eastern Powder River Basin, Wyoming', Water-Resources Investigations Report 02-4045, United States Geological Survey (USGS), pp. 1-96, U.S. Department of the Interior. Retrieved 06 August 2023 from <https://pubs.usgs.gov/wri/wri024045/>.

Belkhiri, L, Boudoukha, A, and Mouni, L 2011, 'A multivariate Statistical Analysis of Groundwater Chemistry Data', *International Journal of Environmental Research*, vol. 5(2), pp. 537-544, < https://www.researchgate.net/publication/236612300_A_multivariate_Statistical_Analysis_of_Groundwater_Chemistry_Data>.

Boyd, CE 2000, *Water quality: an introduction*, Kluwer Academic, Springer New York, NY, DOI: 10.1007/978-1-4615-4485-2.

Carucci, V, Petitta, M, and Aravena, R 2012 "Interaction between Shallow and Deep Aquifers in the Tivoli Plain (Central Italy) Enhanced by Groundwater Extraction: A Multi-Isotope Approach and Geochemical Modelling." *Applied Geochemistry*, vol. 27(1), pp. 266–80, DOI: 10.1016/j.apgeochem.2011.11.007.

Cary, Lise, *et al.* 2015 "Origins and Processes of Groundwater Salinization in the Urban Coastal Aquifers of Recife (Pernambuco, Brazil): A Multi-Isotope Approach", *The Science of the Total Environment*, vol. 530–531, pp. 411–29, DOI: 10.1016/j.scitotenv.2015.05.015.

Chander, KS, Kumar, An, Shashtri, S, Kumar, Al, Kumar, P, and Mallick, J 2017, 'Multivariate statistical analysis and geochemical modelling for geochemical assessment of groundwater of Delhi, India', *Journal of Geochemical Exploration*, vol. 175, pp. 59-71, DOI: 10.1016/j.gexplo.2017.01.001.

Chowdhury, P, Mukhopadhyay, BP, Nayak, S, and Bera, A 2022, 'Hydro-chemical characterization of groundwater and evaluation of health risk-assessment for fluoride contamination areas in the eastern blocks of Purulia district, India', *Environment, Development and Sustainability*, vol. 24(9), pp. 11320-11347, DOI: 10.1007/s10668-021-01911-1.

Clark, I 2015, *Groundwater Geochemistry and Isotopes*, CRC Press, Taylor and Francis Group, 428 p., DOI: 10.1201/b18347.

Clark, ID and Fritz, P 1997, *Environmental Isotopes in Hydrogeology*, CRC Press, Taylor & Francis Group, 328 p., ISBN 1-56670-249-6.

Cooper, CA, Hershey, RL, Healey, JM, and Lyles, BF 2013, 'Estimation of Groundwater Recharge at Pahute Mesa using the Chloride Mass-Balance Method', Publication No. 45251, National Nuclear Security Administration, US Department of Energy, Las Vegas, Nevada.

Creek to Coral 2007, *A Summary Review of Groundwater Research and Knowledge for the Black River and Ross River Basins*, Townsville City Council – Creek to Coral, Townsville. Retrieved from <http://www.creektocoral.org/draftwqip/backround/CCIbackground/>.

Crosbie, R, Morrow, D, Cresswell, R, Leaney, F, Lamontagne, S, and Lefournour, M, 2012, 'New insights to the chemical and isotopic composition of rainfall across Australia', CSIRO Water for a Healthy Country Flagship, Australia, CSIRO:EP125581, DOI: 10.5072/83/5849a0d6c685a.

Eaton, FM 1950, 'Significance of carbonates in irrigation waters', Soil Science, *69*(2), pp. 123–134, DOI: 10.1097/00010694-195002000-00004.

Eriksson, E and Khunakasem, V 1969, Chloride Concentration in Groundwater, Recharge Rate and Rate of Deposition of Chloride in the Israel Coastal Plain. Journal of Hydrology, vol. 7(2), pp. 178-197, DOI: 10.1016/0022-1694(69)90055-9.

Farnham, IM, Singh, AK, Stetzenbach, KJ and Johannesson, KH 2002, 'Treatment of nondetects in multivariate analysis of groundwater geochemistry data', *Chemometrics and Intelligent Laboratory Systems*, vol. 60(1-2), DOI: 10.1016/S0169-7439(01)00201-5.

Freeze, RA, and Cheery, JA 1979, Groundwater: Englewood Cliffs, NJ, Prentice-Hall, pp. 604.

Gibbs, RJ 1970 'Mechanisms Controlling World Water Chemistry.', *Science*, vol. 170, no. 3962, pp. 1088–90, https://doi.org/10.1126/science.170.3962.1088.

Gosselin, DC, Harvey, FE, and Frost, CD 2001, 'Geochemical Evolution of Ground Water in the Great Plains (Dakota) Aquifer of Nebraska: Implications for the Management of a Regional Aquifer System', Groundwater, vol. 39(1), pp. 98-108. DOI: 10.1111/j.1745-6584.2001.tb00355.x.

Güler, C, Thyne, GD, McCray, JE, and Turner, KA 2002, 'Evaluation of graphical and multivariate statistical methods for classification of water chemistry data', *Hydrogeology Journal*, vol. 10, pp. 455–474, DOI: 10.1007/s10040-002-0196-6.

Güler, C, Kurt, MA, Alpaslan, M, and Akbulut, C 2012, 'Assessment of the impact of anthropogenic activities on the groundwater hydrology and chemistry in Tarsus coastal plain (Mersin, SE Turkey) using fuzzy clustering, multivariate statistics and GIS techniques', *Journal of Hydrology*, vol. 414, pp. 435-451, DOI: 10.1016/j.jhydrol.2011.11.021.

Halliwell, DJ, Barlow, KM and Nash, DM 2001, 'A review of the effects of wastewater sodium on soil physical properties and their implications for irrigation systems', *Australian Journal of Soil Research*, vol. 39, pp. 1259-1267, DOI: 10.1071/SR00047.

Hem JD 1985, Study and Interpretation of Chemical Characteristics of Natural Water, 3 ed., U.S. Geological Survey (USGS) Water-Supply Paper 2254, Department of the Interior, United States Geological Survey.

Kaiser, HF 1960 'The Application of Electronic Computers to Factor Analysis', *Educational and Psychological Measurement*, vol. 20(1), pp. 141-151, DOI: 10.1177/001316446002000116.

Kumar, PJS, Elango, E, and James, EJ 2014, 'Assessment of hydrochemistry and groundwater quality in the coastal area of South Chennai, India', *Arabian Journal of Geosciences*, 7, pp. 2641-2653, DOI: 10.1007/s12517-013-0940-3.

Li, P, He, Xiaodong, and Guo, W 2019, 'Spatial groundwater quality and potential health risks due to nitrate ingestion through drinking water: A case study in Yan'an City on the Loess Plateau of northwest China', *Human and Ecological Risk Assessment: An International Journal*, vol. 25(1-2), pp. 11-31, DOI: 10.1080/10807039.2018.1553612.

Liu, J, Fu, G, Song, X, Charles, SP, Zhang, Y, Han, D, and Wang, S 2010, 'Stable Isotopic Compositions in Australian Precipitation", Journal of Geophysical Research, vol. 115(D23), 2010, DOI: 10.1029/2010JD014403.

Marei, A, Khayat, S, Weise, S, Ghannam, S, Sbaih, M, and Geyer, S 2010, 'Estimating groundwater recharge using the chloride mass-balance method in the West Bank, Palestine', *Hydrological Sciences Journal*, vol. 55(5), pp. 780-791, DOI: 10.1080/02626667.2010.491987.

Mazor, E 2004, *Chemical and Isotopic Groundwater Hydrology*, 3 ed., Marcel Dekker Inc., Halsted Press (John Wiley & Sons), United States of America, ISBN: 0-8247-4704-6.

Menció, A and Mas-Pla, J 2008, 'Assessment by multivariate analysis of groundwater-surface water interactions in urbanized Mediterranean streams', *Journal of Hydrology*, Elsevier, vol. 352, pp. 355-356, DOI: 10.1016/j.jhydrol.2008.01.014.

Mensah, FO, Alo, C, and Yidana, SM 2014, 'Evaluation of Groundwater Recharge Estimates in a Partially Metamorphosed Sedimentary Basin in a Tropical Environment: Application of Natural Tracers', *The Scientific World Journal*, Article ID 419508, DOI: doi.org/10.1155/2014/419508.

Mook, WG 2006, *Introduction to Isotope Hydrology: Stable and Radioactive Isotopes of Hydrogen, Oxygen and Carbon*, International Association of Hydrogeologists, Taylor & Francis/Balkema, Great Britain, ISBN 100-415-38197-5.

Munksgaard, NC, Wurster, CM, Bird, MI 2011, 'Continuous analysis of δ18O and δ18D values of water by diffusion sampling cavity ring-down spectrometry: a novel sampling device for unattended field monitoring of precipitation, ground and surface waters', *Rapid Communications in Mass Spectrometry*, vol. 25, pp. 3706-3712, DOI:10.1002/rcm.5282.

Murtha, GG 1975a, 'Soils and Land Use on the Northern Section of the Townsville Coastal Plain, North Queensland', Soils and Land Use Series No. 55, CSIRO, viewed 15 April 2019, <https://publications.qld.gov.au/sl/dataset/soil-townsville-zed/resource/8b49d47d-889e-4632-9cd0-4f68d4c4652b>.

Murtha, GG 1975b, 'Soils and Land Use on the Southern Section of the Townsville Coastal Plain, North Queensland', Soils and Land Use Series No. 55, CSIRO, viewed 15 April 2019, <https://publications.qld.gov.au/sl/dataset/soil-townsville-zed/resource/963b3843-d6db-4866-b1a5-868639986754>.

Piper, AM 1944 '*A Graphical Procedure in the Geochemical Interpretation of Water Analysis*', U S Geological Survey (USGS), Groundwater Note 12. DOI: 10.1029/TR025i006p00914.

Schoeller, H 1977, Geochemistry of Groundwater. In: Groundwater Studies—An International Guide for Research and Practice, UNESCO, Paris, Ch. 15, pp.1-18.

Singh, CH, Kumar, An, Shashtri, S, Kumar, Al, Kumar, P, and Mallick, J 2017, 'Multivariate statistical analysis and geochemical modelling for geochemical assessment of groundwater of Delhi, India', *Journal of Geochemical Exploration*, Elsevier, vol. 175, pp. 59-71, DOI: 10.1016/j.gexplo.2017.01.001.

***The State of Queensland 2019, Queensland Spatial Catalogue – Qspatial, Department of Natural Resources, Mines and Energy, viewed 05 May 2019, <http://qldspatial.information.qld.gov.au/catalogue/custom/index.page>.

Ting, CS, Kerh, T, and Liao, CJ 1998, 'Estimation of groundwater recharge using the chloride mass-balance method, Pingtung Plain, Taiwan', *Hydrogeology Journal*, vol. 6, no. 2, pp. 282-292, DOI: 10.1007/s100400050151.

USSL Salinity Laboratory (1954) Diagnosis and Improvement of Saline and Alkaline Soils. US Department of Agriculture Handbook, No. 60, 160 p.

Villholth, KG and Conti, KI 2018, 'Groundwater governance: rationale, definition, current state and heuristic framework', in Villholth, López, Gunn, Conti, Garrido & van der Gun (eds), *Advances in Groundwater Governance*, CRC Press, Taylor & Francis Group, pp. 3-31. Available from www.un-igrac.org

Werner, AD 2010, 'A review of seawater intrusion and its management in Australia', Hydrogeology Journal, vol. 18(1), viewed 15 February 2018, DOI: 10.1007/s10040-009-0465-8.

Wilcox, LV 1955, 'Irrigation Waters', United States Salinity Laboratory, circular no. 969, United States Department of Agriculture, retrieved 01 July 2023 from <https://www.ars.usda.gov/arsuserfiles/20360500/pdf_pubs/P0192.pdf>.

Wood, WW 1999, 'Use and misuse of the chloride-mass balance method in estimating ground water recharge', *Ground Water*, Vol. 37(1), National Ground Water Association, pp. 1-2, DOI: 10.1111/j.1745-6584.1999.tb00949.x.

Wood, WW and Sanford, WE 1995, 'Chemical and isotopic methods for quantifying ground-water recharge in a regional, semiarid environment', *Ground Water*, Vol. 33(3), National Ground Water Association, pp. 458-468, DOI: 10.1111/j.1745-6584.1995.tb00302.x.

Zaman, M, Shahid, SA, and Heng, L 2018 'Irrigation Water Quality', In: Guideline for Salinity Assessment, Mitigation and Adaptation Using Nuclear and Related Techniques, Springer, Cham, DOI: 10.1007/978-3-319-96190-3_5.

Zaidi, FK, Nazzal Y, Jafri, MK, Naeem, M, and Ahmed, I 2015 "Reverse Ion Exchange as a Major Process Controlling the Groundwater Chemistry in an Arid Environment: A Case Study from Northwestern Saudi Arabia", *Environmental Monitoring and Assessment*, vol. 187(10), pp. 607–618, DOI: 10.1007/s10661-015-4828-4.

THIS PAGE INTENTIONALLY LEFT BLANK

Chapter 4: Hydrochemistry and Multivariate Analysis

4.1 Introduction

The HCA results presented here serve as the basis for subsequent analyses; these include the PCA analysis, Piper diagram, bivariate plots, CAI, ion ratios, Gibbs diagram, stable water isotopes, CMB, and water quality assessment. Water groupings, the products of HCA, play a central role in organizing and interpreting results across the different analyses, including the PCA analysis, hydrogeochemical assessments, and water quality assessments. These groups help identify samples closely related in hydrogeological context, providing a perspective on aquifer affiliations and hydrogeochemical characteristics. The approach ensures a systematic exploration of regional groundwater dynamics, supporting practical applications in sustainable groundwater management.

4.2 Hierarchical Clustering Analysis (HCA) Results

Using data from 86 analyses, HCA was conducted using the variables of Ca^{2+}, Mg^{2+}, Na^{+}, K^{+}, $CaCO_3$, Cl^{-}, and SO_4^{2-}, and EC, and employed the Ward's linkage method. The Kaiser–Meyer–Olkin (KMO) for this study is 0.781 and falls well within the 'satisfactory' category. As detailed in Chapter 3 (section 3.2), in the preliminary stages of factor analysis, it is crucial to evaluate the sampling adequacy and the KMO measure serves this purpose, assessing whether the responses from the sample are adequate (Güler *et al*. 2012). According to Kaiser (1960), a KMO value around 0.5 is minimally acceptable, while values between 0.7 and 0.8 are considered satisfactory, and those above 0.9 are excellent. This analysis yielded the identification of four prominent clusters depicted in a dendrogram (fig. 4.2.1), with each cluster further subdivided into 'A' and 'B' subgroups. The 'A' subgroups are indicative of lower salinity levels, whereas the 'B' subgroups reflect higher salinity conditions. Stiff diagrams have been employed to visually represent the average hydrochemistry of the subgroups for visual reference (fig. 4.2.1). Detailed average ionic concentrations for each of these groups and subgroups are provided in Table 4.2.1 and discussed below.

The hydro-chemical distinctions among the water groups delineated by HCA reveal clear hydrogeochemical patterns. The HCA method categorized the dataset into four primary water groups.

Group 1, symbolizing the least saline composition overall, represents freshwater characteristics. In this context, Group 1A shows the lowest average EC at 201 µs/cm, with a gradual increase noted across subsequent groups. With an average EC of 1246 µs/cm, Group 2 displays a significant increase in salinity compared to Group 1. Differentiating the major ion chemistry between Group 1 subgroups, Group 1B shows significantly higher concentrations of $CaCO_3$, Ca^{2+}, Mg^{2+}, and moderately more Cl^{-}. Group 1A is considered limited geographically, as it encompasses only two samples; one sample is located along the coastal area north of Townsville (Bushland Beach), and the other around 25 km inland near Woodstock.

Table 4.2.1: Average hydrogeochemical results of Water Groups 1-4 (bold) and sub-groups; major ions and **$CaCO_3$** ***are in mg/L, temperature (T) in Celsius (C), electrical conductivity (EC) in µS/cm.***

Group	Sub-Group	n	CaCO3	SO4	Cl	Ca	Mg	K	Na	Ph	T.C	EC
1	A	2	24	11	32	2	2	2	31	6.2	27.5	201
	B	12	116	11	51	23	10	1	48	6.7	28.0	432
	Avg.	19	***70***	***11***	***42***	***13***	***6***	***1***	***39***	***6.5***	***27.7***	***316***
2	A	19	257	6	167	50	22	0	126	7.0	28.5	968
	B	20	326	15	329	97	50	0	145	6.8	28.5	1524
	Avg.	39	***292***	***11***	***248***	***74***	***36***	***0***	***136***	***6.9***	***28.5***	***1246***
3	A	10	129	49	303	25	17	6	204	6.7	28.1	1202
	B	9	343	153	480	24	26	11	445	6.9	28.2	2224
	Avg.	19	***236***	***101***	***391***	***24***	***21***	***8***	***325***	***6.8***	***28.1***	***1713***
4	A	5	509	50	787	119	184	0	439	7.1	29.0	2854
	B	9	405	175	1709	214	111	6	953	6.8	28.6	5019
	Avg.	14	***457***	***112***	***1248***	***166***	***147***	***3***	***696***	***6.9***	***28.8***	***3936***

While these two samples are unique yet sufficiently similar for HCA grouping, they might be considered as outliers. Consequently, Group 1 signatures capture the freshest water composition in the dataset and these samples were retained as part of the grouping.

Group 2, exhibiting an average EC of 1245 µs/cm, has a fourfold increase in average salinity compared to Group 1. Notable variations between Group 2A and 2B are evident in SO_4^{2-}, Ca^{2+}, and Mg^{2+} concentrations, with Group 2B characterized by double the concentrations of these elements compared to Group 2A. Similar patterns extend to the Cl^- concentrations in Group 2B, and the Na^+ concentration shows a minor increase from an average of 126 mg/L in Group 2A to 145 mg/L in Group 2B.

Group 3A and 3B are generally similar to Group 1 and 2, with slight variations in concentration. The EC for Group 3A and 3B is 1202 µs/cm and 2224 µs/cm, respectively, and averages 1712 µs/cm. In Group 3B, the SO_4^{2-} concentration is significantly higher at 153 mg/L, a threefold increase compared to Group 3A; this is more closely affiliated with Group 2 and Group 4 waters. Unlike in Groups 1, 2, and 4, the Cl^- concentration shift between the ‘A’ and ‘B’ subgroups within Group 3 is less pronounced.

A twofold difference in Na^+ concentration distinguishes Group 3B from 3A, a commonality shared with Group 4 waters. Ca^{2+} remains generally unchanged between subgroup A and B

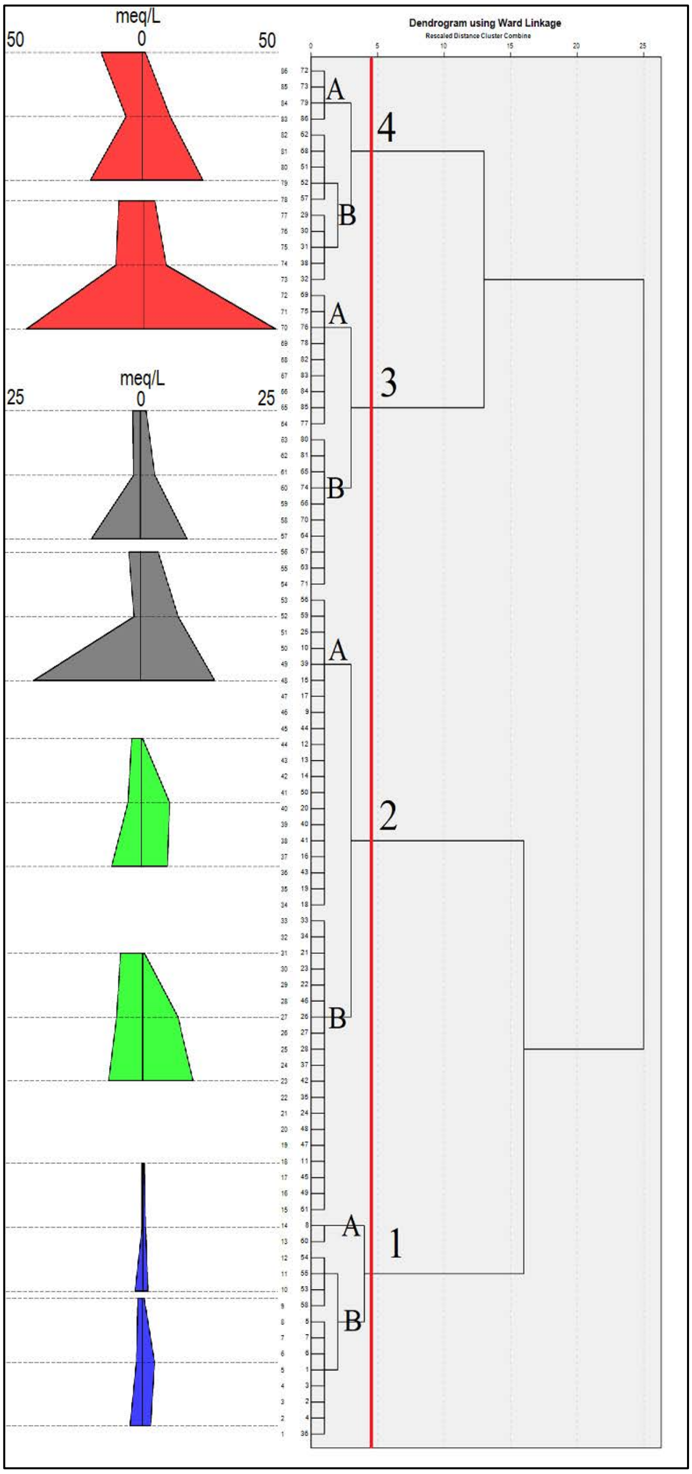

Figure 4.2.1: Dendrogram of HCA results showing classification of groundwater samples into 4 Water Groups, each with subcategory A and B; subgroup A being the freshest within each Water Group. Stiff diagrams at left visualize average hydrochemistry of each subgroup; Water Groups 1-3 are scaled at 25 meq/L, while Water Group 4 is scaled at 50 meq/L.

in Group 3, while Mg^{2+} is much higher in Group A, nearly double from 17 mg/L to 26 mg/L, respectively.

The EC for Group 4 A and B is 2854 µs/cm and 5019 µs/cm, respectively, with an average of 3936 µs/cm. In Group 4 waters, subgroup B demonstrates notably higher Ca^{2+} concentrations compared to subgroup A, averaging 214 mg/L versus 119 mg/L, respectively, and a considerably lower Mg^{2+} concentration. Group 4A and B exhibit Mg^{2+} concentrations of 184 mg/L and 111 mg/L, respectively, marking the sole subgrouping with a decrease in average Mg^{2+} concentration.

Group 4 waters also display higher average $CaCO_3$ concentrations than other subgroups, from 509 mg/L to 405 mg/L for A and B subgroups, respectively, corresponding with lower Mg^{2+} concentrations. Substantially different Na^+ and Cl^- concentrations are evident between Group 4A and Group 4B. Average Na^+ concentrations of Group 4A and B subgroups measure 439 mg/L and 953 mg/L, respectively, while average Cl^- concentrations show 787 mg/L and 1709 mg/L, again respectively. Group 4 features the highest average Cl^- concentration (1248 mg/L), nearly three times higher than the second-highest, Group 3 waters, with an average Cl^- concentration of 391 mg/L.

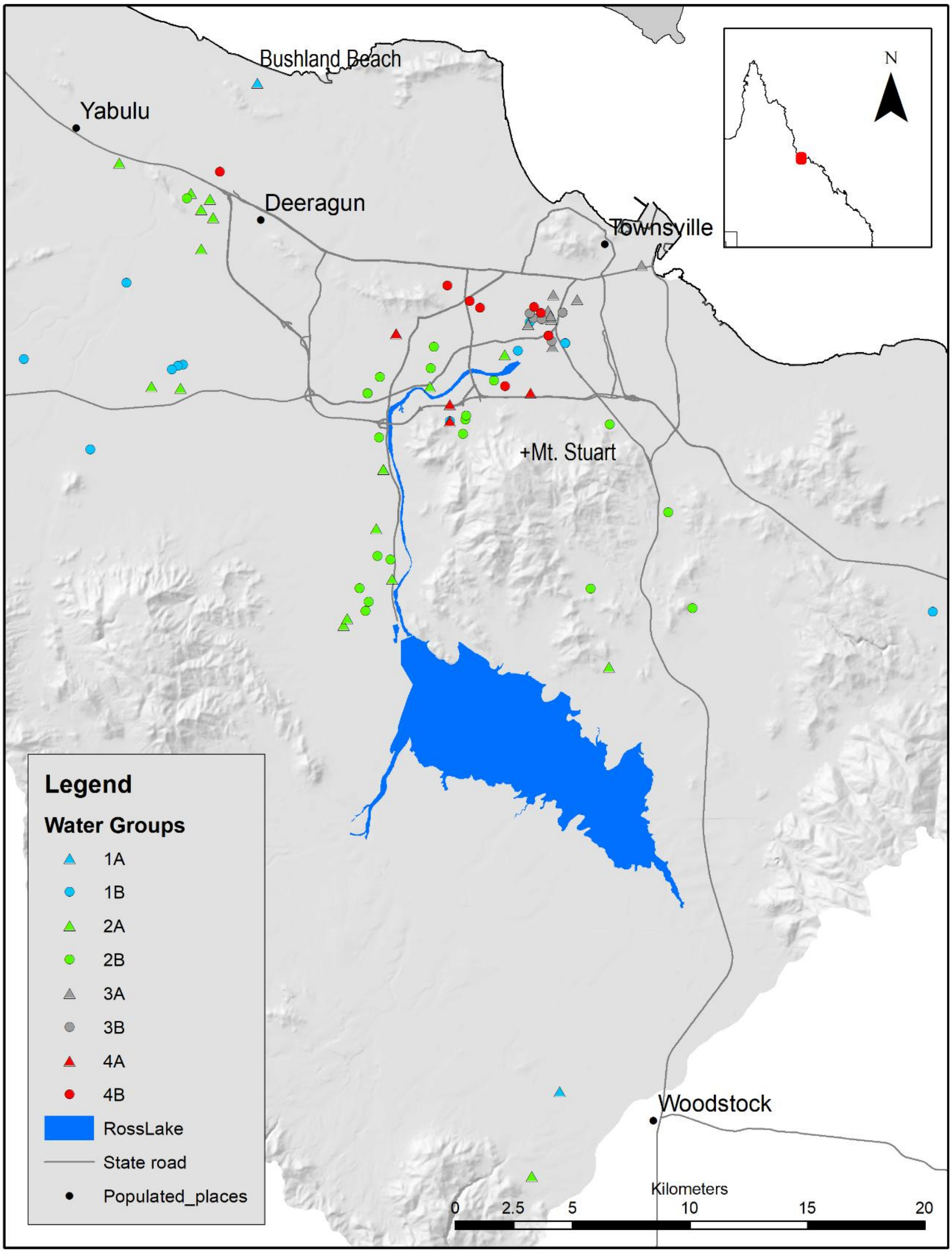

Figure 4.2.2: Regional map of study area displaying water group classification from HCA clustering. Water group 1A samples (blue triangle), the freshest groundwaters, are located near Woodstock, in the upper catchment of Ross Basin, and near Bushland Beach, on the coast north of Townsville.

Figure 4.2.2 displays the spatial distribution of the water groups determined by HCA analysis. Group 1A (n=2) are located in the upper reaches of the upper Ross Basin catchment near Woodstock, and near Bushland Beach, north of Townsville on the coast. Group 1A waters represent the freshest waters. In the upper reaches near Woodstock, this groundwater is sourced from local precipitation that has reached the water table as recharge. The sample near Bushland Beach is in very close proximity to the coast and by having the freshest signature implies that the hydraulic gradient at this location is sufficient to avert any seawater intrusion. On the west side of Mount Stuart, the samples near the Ross River generally shows only Group 2 until the end of the Ross River into the estuary. There are a few exceptions to this, with Group 4 on the northern side of Mount Stuart, which include the suburbs of Annandale and Douglas. These suburbs are characterized by the highest Ca^{2+} and Mg^{2+} concentrations in the TCP. Group 3 is generally found near the end of the Ross River in estuarine areas.

In conclusion, the HCA analysis of hydro-chemical data has revealed distinct hydrogeochemical patterns within the identified water groups. Four primary groups, each further divided into 'A' and 'B' subgroups, exhibit varying levels of salinity and chemical compositions. Group 1 represents the freshest water composition, averaging 316 μs/cm, while subsequent groups show increasing EC, with Group 2 and 3 averaging 1246 μs/cm and 1713 μs/cm, respectively, and distinct variations in major ion concentrations. Notably, Group 4 demonstrates the highest salinity, with an average of 3936 μs/cm, and significant shifts in major ion concentrations between subgroups.

4.3 Principal Component Analysis (PCA) Results

The PCA analysis considered eight common hydro-chemical variables across all samples. The correlation matrix, derived from these eight variables for PCA and HCA analysis (table 4.3.1) reveals significant (r > 0.70) (bold) and moderate (r2 = >0.60) hydro-chemical relationships

Concentrations of $CaCO_3$ shows strong correlation with concentrations of Mg^{2+} (r^2 = 0.79) and EC (r^2 = 0.74), and moderate correlation with concentrations of Ca (r^2 = 0.69) and Na^+ (r^2 = 0.63). Concentrations of SO_4^{2-} exhibits strong correlations with concentrations of K (r^2 = 0.72) and Na^+ (r^2 = 0.70). Concentrations of Cl^- shows substantial correlations with concentrations of Mg (r^2 = 0.78), concentrations of Na^+ (r^2 = 0.92), and EC (r^2 = 0.97), though is moderately correlated to concentrations of Ca^{2+} (r^2 = 0.62). Concentrations of Ca^{2+} are most strongly correlated with concentrations of Mg^{2+} (r^2 = 0.83) and moderately to EC (r^2 = 0.67). Concentrations of Mg^{2+} shows the strongest correlation with concentrations of Ca^{2+} (r^2 = 0.83) and EC (r^2 = 0.84), followed by CaCO3 (r^2 = 0.79) and Cl^- (r^2 = 0.78). Interestingly, K^+ shows only one correlation, a strong positive correlation with SO_4^{2-} (r^2 = 0.72). Concentrations of Na^+ are highly correlated to concentrations of Cl^- (r^2 = 0.92) and EC (r^2 = 0.93), but still strong to moderately correlated with concentrations of SO_4^{2-} (r^2 = 0.70), Mg^{2+} (r^2 = 0.65), $CaCO_3$ (r^2 = 0.63). Conspicuously, EC does not show a correlation with concentrations of K^+.

Table 4.3.1: Correlation matrix of variables selected for PCA and HCA analysis, highlighting several relevant (r = >0.70) relationships (underlined values). EC and magnesium concentration are strongly correlated to concentration*s of $CaCO_3$*, with Ca^{2+} concentrations near the cut-off. Concentrations of* SO_4^{2-} *show high correlation with concentrations of K and Na, while Cl concentrations show strong relationships with concentrations of Mg, Na, and EC. Concentrations of Ca and Mg share a strong correlation as does Mg concentrations with EC and Na concentration.

	CaCO3	SO4	Cl	Ca	Mg	K	Na	EC
CaCO3	1							
SO4	0.273	1						
Cl	0.59	0.582	1					
Ca	0.687	0.049	0.619	1				
Mg	***0.786***	0.308	**0.779**	**0.832**	1			
K	-0.077	**0.718**	0.381	-0.273	-0.004	1		
Na	0.632	**0.703**	**0.916**	0.446	0.646	0.494	1	
EC	**0.737**	0.596	**0.966**	0.672	**0.837**	0.348	**0.931**	1

Examining these correlations between ions suggests certain common minerals are influencing the composition of the water. Examples include limestone (calcite, or $CaCO_3$), dolomite

Table 4.3.2: Results of principal component (PC) analysis (PCA) showing two PCs with Eigenvalues greater than 1.0 and comprising 88.0% of variance explained.

PC	Initial Eigenvalues			Rotation Sums of Squared Loadings		
	Total	% of Variance	Cumulative %	Total	% of Variance	Cumulative %
1	5.08	63.477	63.477	4.26	53.275	53.275
2	1.96	24.482	87.958	2.78	34.684	87.958
3	0.37	4.625	92.584			
4	0.24	3.037	95.621			
5	0.19	2.446	98.067			
6	0.11	1.441	99.508			
7	0.02	0.355	99.864			
8	0.01	0.136	100			

($Ca:MgHCO_3$), and magnesite ($MgCO_3$), which could result in the correlations between the associated ions. Other correlations are more obscure, such as the correlation between potassium and sulphate ($r^2 = 0.72$). Rare evaporative minerals, like arcanite (K_2SO_4), are known to occur in natural brines and playa environments (Wells 1923 pp. 2), but it may also be that these correlations are a result of the occurrence of different minerals (e.g. K-feldspar and sulfate bearing minerals).

Table 4.3.3: Rotated component loadings for PCA analysis. PC1 factors are concentrations of Mg, Ca, and CaCO3, and EC. PC2 factors are concentrations of K and SO_4^{2-}. Na is slightly more associated with PC2, while Cl is loading more on PC1.

	PC 1	PC 2
Mg	**0.937**	0.126
Ca	**0.919**	-0.172
CaCO3	**0.866**	-
EC	**0.837**	0.527
Cl	0.767	0.562
K	-0.167	**0.928**
SO4	0.197	**0.887**
Na	0.659	0.695

A summary of the PCA results including loadings, eigenvalues, and variance explained by each principal components (PC), and cumulative variance, is presented in Table 4.3.2.

The results of the PCA analysis indicate two principal components with Eigenvalues greater than 1, comprising a total variance of 88.0%, with the first and second principal component (PC1 and PC2) each explaining 53.3% and 34.7% respectively.

Two PCs were derived and subjected to a varimax normalization for rotation, following the methods of Kaiser (1960) (Menció and Mas-Pla 2008 pp. 362, Belkhiri, Boudoukha, and Mouni 2011 pp. 542). This rotation aimed to enhance the separation of original variables within each principal component (Menció and Mas-Pla 2008 pp. 362). The outcomes of this rotation are summarized in Table 4.3.3, which presents the postrotation PC loading results. Notably, the most significant loadings that underscore the involvement of each chemical component in the respective PC have been emphasized (bold).

The principal component analysis yielded PC1 with a substantial variance contribution rate of 53.3%. PC1 is mainly influenced by concentrations of Mg^{2+} (0.94), Ca^{2+} (0.92), and $CaCO_3$ (0.87), and EC (0.84), as displayed in Table 4.3.3. Although concentrations of Cl^- and Na^+ exhibit comparatively lower loadings of 0.77 and 0.66 respectively, they still contribute to the component. In PC2, accounting for 34.7% of the variance, concentrations of K^+ (0.93) and SO_4^{2-} (0.89) exhibit the highest loadings, accompanied by concentrations of Na^+ (0.70), and Cl^- (0.56), and EC (0.53) to a lesser extent. However, $CaCO_3$ concentration's loading for PC2 is <0.10, rendering it insignificant and therefore excluded. The rotated loadings for PC1 highlight concentrations of Mg^{2+} and Ca^{2+} as the principal ionic species influencing groundwater chemistry. These two variables may be the result of separate or related processes. This implies that alkalinity (as $CaCO_3$) and, to a larger extent, EC, are primarily influenced by concentrations of Mg^{2+} and Ca^{2+}. While concentrations of Na^+ and Cl^- still play a role in PC1, their significance is overshadowed by concentrations of Mg^{2+} and Ca^{2+}. PC1 does not involve concentrations of K^+ (-0.17) and SO_4^{2-} (0.20), highlighting a clear distinction between the processes impacting groundwater chemistry. PC2, on the other hand, identifies concentrations of K^+ and SO_4^{2-} as primary ions influencing the hydrogeochemistry. Concentrations of Mg^{2+} and Ca^{2+} have minimal association with PC2, indicated by their loadings of 0.13 and -0.17, respectively. The EC loadings for PC1 and PC2 stand at 0.84 and 0.53, respectively, signifying that while EC is significantly influenced by PC1 processes, PC2 processes are also contributing to EC.

These established connections are visually represented in figure 4.3.1, which displays PC1 factor scores along the x-axis and PC2 along the y-axis. Notably, concentrations of Ca^{2+}, Mg^{2+}, and $CaCO_3$ predominantly cluster around the PC1 axis, indicating their primary influence on PC1. In contrast, concentrations of K^+ and SO_4^{2-}, the key ions of PC2, are positioned towards the upper part of the graph, straddling the y-axis. Notably, SO_4^{2-} concentration resides on the positive side of PC1, while K^+ rests on the negative side. The difference in the position of these points in relation to the y-axis is noteworthy because large variations in PC1 do not effectively result in significant change in PC2 (Helena *et al*. 2000 pp. 814).

Concentrations of Na^+ and Cl^-, and EC plot well in-between the PCs, denoting that these contribute to the variance of both principal components. This signifies that these are involved in the underlying processes controlling the fundamental processes governing both PC1 and PC2.

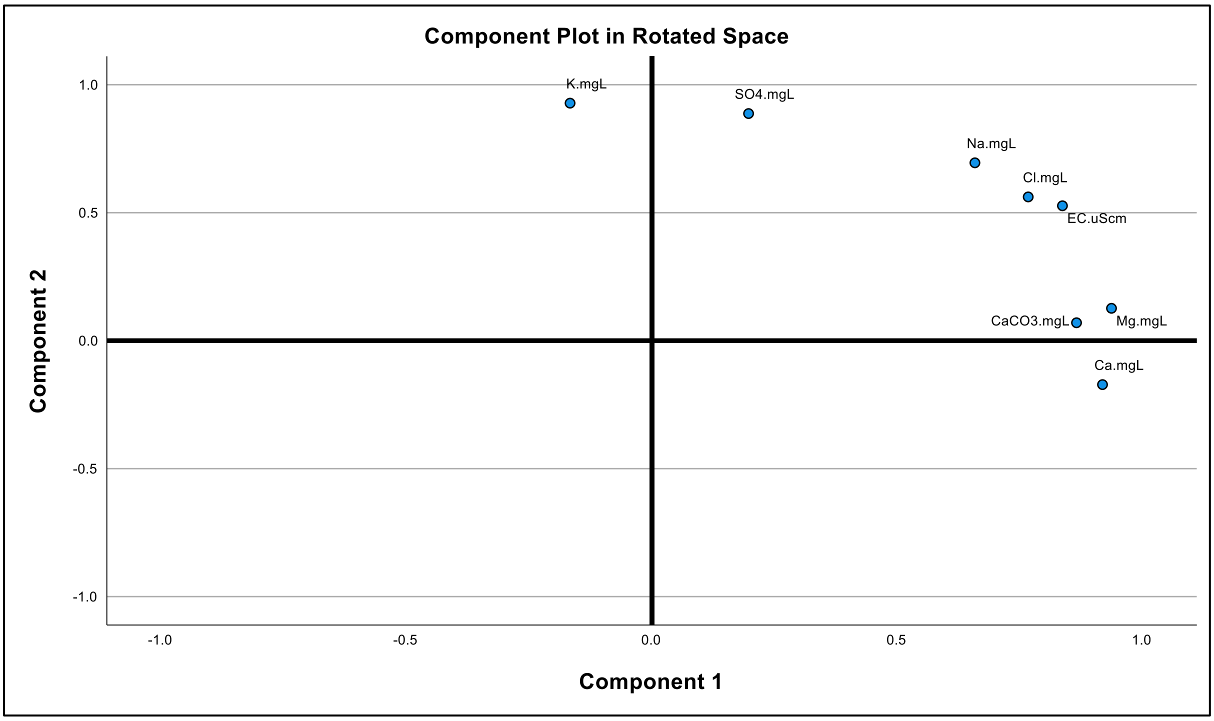

Figure 4.3.1: Graph displaying component plot of PC1 (component 1) and PC2 (component 2) factor loadings. Ca^{2+}, Mg^{2+}, and $CaCO_3$ are primarily located near the PC1 axis, signifying the primary effects on PC1. The main ions of PC2, K^+ and SO_4^{2-}, are located near the top of the graph, straddling the y-axis. SO_4^{2-} is in the positive side of PC1 while K^+ is located on the negative side. Na^+, Cl^-, and EC plot well in-between the PCs, signifying that these contribute to the variance of both PCs and that these are involved in the underlying processes controlling the respective PC.

The integration of sample factor scores from the PCA analysis with the water groups established through HCA (fig. 4.3.2) shows further insights. This is best depicted in figure 4.3.2, where PC1 is plotted along the x-axis and PC2 along the y-axis, revealing distinct divisions among the water groups.

The location of Group 1 waters in relation to PC1 is noteworthy. These waters predominantly reside within the negative PC1 realm, signifying a limited influence of PC1. This trend is understandable for Group 1A waters, which are the freshest samples in the study with the lowest EC values. They are positioned far to the left (blue triangle), representing PC1's most negative zone. Among Group 1A waters, a noticeable variance in PC2 (concentrations of K^+ and SO_4^{2-}) can be observed, with one sample plotting above and the other below the PC1 axis; the Group 1A sample with a positive PC2 score originates from Bushland Beach, a coastal suburb north of Townsville. Conversely, the counterpart with a negative PC2 score comes from Woodstock, a rural area about 25km inland.

Within Group 2A waters, a distinct trend toward the negative end of PC2 is evident, implying that concentrations of K^+ and SO_4^{2-} have limited significance in affecting the water chemistry.

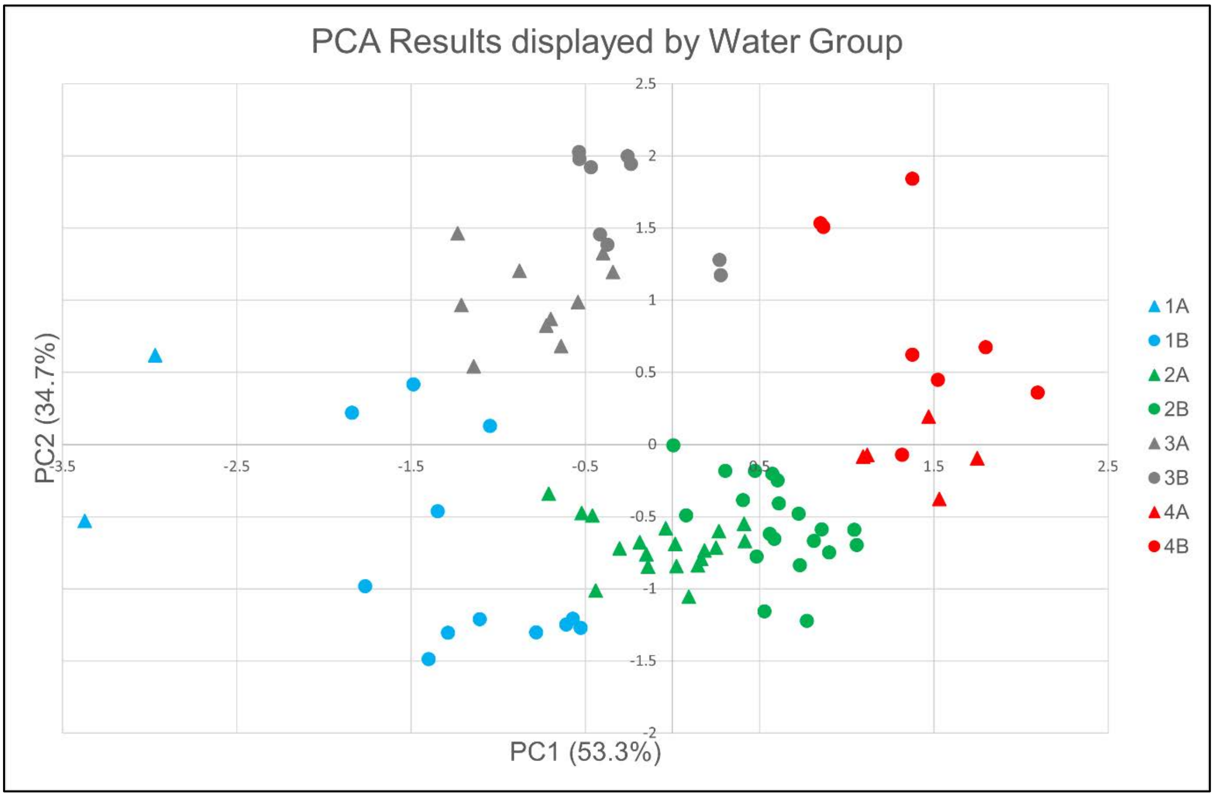

Figure 4.3.2: Plot of sample factor scores calculated during PCA analysis displayed by water group. PC1 is the x-axis and PC2 is represented on the y-axis. Clear distinctions can be seen between the HCA determined water groups.

Furthermore, Group 2A is clearly differentiated from Group 2B, which constitutes the more saline samples within Group 2.

While Group 2A spans the positive and negative spectrum of PC1, indicating a mixed impact of Ca^{2+} and Mg^{2+}, Group 2B is situated exclusively on the positive side of PC1, revealing the prominent role of Ca^{2+}, Mg^{2+}, and essentially $CaCO_3$, in influencing the chemistry of this group.

Group 3 waters are predominantly leveraged by concentrations of K^+ and SO_4^{2-}, as is evident from their positioning mainly on the negative side of PC1. The distinction between Group 3A and 3B waters lies in the impact of PC1. Notably, Group 3B shows a few samples affected by PC1, indicating the potential influence of Ca^{2+} and Mg^{2+} in Group 3B aquifers.

In the case of Group 4 waters, a clear interplay between PC1 and PC2 factors is visible, with a distinct separation along the y-axis. This is evident from the positioning of Group 4A mainly around or below the x-axis, highlighting the limited role of K^+ and SO_4^{2-} in the less saline waters within this subset. Conversely, Group 4B, with the most saline samples, clusters within the positive domains of both PC1 and PC2. An exception within this group is a sample from Vincent, a centrally located suburb within the study area.

4.4 Hydrogeochemical Results

Hydrogeochemistry is shaped by interactions between rock and water, as well as various chemical processes within the area, which is depicted in the hydrogeochemical results of the groundwater samples (n=86) (table 4.4.1).

Table 4.4.1: Summary statistics of hydrogeochemical results of groundwater samples (n=86) in the TCP.

	Na	K	Ca	Mg	CaCO3	Cl	SO4	Ph	T	EC
	mg/L	mg/L	mg/L	mg/L	meq/L	mg/L	mg/L	-	C	µs/cm
Min	17	0	0	0	0	18	0	5.5	26.1	137
Max	1460	29	461	542	13	2670	476	7.5	29.9	7060
Median	160	1	52	25	5	281	20	6.8	28.4	1349
Average	265	3	72	45	5	431	50	6.8	28.4	1697
St.Dev	299	5	73	66	3	511	89	0.3	0.9	1389

The pH values of the collected samples (n=86) vary between 5.5 and 7.5, with an average of 6.8, indicating a generally neutral to slightly acidic groundwater nature. Notably, there's a significant range in EC, spanning from 137 to 7060 Ms/cm, and averaging at 1697 Ms/cm. Among the samples, the lowest EC was noted in the Upper Ross River basin, while the highest was recorded in the Mount Low suburb, northeast of Mount Louise. Temperature readings ranged from 26.1 to 29.9 degrees Celsius, with an average of 28.4°C.

Na^+ is the dominant ion in the cation chemistry, exhibiting higher concentrations on the proper coastal plain and decreasing towards the up-catchment or inland areas. The highest concentration of Na^+ (1460 mg/l) aligns with the Mount Low location of the high EC, while the minimum (17 mg/l) was found in Douglas. Elevated Na^+ levels can be attributed to silicate weathering, halite dissolution, connate water, and potentially, saltwater intrusion (Hem 1985 pp. 100).

The Ca^{2+} content in groundwater samples exhibits a range from 17 to 674 mg/l. Ca^{2+} is a common element found in rocks and minerals and significantly influences the solute composition of natural waters (Hem 1985 pp. 89). The behaviour of Ca^{2+} in aqueous systems is primarily controlled by the dissolution of calcium-rich minerals, the dynamics of carbon dioxide species, and the equilibrium involving the sulphates gypsum and anhydrite (Hem 1985 pp. 90).

The Mg^{2+} concentrations ranged from 0-542 mg/L, averaging 45 mg/L. Magnesium is a significant constituent of various geological formations. In igneous rocks, it's often present in dark-coloured ferromagnesian minerals like olivine, pyroxenes, and amphiboles, whereas altered rocks can feature magnesian minerals such as chlorite and serpentine (Hem 1985 pp. 97). Within sedimentary contexts, Mg^{2+} appears as various carbonates and combinations of magnesium and calcium carbonate, such as dolomite, which features a crystal structure with balanced proportions of calcium and magnesium ions (Hem 1985 pp. 97), and in the coastal areas, higher Mg^{2+} content in the seawater might be a reason for elevated Mg^{2+} concentration in groundwater due to saline intrusion (Kumar *et al*. 2012 pp. 2644).

Additionally, Mg^{2+} is a prevalent ion found in most limestone formations. During the dissolution process, limestone releases magnesium into the solution; however, this reaction is not readily reversible because magnesium's hydrogeochemical behaviour is significantly different than Ca^{+2} (Hem 1985 pp. 97). Therefore, as groundwater evolves along its flow path, the concentration of Mg^{2+} tends to increase until it reaches a relatively high ratio compared to Ca^{+2} (Hem 1985 pp. 97).

Potassium concentrations in the study area were limited, ranging from 0-29 mg/L, averaging 3 mg/L. K^+ is less abundant than sodium in igneous rock but more prevalent in sedimentary formations (Hem 1985 pp. 104). The primary sources of K^+ minerals in silicate rocks include orthoclase and microcline feldspars, as well as micas and leucite feldspathoids, but unlike other feldspars, potassium feldspars exhibit higher resistance to water erosion, gradually transforming into silica, clay, and K^+ ions over time (Hem 1985 pp. 104). In sedimentary deposits, K^+ is often found within unaltered feldspar or mica particles or bound to illite and other clay minerals (Hem 1985 pp. 104). Evaporite formations may contain K^+ salt beds, contributing to increased K^+ concentrations in brines (Hem 1985 pp. 104).

The alkalinity of a solution can be described as its ability for the solutes it holds to interact with and counteract acidity, and in natural groundwaters, HCO_3^- and alkalinity originate primarily from the dissolution of carbon dioxide species (Hem 1985 pp. 106). The prevalent approach involves expressing alkalinity as an equivalent quantity of calcium carbonate (as $CaCO_3$) in milliequivalents per litre (meq/L). $CaCO_3$ ranged 0-13 meq/L, averaging 5 meq/L.

The process for introducing alkalinity into groundwater begins with the absorption of carbon dioxide from the atmosphere into the water, forming carbonic acid (H_2CO_3), which then dissociates into HCO_3^- ions and hydrogen ions (Hem 1985 pp. 106). Carbonate ions may also contribute to alkalinity through various chemical reactions (Hem 1985 pp. 106), but only at pH >8 (Hem 1985 pp. 107). Consequently, the alkalinity of TCP groundwaters is primarily attributed to the presence and dissociation of H_2CO_3 and HCO_3^-. The dissolution of carbonate minerals in the aquifer material can also release carbonate ions into the groundwater, further increasing alkalinity levels.

Among the anions, HCO_3^- is dominant, followed by chloride and sulphate. Elevated levels of bicarbonate concentration often indicate the presence of minerals containing carbonates. This increase could be attributed to the breakdown of silicate and carbonate minerals, as well as the decomposition of organic matter, both contributing to the higher levels of bicarbonate in the groundwater (Singh *et al*. 2017 pp. 67).

Chloride concentrations in the TCP ranged from 18-2670 mg/L and averaged 431 mg/L (tab. 4.4.1). Notable sources of chloride are linked with sedimentary rocks, especially those formed from evaporites (Lloyd and Heathcote 1986 pp. 118), which may be present in the study area. Chloride can be found in sedimentary rocks due to the presence of connate brine and cementing material (Lloyd and Heathcote 1986 pp. 118). It is also commonly found in deposits that have not been fully leached and were deposited in marine environments or closed drainage basins (Lloyd and Heathcote 1986 pp. 118).

Sulphate concentrations in the study area ranged from 0-476 mg/L and averaged 50 mg/L (tab. 4.4.1). Sulphate in groundwater has few sources, which include dissolution of anhydrite and gypsum (Singh *et al*. 2017 pp. 67) and reduction by bacteria (Lloyd and Heathcote 1986 pp. 214).

The results illustrated by the Piper (1944) diagram (fig. 4.4.1) distinctly highlight the differentiation among the various Water Groups and their respective water classifications, with the regional distribution in the TCP shown in figure 4.4.2.

Ordered in a descending hierarchy of prevalence, the water types inside the TCP, alongside their corresponding sample proportions, are as follows: Na-Cl (60.5%), Na-HCO_3 (25.6%), Ca-HCO_3 (5.8%), Ca-Cl (4.7%), and Mg-Cl (3.5%). Analysis of the water types present within each Water Group reveals that Water Groups 1A, 3A, and 4B are all classified as Na-Cl water. Notably, Water Group 1A exclusively comprises Na-Cl water types, albeit with a limited sample count. Similarly, Water Group 3B and 4A both exclusively consist of Na-Cl water types, barring one sample in each group that is categorized as Na-HCO_3 and Mg-Cl types, respectively.

Water Groups 2B and 3 have the most diverse range, with water types spanning Na-HCO_3, Na-Cl, and Ca-Cl within each group. Water Group 3 incorporates the additional water type of Ca-HCO_3, albeit in limited numbers. This analysis underscores the intricate interplay of hydro-chemical processes taking place both within and between each water group. Distinct clusters are discernible based on these Water Groups. Notably, Water Groups 1B and 2A predominantly align between the areas of freshening and mixing. In contrast, Water Groups 3 and 4 are situated within the mixing-to-seawater signature range, while also showing samples in the intrusion area on the diamond field.

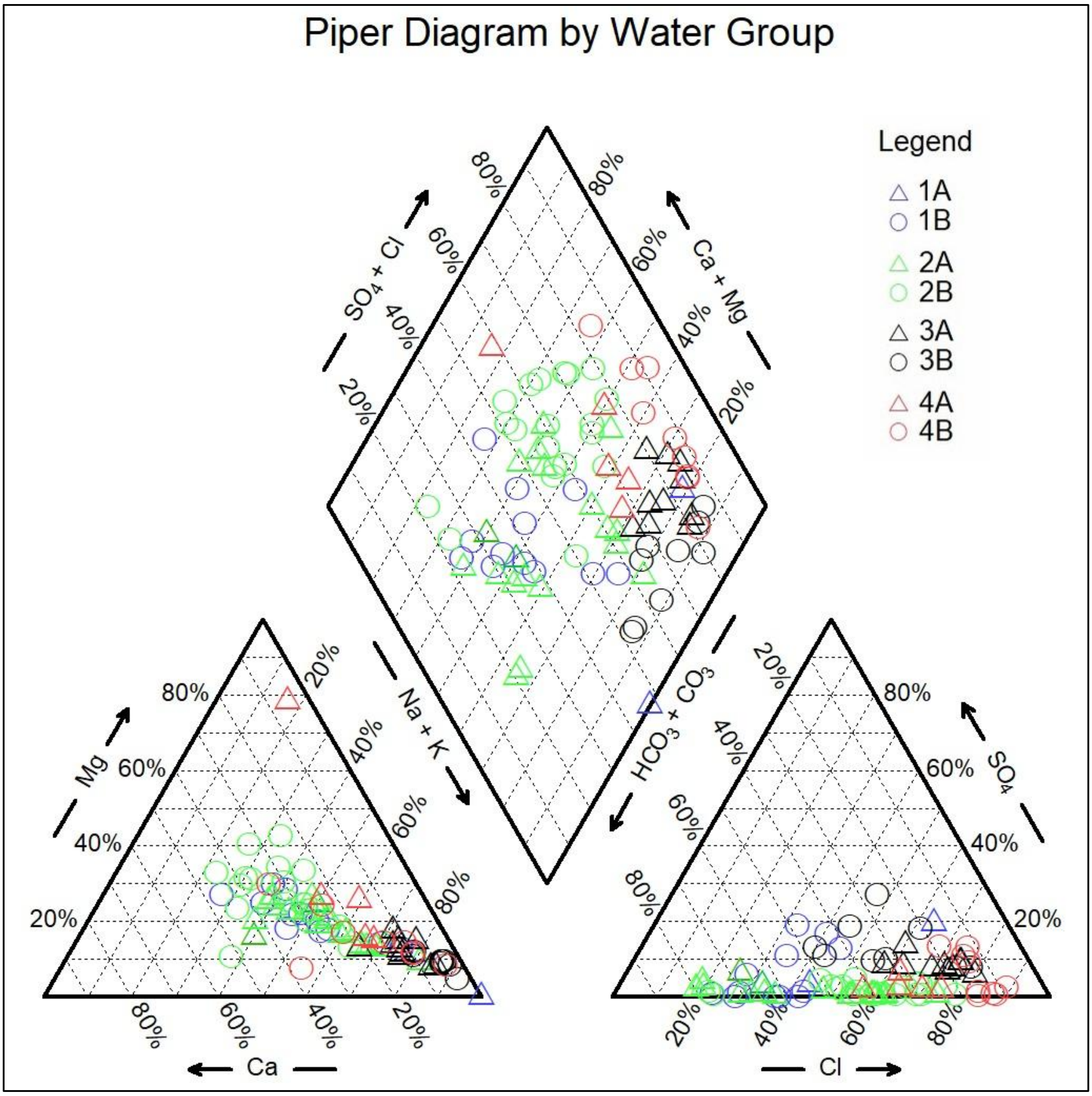

Figure 4.4.1: Piper diagram of groundwater samples, displayed by water groups determined from HCA analysis.

An excess of calcium in coastal groundwater samples, compared to a conservative mixture, may imply seawater intrusion while, conversely, an abundance of Na^+ could signal aquifer freshening (Appelo and Postma 2005 pp. 244). Water Group 2A exhibits a few samples that align well with the freshening field. Meanwhile, Water Groups 3 and 4 feature elevated chloride concentrations, pushing their compositions toward the seawater signature and intrusion areas on the diamond plot. Water Group 2B is primarily indicative of mixing, yet a subset of samples leans toward the seawater intrusion region. Water Group 3B, characterized by higher SO_4^{2-} and HCO_3^- concentrations, forms a distinct grouping beneath the seawater signature region. Broadly speaking, the fresher samples, represented by Water Groups 1 and 2, tend to align predominantly with the freshwater signature, indicating mixing. In contrast, the more saline water groups, Water Groups 3 and 4, are typically situated within the mixing region, extending toward the seawater signature and seawater intrusion areas.

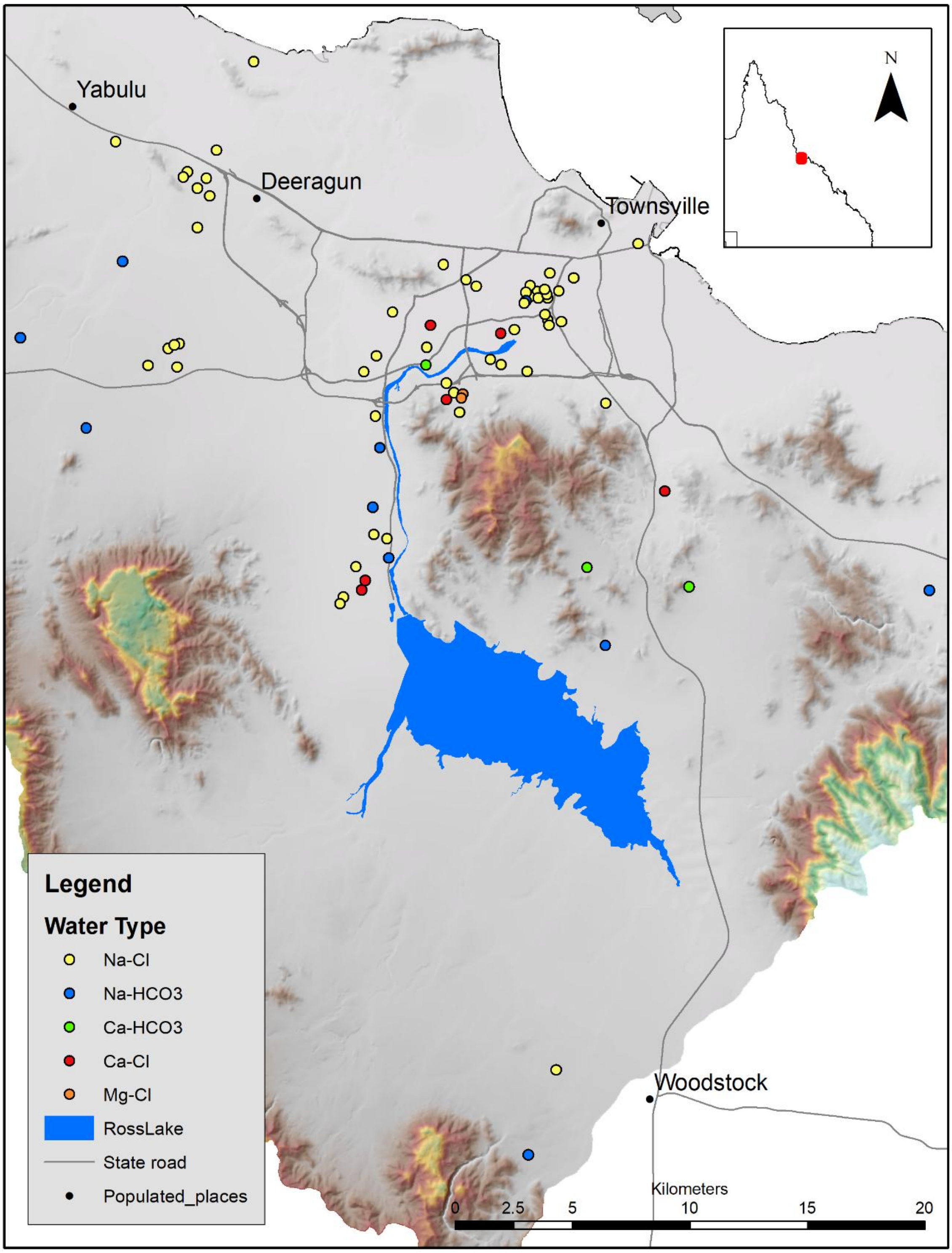

Figure 4.4.2: Regional map showing spatial distribution of water types based on Piper diagram classification of groundwater samples.

4.5 Groundwater Processes

4.5.1 Weathering and Dissolution

In the context of an aquifer, the alignment of the plot involving SO_4^{2-}+ HCO_3^- and Ca^{2+} and Mg^{2+} ions near the equiline (1:1) represents the relationship (fig. 4.5.1) that occurs when the dominant processes within the system involve the dissolution or weathering of calcite, dolomite, and gypsum (Kovalevsky, Kruseman and Rushton 2004 pp. 56, Kaur *et al*. 2019 pp.1248). This graph can show ion exchange and reverse-ion exchange reactions depending on the samples relative position to the equiline (Singh *et al*. 2017 pp. 69). From figure 4.5.1, most groundwater samples in the TCP exhibit positions above the 1:1 equiline, suggesting carbonate weathering (Kaur *et al*. 2019) and reverse-ion exchange reactions (Singh *et al*. 2017 pp. 69; Zaidi *et al*. 2015 pp. 607). Both samples from Group 1A and most samples from Group 3B plot near the equiline which indicates dissolution of calcite, dolomite, or gypsum (Singh *et al*. 2017 pp. 69); no samples plotted to the right of the equiline, indicating that silicate weathering isn't a significant process (Kaur *et al*. 2019 pp. 1248) and ion exchange reactions are limited (Singh *et al*. 2017 pp. 69).

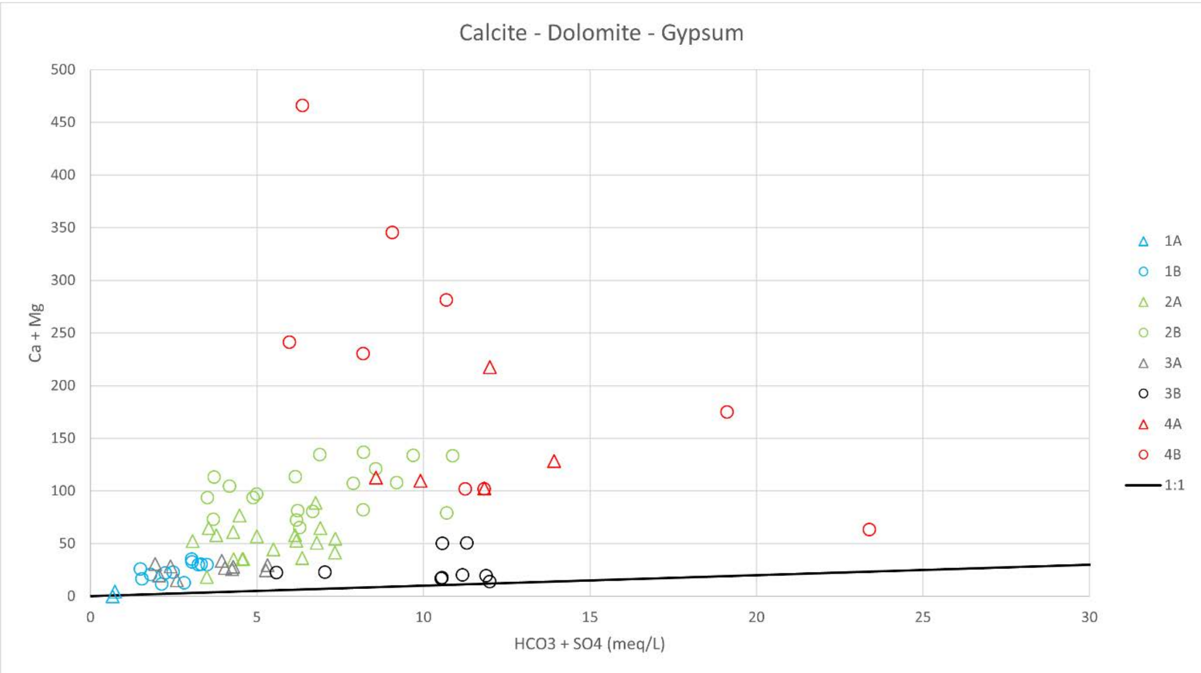

Figure 4.5.1: Plot of Ca+Mg and HCO_3+ SO_4^{2-} and 1:1 equiline, showing the influence of carbonate dissolution.

Patterns emerge within the water groupings of the Ca^{2+}:Mg^{2+} ratio (fig. 4.5.2) wherein linear trends suggest behaviours. The dissolution of calcite and dolomite can be evaluated using the Ca^{2+}/Mg^{2+} ratio, with values <1 indicating dissolution of dolomite and values >1 indicating dissolution of calcite (Singh *et al*. 2017 pp. 69). Group 3B, for instance, consistently plots below the 1:1 line, while Group 3A predominantly aligns either on or above the equiline, indicating that dolomite dissolution affects the hydrogeochemistry of Group 3B groundwaters while the dissolution of calcite influences Group 3A. Notably, Group 3B includes several samples with elevated concentrations of magnesium relative to calcium, as indicated by their linear distribution along the x-axis at lower concentrations. Within Group 2A and 2B, a clear positioning above the equiline is evident. In a few instances, at relatively higher concentrations, Group 2B deviates either above or below the equiline.

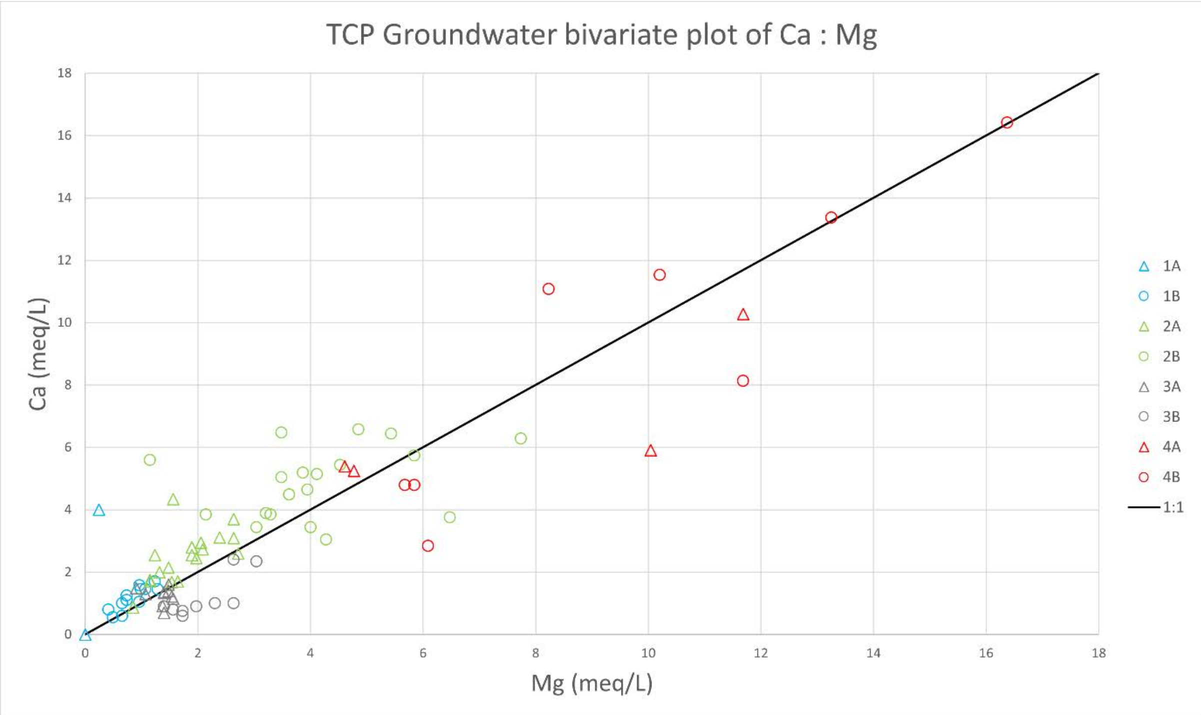

Figure 4.5.2: Bivariate plot of Ca:Mg ratio for groundwater samples, displayed by water group and subgroup.

For Group 4, a discernible trend is apparent with most samples positioned near the 1:1 line while others diverge, locating themselves above and below this reference. Amongst the samples located above or below this reference, the suburb of Annandale stands out, with the highest Ca^{2+}/ Mg^{2+} ratio of 23.1 (Ca^{2+}) to 4.8 (Mg^{2+}); this observation is attributed to the area's record-high Ca^{2+} concentration of 461 mg/L. This indicates that Group 4 waters are influenced by both calcite and dolomite dissolution.

The dissolution of halite and rock weathering can be assessed through the bivariate plot of Na^{+} and Cl^{-} (fig. 4.5.3 a and b), as samples that fall on the 1:1 equiline are considered to be influenced by halite dissolution, while samples plotting above, or below, the equiline are designated as influenced by cation exchange and rock weathering, or reverse ion exchange reactions, respectively (Gugulothu *et al*. 2022 pp. 5).

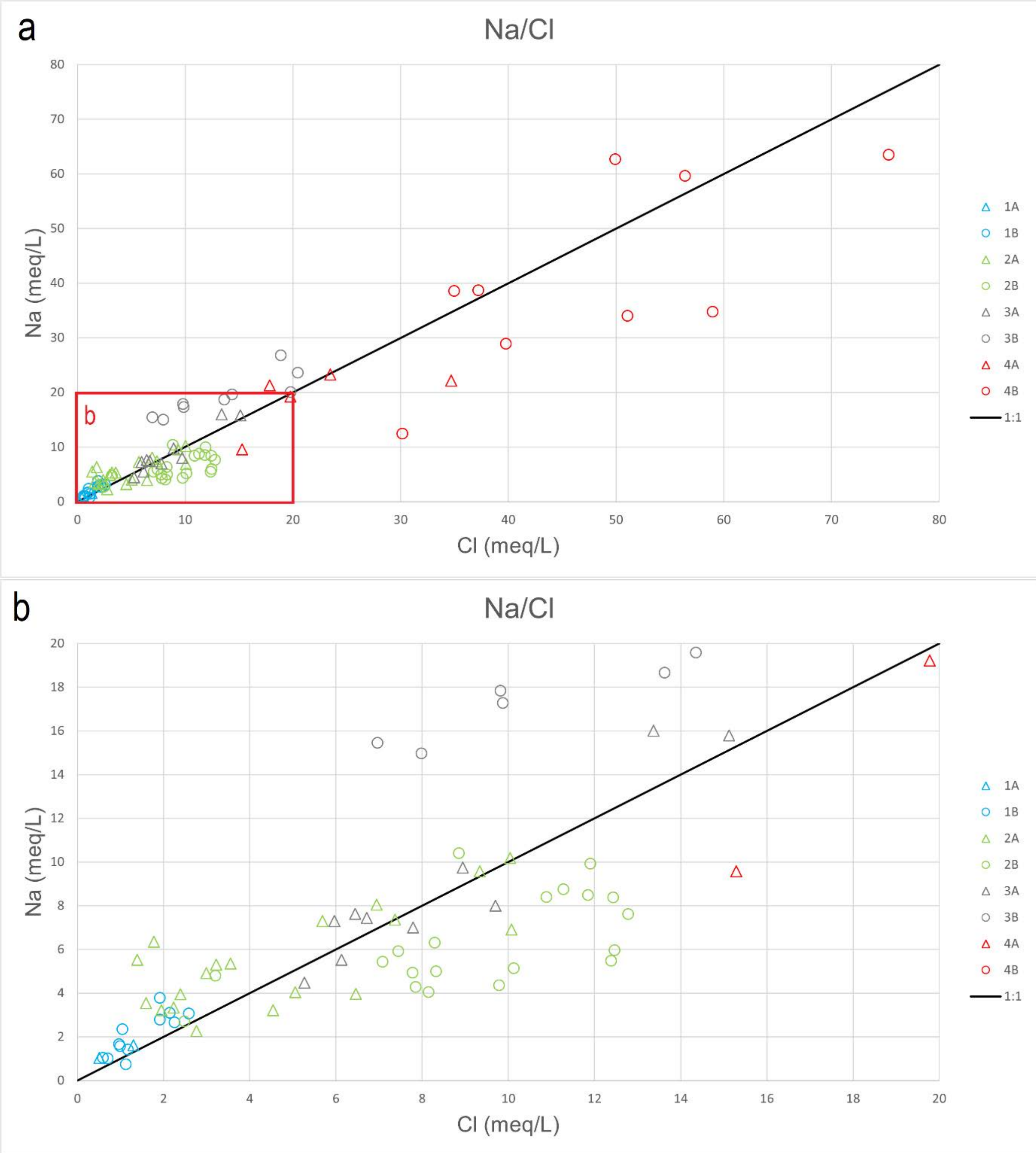

Figure 4.5.3: (a) Bivariate plot of Na and Cl for groundwater samples, displayed by water group and subgroup, and (b) reduced scale (20 meq/L) to show detail of fresher water groups.

In the bivariate plot of Na^+ and Cl^- (fig. 4.5.3) all samples from Group 1, except for a single sample from Group 1B, lie above the 1:1 equiline, suggesting rock weathering or ion exchange processes are dominant (Gugulothu *et al*. 2022 pp. 5). Similarly, the majority of Group 2A samples also fall above the line, while Group 2B samples are predominantly below the equiline, indicative of reverse ion exchange processes (Gugulothu *et al*. 2022 pp. 5).

Group 3 exhibits a pattern whereby fresher Group 3A groundwaters appear both above and below the line, whereas 3B waters are consistently positioned above the equiline. It is important to highlight that Group 3A waters closely cluster around the equiline (fig. 4.4.3b), unlike Group 3B waters, which plot notably higher due to elevated Na^+ levels. This suggests that halite dissolution potentially exerts a greater influence on Group 3A groundwaters, whereas Group 3B is primarily impacted by ion exchange or rock weathering reactions (Gugulothu *et al*. 2022 pp. 5).

The molar ratio of Na^+/Cl^- in groundwater samples varied from 0.41 to 4.0 meq/L, with an average of 1.17 meq/L across all samples. The majority of samples (58.1%) exhibited a ratio greater than 1, indicating non-halite sources for the excess Na^+ (Ansari and Umar 2019 pp. 40), with potential sources being silicate weathering, saline soils, or anthropogenic sources (Ansari and Umar 2019 pp. 40). A Na^+/Cl^- ratio of 1.0 (+/- 0.05), indicating the dissolution of halite (Gugulothu *et al*. 2022 pp. 5), was observed in 8 samples, with three from Group 2A, one from Group 3A and 3B, respectively, two from Group 4A, and one in 4B. Only one sample, located in Group 2A, had a Na^+/Cl^- ratio of exactly 1.0.

The scatterplot of Na^++K^+/Cl^- was further used to assess the source of excess cations (fig. 4.5.4). Samples positioned above the 1:1 line for Na^++ K^+/Cl^- indicate that excess cations may originate from silicate weathering, while those below the line are likely influenced by processes such as evaporation and reverse ion exchange (Singh *et al*. 2017 pp. 69; Gugulothu *et al*. 2022 pp. 5). In Group 1, all samples, with one exception, lie above the equiline and indicate silicate weathering. Group 2 samples exhibit a split distribution, with Group 2A predominantly above and Group 2B below the line, indicating evaporation or reverse ion exchange processes. Similarly, Group 3A has samples both above and below the equiline, whereas Group 3B is primarily positioned above the equiline. Group 4 samples have a mixed distribution, with a majority falling below the equiline.

In summary, the bivariate plots have indicated both ion exchange and reverse ion exchange reactions are occurring in the TCP. Halite dissolution is indicated to a limited extent. Rock weathering or ion exchange is mainly occurring in the fresher groundwaters, though does occur at higher salinities. Reverse ion exchange is shown to occur in most high salinity samples, with greater variability in Group 4B waters than the fresher 4A groundwaters. This distribution underscores the variable processes responsible for the hydrogeochemical characteristics of the water groups, with fresher groundwater typically influenced by rock weathering and ion exchange, while higher salinity waters tend to reflect the effects of reverse ion exchange and evaporation.

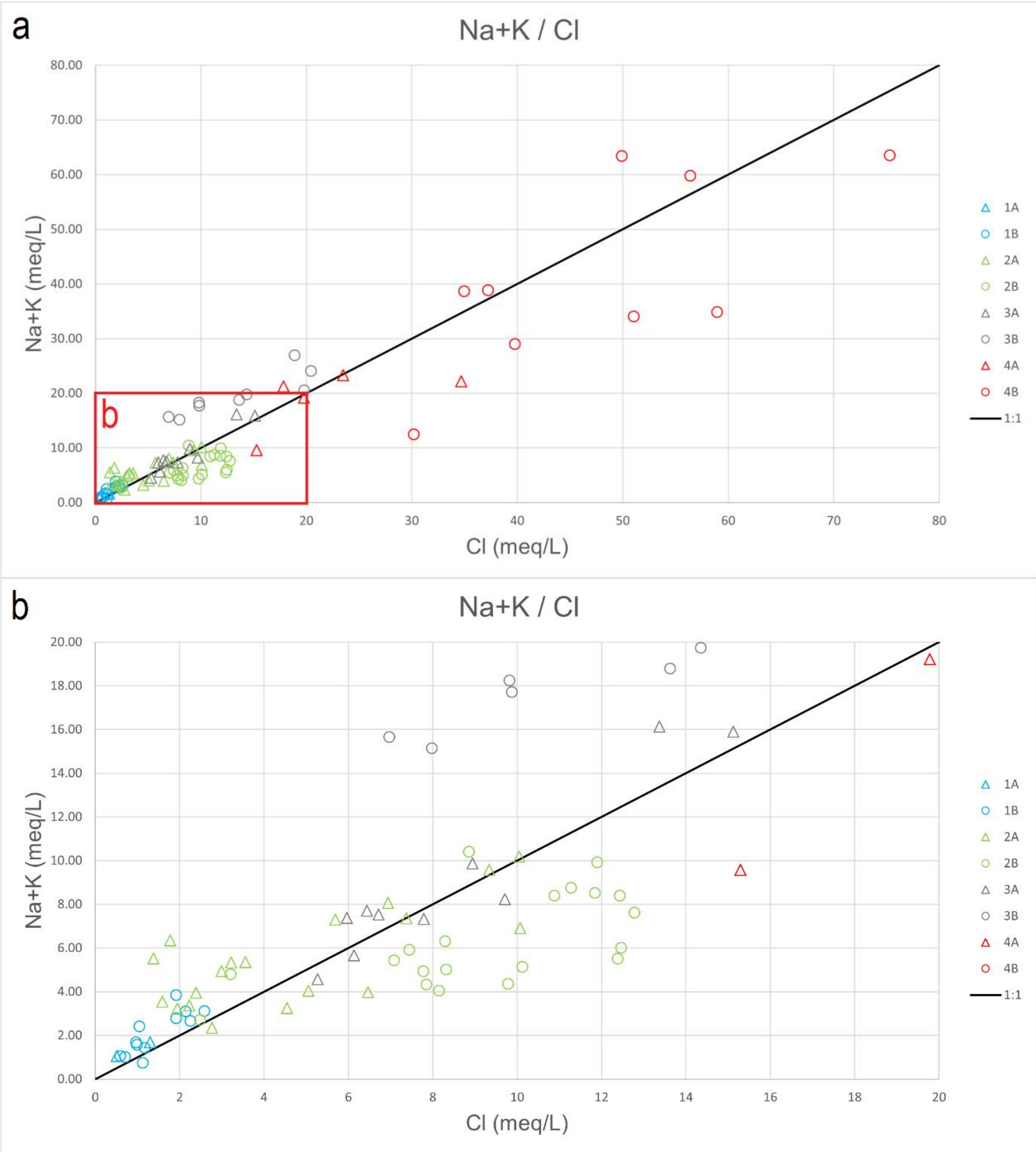

Figure 4.5.4: (a) Bivariate plot of Na+K / Cl for groundwater samples, displayed by water group and subgroup, and (b) reduced scale (20 meq/L) to show detail of fresher water groups.

4.5.2 Chloro-Alkaline Indices (CAI)

An interchange of Na^+ and K^+ within the groundwater and Ca^{2+} and Mg^{2+} within the aquifer is shown through the CAI (fig 4.5.5) (Schoeller 1977):

In the study area, the CAI(I) and CAI(II) indices ranged between -3.00 and +0.59 and -0.82 to +2.96, respectively, with average values of -0.18 for CAI(I) and +0.12 for CAI(II). Out of all samples (n=86), 37 of 86 samples (43%) displayed positive indices, indicating reverse ion exchange (Chowdhury *et al*. 2022).

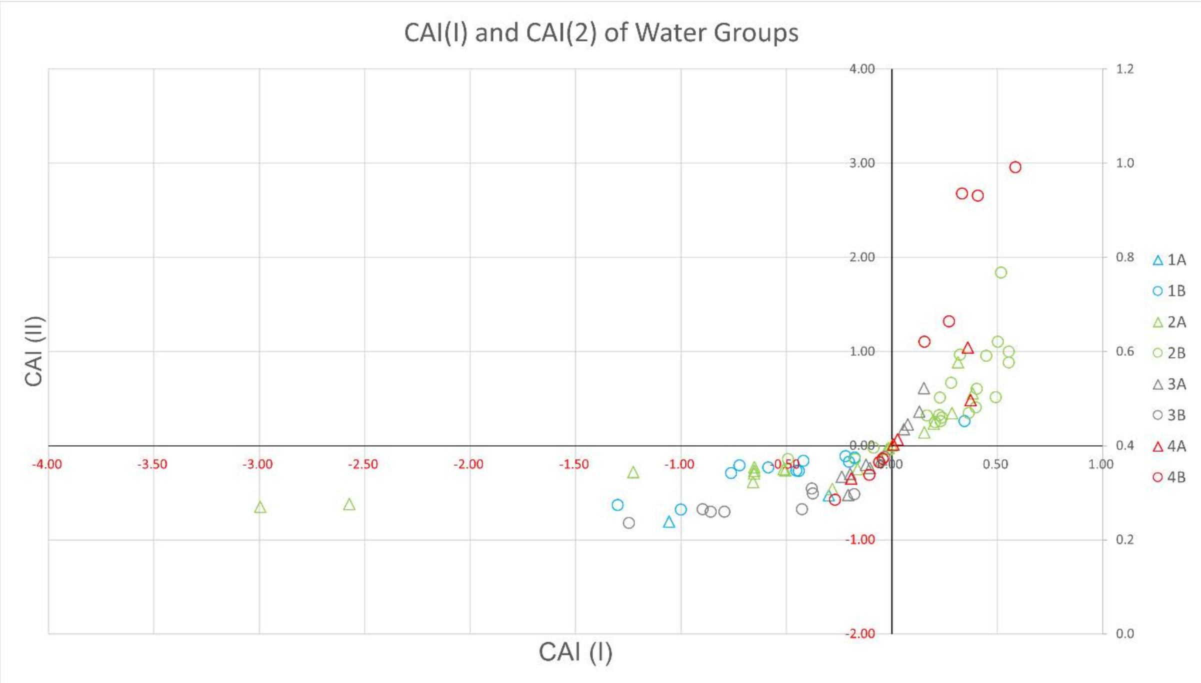

Figure 4.5.5: Bivariate plot of CAI (I) and CAI (II), indicating ion exchange (negative indices) and reverse ion exchange (positive indices) for groundwater samples in the TCP.

The various water groups have different distributions of indices. Within Water Group 1, all indices were negative, except for a single sample. Water Group 2A has positive indices in 26% of the samples, while 85% of samples in Water Group 2B showed positive values. In Water Group 3A, positive indices were noted for 40% of samples, while Group 3B shows exclusively negative values, indicating ion exchange as the dominant process (Gugulothu *et al*. 2022 pp. 7). Among Water Group 4A samples, 80% displayed a positive index, while in the case of Water Group 4B, only 55% yielded positive values.

As indicated by the CAI(I) and CAI(II) indices, both ion exchange and reverse ion exchange reactions are occurring in Townsville's groundwater systems. The fresher waters appear to be more influenced by ion exchange reactions, though there are exceptions. While the more saline waters of Groups 3 and 4 are split, such that just over half of Group 3A is dominated by

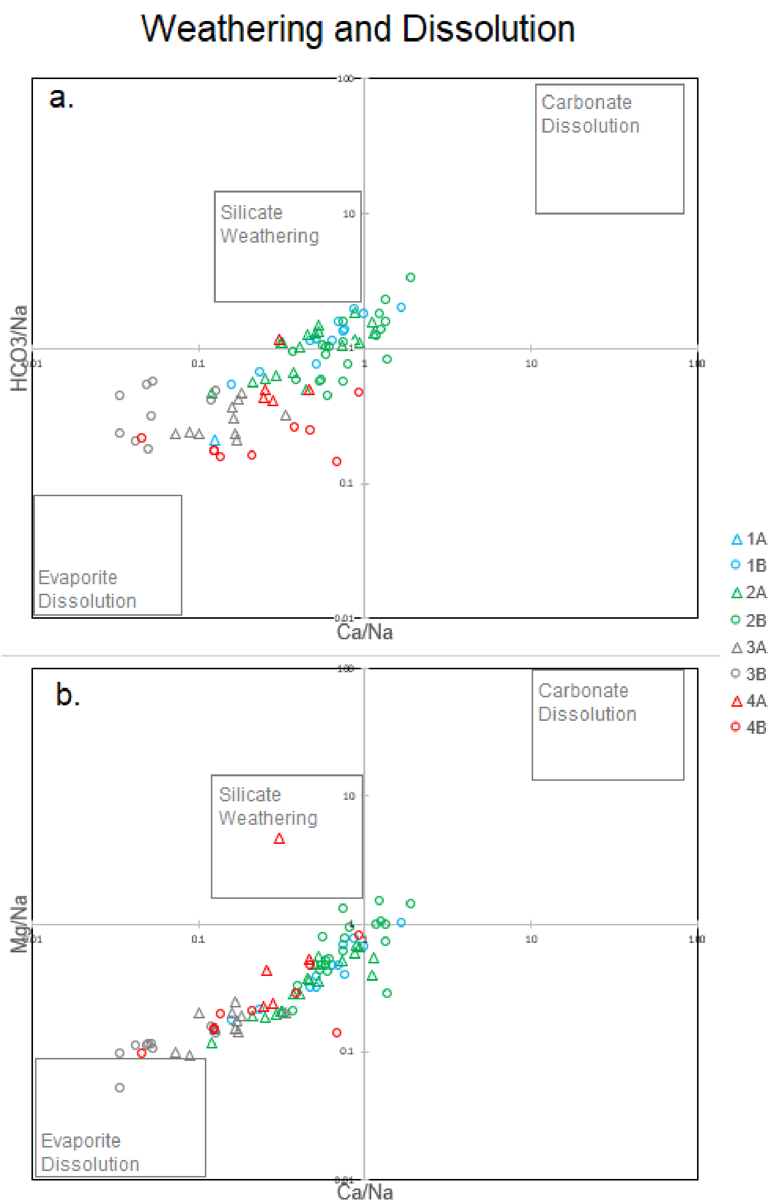

Figure 4.5.6a (top): Weathering and dissolution associations by ionic ratio comparison displayed by Water Group. Magnesium graph (b) shows Water Group 3A/B and 4B waters close or within the Evaporite Dissolution field, and one sample from Water Group 4A locates within the Silicate Weathering field; this sample is located in Douglas, within a suspected internally draining basin.

Figure 4.5.6b (bottom): Weathering and dissolution associations by ionic ratio comparison displayed by Water Group. Magnesium graph (b) shows Water Group 3A/B and 4B waters close or within the Evaporite Dissolution field, and one sample from Water Group 4A locates within the Silicate Weathering field; this sample is located in Douglas, within a suspected internally draining basin.

ion exchange and just over half of Group 4B is dominated by reverse ion exchange, Group 1 and 2A waters are controlled by ion exchange.

The Na^{+} normalized Ca^{2+} to HCO_3^{-} and Mg^{2+} ratio plots (fig. 4.5.6) have differences among water groups that offer insight to processes influencing the water chemistry (Singh *et al.* 2017 pp. 68). In the graphical depiction of weathering and dissolution processes, the relationships between the Ca^{2+}/Na^{+} ratio and the HCO_3/Na^{+} as well as Mg^{2+}/Na^{+} ratios (fig. 4.5.6a and 4.5.6b respectively) illuminates the impact of these processes on different water groups. Notably, the plot of Ca^{2+}/Na^{+} ratio against HCO_3^{-}/ Na^{+} ratio (fig. 4.5.6a) distinctly underscores distribution variations among the water groups (Singh *et al*. 2017 pp. 66).

Water Groups 3 and 4 exhibit a tendency towards evaporite dissolution, while Water Groups 1 and 2 predominantly cluster toward the silicate weathering region. Although some intermingling is observed within the 'A' subgroups, this distinction becomes more pronounced in the ‘B’ subgroups, as a result of the variable calcium concentration. The broader spread of samples along the x-axis in Water Group 4B is a result of the higher calcium concentration. Conversely, Groups 1 and 2 cluster around the 1:1 range, aligning them closer to the silicate weathering zone. Notably, the analysis does not indicate any instances of carbonate dissolution.

For the Mg^{2+}/Na^{+} ratio (fig. 4.5.6b), the alignment of water groups becomes more linear, with a few exceptions. Consistent with the calcium trend, several samples align with evaporite dissolution. Notably, a solitary Group 3B sample resides within this range. Additionally, several samples from Groups 3A/B and 4B are positioned near the boundary, potentially indicating the influence of evaporitic dissolution. A sample from Group 4A is positioned within the silicate weathering region. As previously noted, the absence of samples affected by carbonate dissolution is evident. The data highlights a potential role of calcium in influencing groundwater composition on a broader scale.

This analysis provides significant insights into the interplay of weathering and dissolution processes, offering a comprehensive understanding of the underlying hydro-chemical mechanisms influencing water chemistry across different water groups.

4.5.3 Gibbs Diagram

As showcased in figure 4.5.7, the Gibbs diagram illustrates the primary factors shaping the chemical composition of groundwater, encompassing rock-water interaction, evaporation, and precipitation. Group 1 samples cluster around rock-water interaction and evaporation, while Group 4 samples show evaporation and seawater influences. Group 2 and Group 3 waters occupy intermediate spaces between rock-water interaction and seawater effects, with Group 3 samples edging slightly towards seawater.

Calcium is the dominate ion in fresh waters and Na^{+} is dominant in saline water bodies, with the composition of low-salinity water controlled by the concentration of salts in the precipitation in tropical areas (Gibbs 1970 pp. 1089). This shows that most samples in the study area come from groundwaters controlled by evaporative processes.

Given that samples in the rock-dominance area are considered in equilibrium with basin sediments and the exact position is determined by climate, landscape relief, and composition of the basin’s sediments (Gibbs 1970 pp. 1089), Group 1 samples in the cation plot show that there is an excess source of Na^{+} influencing the water chemistry for some samples, as demonstrated by the samples plotting further to the right on the graph.

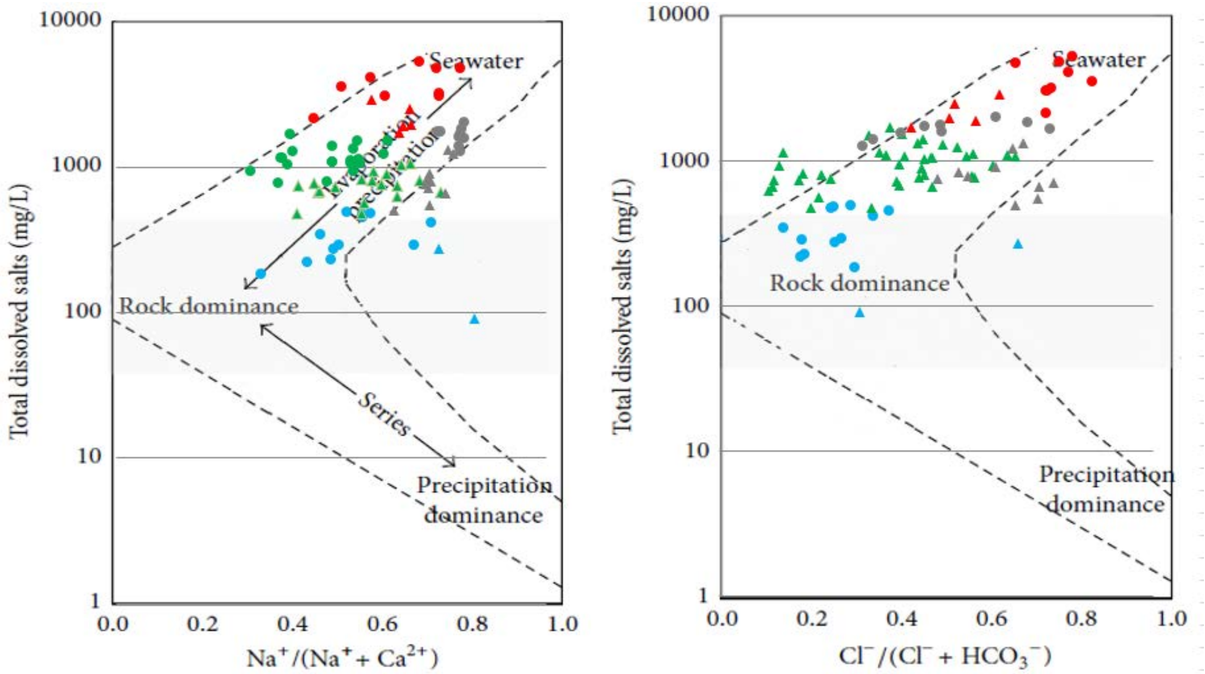

***Figure 4.5.7**: Gibbs diagram displaying water groups, with Group 1 (blue), Group 2 (green), Group 3 (grey), Group 4 (red), with A and B designated by triangles and circles, respectively.*

In the anion graph, Group 2A waters are distributed in two areas, one more toward rock-dominance and the other more toward seawater composition. The noticeable difference between these two groups is the concentration of HCO_3^- which decreases moving to the right on the graph. This is typical of an evaporation trend, whereby as the salinity increases and calcium carbonate ($CaCO_3$) precipitates, the relative proportion of Na^+ to Ca^{2+} and HCO_3^- to Cl^- increases.

This integrated approach, utilizing the Gibbs diagram and major ion concentrations, provides valuable insights into the processes impacting groundwater chemistry within different water groups.

4.6 Discussion of Findings

Hydrogeochemistry provides a systematic framework to explore the relationship between the aquifer and groundwater chemistry. Elevated concentrations of specific ions are indicators of underlying hydrological processes, indicating the processes that shape groundwater chemistry (Gugulothu *et al*. 2022).

PCA can be a powerful tool to decipher multi-dimensional hydrogeochemistry (Singh *et al*. 2017). By distilling complex data into two principal components, PCA shows nuanced relationships among various ions, allowing determination of the underlying drivers behind the composition of different water groups (Gugulothu *et al*. 2022). The PCA analysis resulted in the identification of two principal components that comprised 88.0% of total variance. The first principal component explained 53.3% of total variance and identified Ca^{2+}, Mg^{2+}, and $CaCO_3$ concentrations as the controlling factors. The second principal component explained 34.7% of variance and identified K^+ and SO_4^{2-} as the controlling variables. These results offer insights into how geological factors interact with hydro-chemical variables, revealing correlations between seemingly unrelated ions and additional mineral sources impacting water chemistry.

HCA complements PCA by delineating distinct water groups and subgroups, providing deeper insights into the hydro-chemical profiles present (Gugulothu *et al*. 2022). This analysis resulted in the classification of four separate water groups, each bifurcated into subgroups of A and B based on salinity. Each water group, and subgroup, has generally distinct hydrogeochemical signatures. Clustering of samples reveals patterns of salinity variations and ion concentrations across the study area, underscoring the role of geological factors in determining groundwater chemistry. Water Groups 1 and 2 are the least saline, with EC less than around 300 and 1200 µS/cm, respectively, with Group 2 showing more saline signatures and significantly higher ion ratios. Concentrations of Ca^{2+}, Mg^{2+}, $CaCO_3$, and to a lesser extent Na^+, Cl^-, and EC, are the primary controls on the water chemistry. Water Groups 3 and 4 have considerably higher EC averages, being around 1700 and 4000 µS/cm respectively. Though Ca^{2+}, Mg^{2+}, and $CaCO_3$ play a role in these groups, K^+ and SO_4^{2-} are distinguishing influences. Na^+ and Cl^- also show distinction between the subgroups, consistent with water evolution.

Bivariate plots of relevant ions underscore the distinction between hydrogeochemical characteristics among the water groups, with fresher groundwater typically influenced by rock weathering and ion exchange, while higher salinity waters tend to reflect the effects of reverse ion exchange and evaporation. Rock weathering and cation exchange were shown to occur in most water groups, with Group 2B showing reverse ion exchange processes dominating. Group 3A was indicated as reverse ion exchange processes but also the dissolution of halite having an influence in 3A groundwaters. Carbonate dissolution was identified in the water groups, with Group 1 and 3B groundwaters dominated by calcite dissolution, 3A dominated by dolomite dissolution, and Group 2 and 4 groundwater showing dissolution of both calcite and dolomite, with few samples from each of these groups affected by halite dissolution.

The CAI(I) and CAI(II), offer a quantitative means to examine ion exchange processes between groundwater and aquifer material (Singh *et al*. 2017). In these indices, Groups1 and 2 occur near the silicate weathering zone while Groups 3 and 4 appear more closely linked to evaporite dissolution. Groups 3 and 4 show a greater range in Ca^{2+} concentrations whereas in Groups 1 and 2, Na^+ and Mg^{2+} concentrations are greater. These indices unravel both direct and reverse processes and their influence on groundwater quality (Gugulothu *et al*. 2022).

The Gibbs diagram visually represents complex chemical interactions, positioning major ion compositions against total dissolved salts to indicate the prevailing hydrogeochemical processes (Singh *et al*. 2017). In this diagram, Group 1 samples showed rock-water interaction and evaporation were the dominant mechanisms controlling water chemistry, while Group 4 samples prominently showed evaporation and seawater influences. Meanwhile, Group 2 and Group 3 waters occupied the intermediate spaces between rock-water interaction and seawater effects, with Group 3 samples skewed slightly towards seawater. This graphical format indicates that water-rock interaction and evaporation play variable roles across the TCP.

In sedimentary aquifers originating from marine environments, ion exchange mechanisms significantly influence groundwater composition. Sodium-saturated clays in such aquifers undergo ion exchange with calcium and magnesium ions from recharge waters, leading to proportional increases in Na^+ concentration (Llyod and Heathcote 1985). These analyses have shown ion exchange and rock weathering to be occurring predominately in the freshest water samples, from Groups 1 and 2. Reverse ion exchange reactions are observed in the TCP, mainly in the intermediate waters of Groups 2 and 3. Reverse ion exchange can occur where saline water percolates through terrigenous clays, mainly in river estuaries, replacing Na^+ with Ca^{2+} (Llyod and Heathcote 1985 pp. 14). This implies that reverse ion exchange processes could be occurring in areas that are, or were formerly, Ross River estuaries.

The summary below provides an overview of the key characteristics and influences of each water group in the hydrogeochemical landscape of the Townsville regional study area:

1. **Water Group 1**:
   - **PCA Analysis**: Identifies Ca^{2+}, Mg^{2+}, $CaCO_3$ as controlling factors.
   - **Salinity**: Least saline, EC < 300 µS/cm.
   - **Dominant Ions**: Ca^{2+}, Mg^{2+}, $CaCO_3$; lesser extent of Na^+, Cl^-, EC.
   - **Hydrochemical Characteristics**: Reflects rock weathering and ion exchange.
   - **Chloro-alkaline Indices (CAI)**: Aligned near silicate weathering.
   - **Gibbs Diagram**: Dominated by rock-water interaction and evaporation.
2. **Water Group 2**:
   - **PCA Analysis**: Identifies Ca^{2+}, Mg^{2+}, $CaCO_3$ as controlling factors.
   - **Salinity**: EC < 1200 µS/cm.
   - **Dominant Ions**: Ca^{2+}, Mg^{2+}, $CaCO_3$; higher ion ratios.
   - **Hydrochemical Characteristics**: More saline signatures, significant ion ratios, reverse ion exchange.
   - **Chloro-alkaline Indices (CAI)**: Aligned near silicate weathering.
   - **Gibbs Diagram**: Intermediate between rock-water interaction and seawater effects.

3. **Water Group 3**:
    - **PCA Analysis**: Identifies K^+, SO_4^{2-} as controlling variables.
    - **Salinity**: EC around 1700 µS/cm.
    - **Dominant Ions**: Na^+, Cl^-; greater range in Ca^{2+} concentrations.
    - **Hydrochemical Characteristics**: Influenced by evaporite dissolution, reverse ion exchange.
    - **Chloro-alkaline Indices (CAI)**: Aligned near evaporite dissolution.
    - **Gibbs Diagram**: Intermediate between rock-water interaction and seawater effects.
4. **Water Group 4**:
    - **PCA Analysis**: Identifies K^+, SO_4^{2-} as controlling variables.
    - **Salinity**: Highest, EC around 4000 µS/cm.
    - **Dominant Ions**:Na^+, Cl^-; distinct Na^+, Cl^- concentrations.
    - **Hydrochemical Characteristics**: High EC averages, influenced by K^+, SO_4^{2-}.
    - **Chloro-alkaline Indices (CAI)**: Aligned near evaporite dissolution.
    - **Gibbs Diagram**: Exhibits significant evaporation and seawater influences.

In summary, the integration of these analyses provides valuable insights into the hydro-chemical dynamics within the TCP. This analytical approach highlights the multifaceted nature of hydrogeological systems and outlines the complexities of water sources, processes, and interactions.

4.7 References – Chapter 4

Ansari, AA and Umar R 2019, 'Evaluation of hydrogeochemical characteristics and groundwater quality in the quaternary aquifers of Unnao District, Uttar Pradesh, India', *HydroResearch*, vol. 1, pp. 36-47, DOI: 10.1016/j.hydres.2019.01.001.

Appelo, CAJ and Postma, D 2005, *Geochemistry, groundwater and pollution*, 2 ed., Taylor and Francis, A.A. Balkema Publishers, Great Britain.

Belkhiri, L, Boudoukha, A, and Mouni, L 2011, 'A multivariate Statistical Analysis of Groundwater Chemistry Data', *International Journal of Environmental Research*, vol. 5(2), pp. 537-544, <https://www.researchgate.net/publication/236612300_A_multivariate_Statistical_Analysis_of_Groundwater_Chemistry_Data>.

Chowdhury, P, Mukhopadhyay, BP, Nayak, S, and Bera, A 2022, 'Hydro-chemical characterization of groundwater and evaluation of health risk-assessment for fluoride contamination areas in the eastern blocks of Purulia district, India', *Environment, Development and Sustainability*, vol. 24(9), pp. 11320-11347, DOI: 10.1007/s10668-021-01911-1.

Gibbs, RJ 1970 'Mechanisms Controlling World Water Chemistry.', *Science*, vol. 170, no. 3962, pp. 1088–90, DOI: 10.1126/science.170.3962.1088.

Gugulothu, S, Subbarao, N, Das, R and Dhakate, R 2022, 'Geochemical evaluation of groundwater and suitability of groundwater quality for irrigation purpose in an agricultural region of South India', *Applied Water Science*, vol. 12(142), pp. 1-13, DOI: 10.1007/s13201-022-01583-w.

Güler, C, Kurt, MA, Alpaslan, M, and Akbulut, C 2012, 'Assessment of the impact of anthropogenic activities on the groundwater hydrology and chemistry in Tarsus coastal plain (Mersin, SE Turkey) using fuzzy clustering, multivariate statistics and GIS techniques', *Journal of Hydrology*, vol. 414, pp. 435-451, DOI: 10.1016/j.jhydrol.2011.11.021.

Helena, B, Pardo, R, Vega, M, Barrado, E, Fernandez, JM, and Fernandez L 2000, 'Temporal evolution of groundwater composition in an alluvial aquifer (Pisuerga River, Spain) by principal component analysis', *Water Resources*, Elsevier, Pergamon, vol.34(3), pp. 807-816, DOI: 10.1016/S0043-1354(99)00225-0.

Hem JD 1985, Study and Interpretation of Chemical Characteristics of Natural Water, 3 ed., U.S. Geological Survey (USGS) Water-Supply Paper 2254, Department of the Interior, United States Geological Survey.

Kaiser, HF 1960 'The Application of Electronic Computers to Factor Analysis', *Educational and Psychological Measurement*, vol. 20(1), pp. 141-151, DOI: 10.1177/001316446002000116.

Kaur, L, Rishi, MS, Sharma, S, Sharma, B, Lata, R, and Singh, Gagandeep 2019, "Hydrogeochemical characterization of groundwater in alluvial plains of river Yamuna in northern India: An insight of controlling processes', *Journal of King Saud University – Science*, vol. 31(4), ScienceDirect, DOI: 10.1016/j.jksus.2019.01.005.

Kovalevsky, VS, Kruseman, GP, and Rushton KR 2004, *Groundwater studies: an international guide for hydrogeological investigations*, IHP-VI Series on Groundwater No. 3, UNESCO, United Nations, 430 p., ISBN 92-9220-005-4. Retrieved 10 August 2023 from <https://unesdoc.unesco.org/ark:/48223/pf0000134432>.

Kumar, PJS, Elango, E, and James, EJ 2014, 'Assessment of hydrochemistry and groundwater quality in the coastal area of South Chennai, India', *Arabian Journal of Geosciences*, 7, pp. 2641-2653, DOI: 10.1007/s12517-013-0940-3.

Llyod, JW and Heathcote JA 1985, *Natural inorganic hydrochemistry in relation to groundwater: An introduction*, Clarendon Press, Oxford, United Kingdom.

Menció, A and Mas-Pla, J 2008, 'Assessment by multivariate analysis of groundwater-surface water interactions in urbanized Mediterranean streams', *Journal of Hydrology*, Elsevier, vol. 352, pp. 355-356, DOI: 10.1016/j.jhydrol.2008.01.014.

Piper, AM 1944 '*A Graphical Procedure in the Geochemical Interpretation of Water Analysis*', U S Geological Survey (USGS), Groundwater Note 12. DOI: 10.1029/TR025i006p00914.

Schoeller, H 1977, Geochemistry of Groundwater. In: Groundwater Studies—An International Guide for Research and Practice, UNESCO, Paris, Ch. 15, pp.1-18.

Singh, CH, Kumar, An, Shashtri, S, Kumar, Al, Kumar, P, and Mallick, J 2017, 'Multivariate statistical analysis and geochemical modelling for geochemical assessment of groundwater of Delhi, India', *Journal of Geochemical Exploration*, Elsevier, vol. 175, pp. 59-71, DOI: 10.1016/j.gexplo.2017.01.001.

Wells, RC 1923, 'Sodium Sulphate: Its sources and uses', Department of the Interior, United States Geological Survey, Bulletin 717, pp. 1-43, DOI: 10.3133/b717.

Zaidi, FK, Nazzal, Y, Jafri, MK, and Naeem, M 2015, 'Reverse ion exchange as a major process controlling the groundwater chemistry in an arid environment: a case study from northwestern Saudi Arabia', *Environmental Monitoring and Assessment*, vol. 187(10), pp. 607-618, DOI: 10.1007/s10661-015-4828-4.

THIS PAGE INTENTIONALLY LEFT BLANK

Chapter 5: Water Quality

5.1 Introduction

The following chapter discusses the results of water quality analysis for N=86 samples from the TCP, beginning with the investigation of stable water isotopes as key indicators of groundwater recharge and movement. The results of stable isotope analysis provide insights into the origin and behaviour of groundwater within the study area. Following this, chloride mass balance (CMB) methods are employed to estimate recharge rates across different groundwater systems. The chapter then shifts to evaluating irrigation water quality using several key indices, starting with the Residual Sodium Carbonate (RSC) and Sodium Adsorption Ratio (SAR), both of which assess the potential for soil degradation and salinity issues. The Wilcox diagram is also used to further classify irrigation water suitability based on salinity and sodium hazard. Lastly, the seasonal analysis of stable isotopes is discussed to determine if variations in groundwater chemistry are linked to seasonal changes, providing a comprehensive understanding of how seasonal factors may influence water quality

5.2 Stable Isotope Characteristics of Coastal Plain Groundwater

Results of the stable isotope analysis are displayed in figure 5.2.1. All four water groups obtained from the HCA analysis are distributed along the length of the LMWL, indicating that, with respect to the processes influencing the stable isotope composition, each water group is affected by similar processes. The signature of δD and $\delta^{18}O$ and for most groundwater samples plot on or below the LMWL and indicate that groundwater is influenced by meteoric and subsurface processes (Clark and Fritz 1997 pp. 74). A few of the samples, most noticeably from water groups 1B and 4B, plot above the LMWL (Liu *et al*. 2010) and signify re-evaporation of local surface waters (Clark and Fritz 1997 pp. 74). A few samples from water groups 2A and 2B also plot slightly above the LMLW but generally this effect is considered limited.

The freshest group, 1A, are both ^{18}O enriched and depleted. The ^{18}O enriched sample was obtained from the upper reaches of the Upper Ross River catchment, near the foot of Mount Elliot, while the second sample, considered ^{18}O depleted, was obtained >0.5km from the beach, in the suburb of Bushland Beach. The ^{18}O depleted beach sample can be explained by subsurface paleochannel drainage of evaporated phreatic waters while the ^{18}O enriched sample is characterized by continental and altitude fractionation effects (Clark 2015 pp.124), presumably from rainfall on Mount Elliot infiltrating and moving downslope and into the aquifer system in the upper reaches of the catchment.

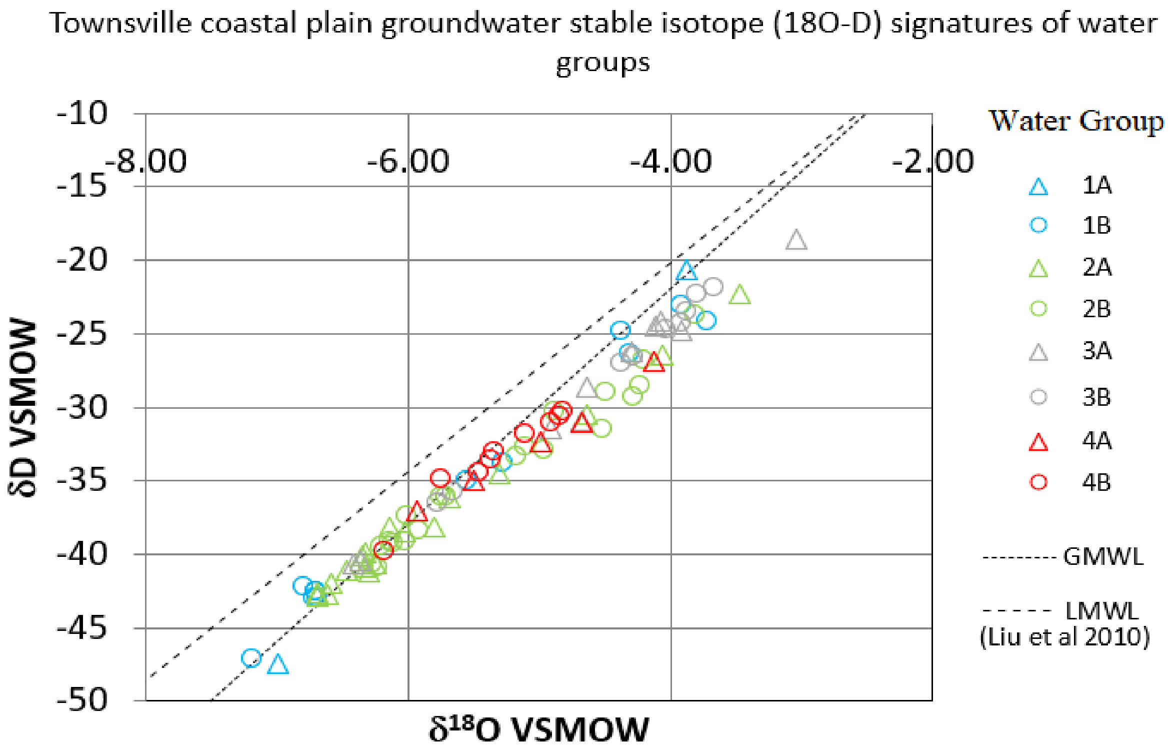

Figure 5.2.1: Stable isotope results of Townsville's groundwater, displayed by water group. Group 1 is most 'fresh' and proceeding to most 'saline' in Group 4, with each group split between A/B and each representing the fresh/saline scale, respectively, within each group. Noticeably, there is no clear discernible groupings based on water group and indicating that similar fractional effects and processes are generally occurring across all systems.

Crosbie *et al*. (2012, pp. 9) lists the weighted average $\delta^{18}O$ and δD compositions as -6.85 and -41.99, respectively, for precipitation in Townsville. From this perspective, and with few exceptions, groundwater samples in the study area all depict evaporative effects. The few exceptions are samples from water groups 1A, 1B, and 2A, as these are less than the weighted average of local precipitation.

The observation suggests that most of the groundwater in the TCP follows slower recharge routes, which allow evaporation to occur. This observation aligns with the prevalence of clay and less permeable sediments across the TCP region. In such conditions, recharge waters experience delays in the unsaturated zone and are influenced by evaporation processes.

This evaporation leads to a deviation from the local meteoric water line, resulting in a line with a shallower slope, which is largely influenced by relative humidity (Clark and Fritz 1997, pp. 43). When humidity is low, kinetic evaporation is maximized, leading to a low slope. Conversely, high humidity levels lead to a steeper slope, reaching approximately 8, the GMWL, at 90% humidity (Clark and Fritz 1997 pp. 44). This distinction is reflected in the isotopic compositions of the water groups. Group 2 generally exhibits more depleted ^{18}O

values compared to groups 3 and 4, with subgroup 2A being more ^{18}O depleted than 2B. Group 3 also displays variations, with some 3A samples showing more depleted ^{18}O signatures than 3B. Group 4 demonstrates the narrowest range of values. Notably, groups 2B and 3A/B typically exhibit signatures consistent with lower relative humidity during recharge precipitation, suggesting recharge during the summer when humidities are highest.

Two of the samples showed nearly identical stable water isotopes values for $\delta^{18}O$ and δD. These samples were from locations on the opposite sides of Mount Stuart, one in the suburb of Kelso (west) and the other in Roseneath (east) (fig. 5.2.2). The $\delta^{18}O$ and δD values for Kelso were -5.69 and -36.23, and Roseneath had values of -5.71 and -36.09. The stable isotope compositions generally do not change once the recharge waters enter the saturated zone, or water table. Because these signatures are unique in their similarity, it can be inferred that the groundwater systems of these sampling points share a common recharge area. The common recharge area is most likely the topographical highs of the Mount Stuart complex. While there are similarities in the stable isotope signatures, differences between the water types of each sampling point are noted. The sample from Kelso has a Na-HCO_3 water type, which is typical of ion exchange and freshening processes (Lloyd and Heathcote 1985 pp. 132), while the Roseneath sample is Ca-Cl type. The Ca-Cl water type can result from reverse-ion exchange processes of Na-Cl waters, or cement pollution (Lloyd and Heathcote 1985 pp. 132) or could be basinal brine from evaporation of paleoseawaters in Phanerozoic sedimentary basins (Lowenstein *et al*. 2003 pp. 857). Thus, the stable isotope composition serves to identity common recharge processes and the water types generally indicate within aquifer processes.

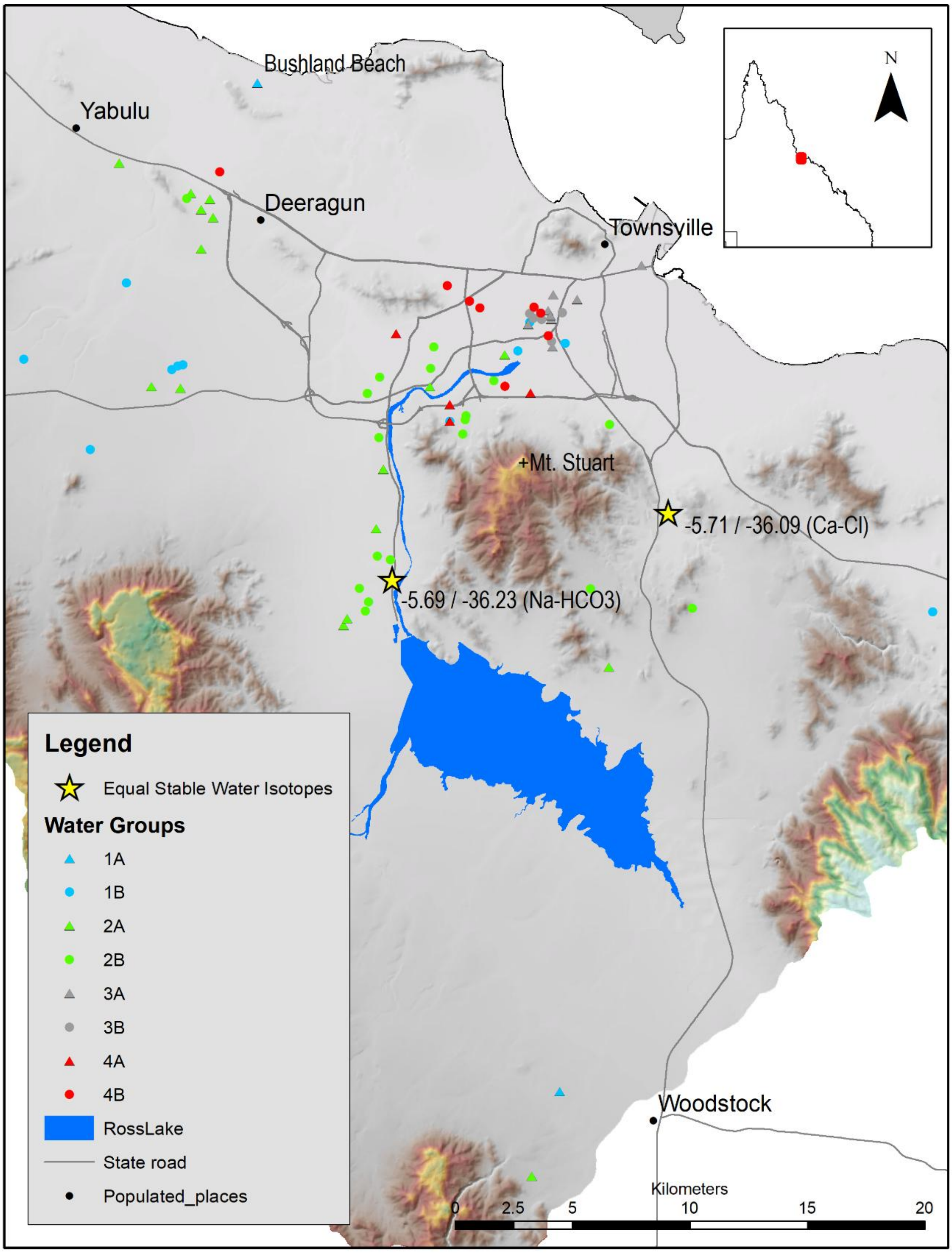

Figure 5.2.2: Regional map of the study area showing locations of equal value stable water isotope results (yellow star). Sample are located on opposite sides of the Mt. Stuart complex and are of two different water types: Kelso, on the western side is Na-HCO_3 while Roseneath, on the east side, is Ca-Cl.

5.3 Estimation of Recharge Using Chloride Mass Balance Analysis

Estimation of recharge rates was undertaken for each of the samples (n=86) and analysed based on water groups determine by HCA (fig. 5.3.1) with estimates provided in Table 5.3.1; Water group 1A is not included in this assessment as this group only contains two samples.

Group 1 has an estimated recharge rate of 31-160 mm/yr, with an average of 75 mm/yr, while Group 2 shows a significantly narrower range, calculated at 6-59 mm/yr, averaging 18 mm/yr. Group 3 has lower recharge rates, ranging from 5-15 mm/yr, with an average of 11 mm/yr, and Group 4 has the lowest estimated recharge values, ranging from 1-5 mm/yr, averaging only 3 mm/yr. On examination of subgroups, Group 2A has an estimated recharge over twice that of Group 2B, at 25 mm/yr and 11 mm/yr, respectively. Similarly, subgroups 3A and 3B follow a comparable pattern, with Group 3A having nearly double the recharge of 3B, estimated to be 11 mm/yr and 7 mm/yr, respectively. These trends are also present in subgroups 4A and 4B, where the estimated recharge for 4B waters, at 2 mm/yr, is half that of 4A waters, which is 4 mm/yr.

When these recharge rates are contextualised as a percentage of rainfall, the results of the CMB analysis show that recharge to group 1 waters is between 2.7-13.9% of the average annual rainfall of 1143 mm/yr, which is the highest among water groups. Group 2 and 3 water receive between 0.5-5.1% and 0.4-1.3% respectively, while group 4 is the lowest, with estimated recharge only 0.08-0.4% of average annual precipitation.

Overall, the recharge rates calculated for the study area are relatively low when compared to global averages, which is consistent with Townsville's designation as a dry tropics region. As previously mentioned, projections indicate a decline in annual rainfall, which directly translates to reduced recharge of the groundwater system. Meanwhile, the number of groundwater bore installations continues to grow at a rate of 11% annually, further increasing demand on these limited resources. With more users relying on groundwater and a predicted decrease in natural recharge, the risk of over-extraction becomes a significant concern.

The estimated recharge was also compared to the bore depth (fig. 5.3.2). The subgroup samples are spread across the depth profile with few discernible trends. For example, subgroup 2B samples range in depth from 7 to 43m with most recharge estimates ranging below 20 mm/yr, while subgroup 1B waters have a similar range of depth with estimated recharge that is much more variable.

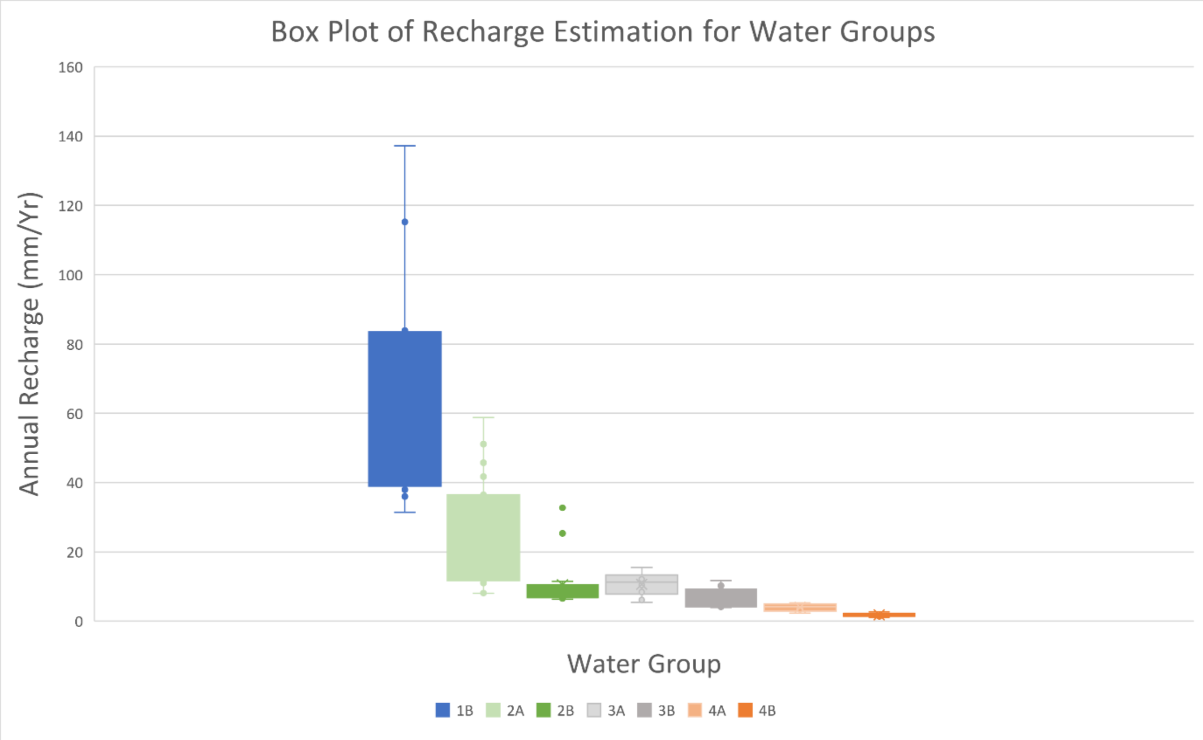

Figure 5.3.1: Box plot of results of CMB analysis showing estimated annual recharge values per water group (water group 1A consists of two samples and is not displayed).

Table 5.3.1: Summary statistics of results of CMB analysis showing estimated annual recharge values per water group.

	Recharge Estimate by Water Group (mm/yr)					
	n	Min	Max	Average	Median	St.Dev
Group 1	**14**	**31**	**160**	**75**	**71**	**39**
1A	2	63	160	-	-	-
1B	12	31	137	69	71	33
Group 2	**39**	**6**	**59**	**18**	**11**	**14**
2A	19	8	59	25	23	16
2B	20	6	33	11	9	7
Group 3	**19**	**5**	**15**	**11**	**11**	**3**
3A	10	5	15	11	11	3
3B	9	4	12	7	6	3
Group 4	**14**	**1**	**5**	**3**	**2**	**1**
4A	5	2	5	4	4	1
4B	9	1	3	2	2	1

The other subgroups have recharge rates under 60 mm/yr across all depths. An exception is Group 3 waters which all come from bores of less than 18m in depth and have consistently less than 20 mm/yr estimated recharge. Subgroup 1A samples come from variable depths but consistently have higher recharge estimates, unlike Group 4 waters that vary across depths but have very low estimated recharge.

The general trend of all the samples indicates that higher rates of recharge are associated with the fresher groundwaters, with recharge rate decreasing as EC concentrations increase across the water groups. This is not unexpected as higher recharge rates are generally associated with relatively less rock-water interaction and, consequently, lower solute loads.

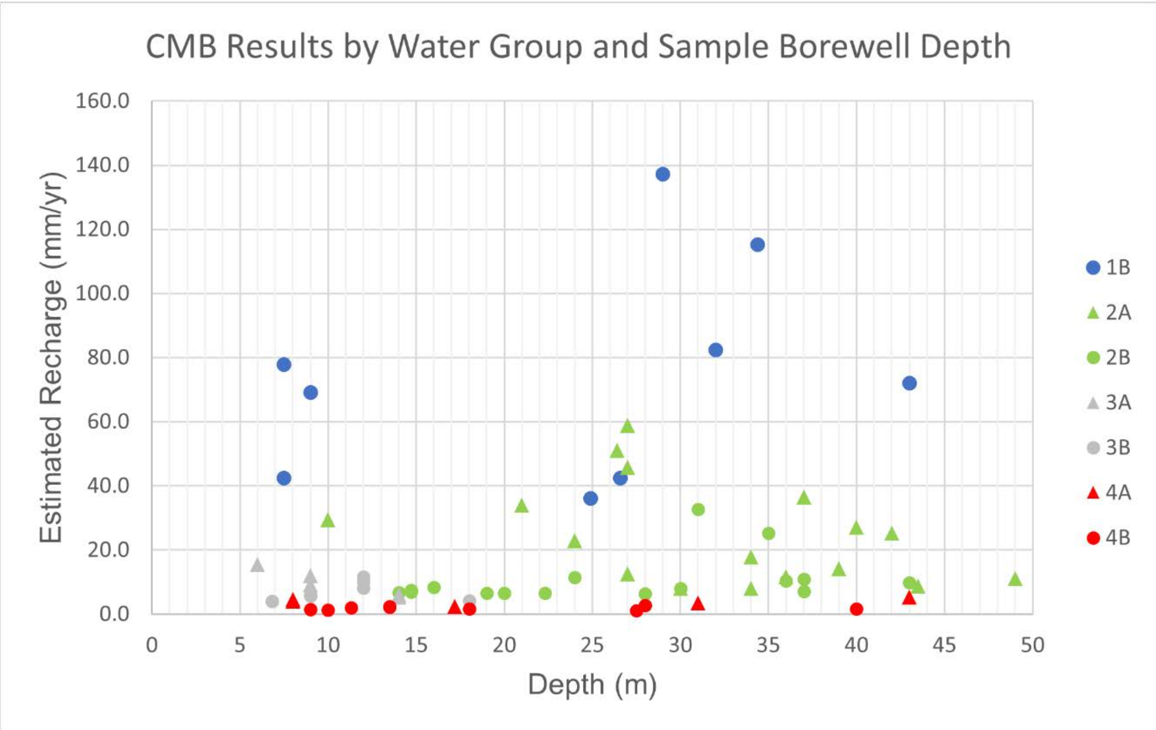

Figure 5.3.2: Scatter plot of results of CMB analysis showing estimated annual recharge values by depth, for each water group (water group 1A consists of two samples and is not displayed).

5.4 Water Quality Assessment and Suitability for Irrigation

This section presents an analysis of groundwater quality in the study area, with a focus on its suitability for irrigation. The assessment is based on key indicators, including the residual sodium carbonate (RSC), sodium adsorption ratio (SAR), and the Wilcox diagram. The results are analysed in relation to the four identified Water Groups (Groups 1-4) and their sub-divisions (A and B), highlighting the variability in water quality across the different groups. These metrics provide insight into the potential impacts of groundwater quality on soil health and agricultural productivity, with particular emphasis on the classification of groundwater as suitable or unsuitable for irrigation.

5.4.1 Residual Sodium Carbonate (RSC) Results

The RSC was calculated for all samples (n=124) with values in the study area ranging between –36.19 and 6.17 meq/L, indicating a wide range of RSC values in the groundwater systems. The samples showed 80.6% were classified as 'suitable', while 10.5% and 8.9% were classified as 'marginally suitable' and 'unsuitable', respectively.

Table 5.4.1: Residual sodium carbonate (RSC) classification of water groups.

Group	Subgroup	n	Suitable <1.25 meq/L	Marginally Suitable 1.25-2.5 meq/L	Unsuitable >2.5 meq/L
1	A	2	2	-	-
	B	12	12	-	-
2	A	19	9	7	3
	B	20	19	-	1
3	A	10	10	-	-
	B	9	2	-	7
4	A	5	5	-	-
	B	9	8	-	1
	Percentage (%)		**77.9**	**8.1**	**14.0**

Further analysis based on the results of the HCA analysis was undertaken (table 5.1 and fig. 5.4.1). The classification (Hem 1985 pp. 217) revealed that 77.9% of the samples were categorized as 'suitable' for irrigation, while 8.1% and 14.0% were classified as 'marginally suitable' and 'unsuitable' respectively. The water groups identified through the HCA analysis indicated that the RSC values generally fell within the 'suitable' category for irrigation purposes. Specifically, Group 1 waters were all classified as 'suitable,' and the majority of samples from other groups also met the suitability criteria. However, a few exceptions, such as Group 2A waters and Group 3B waters were noted. Only 47.3% of the 2A waters were classified as suitable, with the majority falling under the 'marginally suitable' category. Group 3B waters showed 7 of the 9 samples (77.8%) classified as 'unsuitable'.

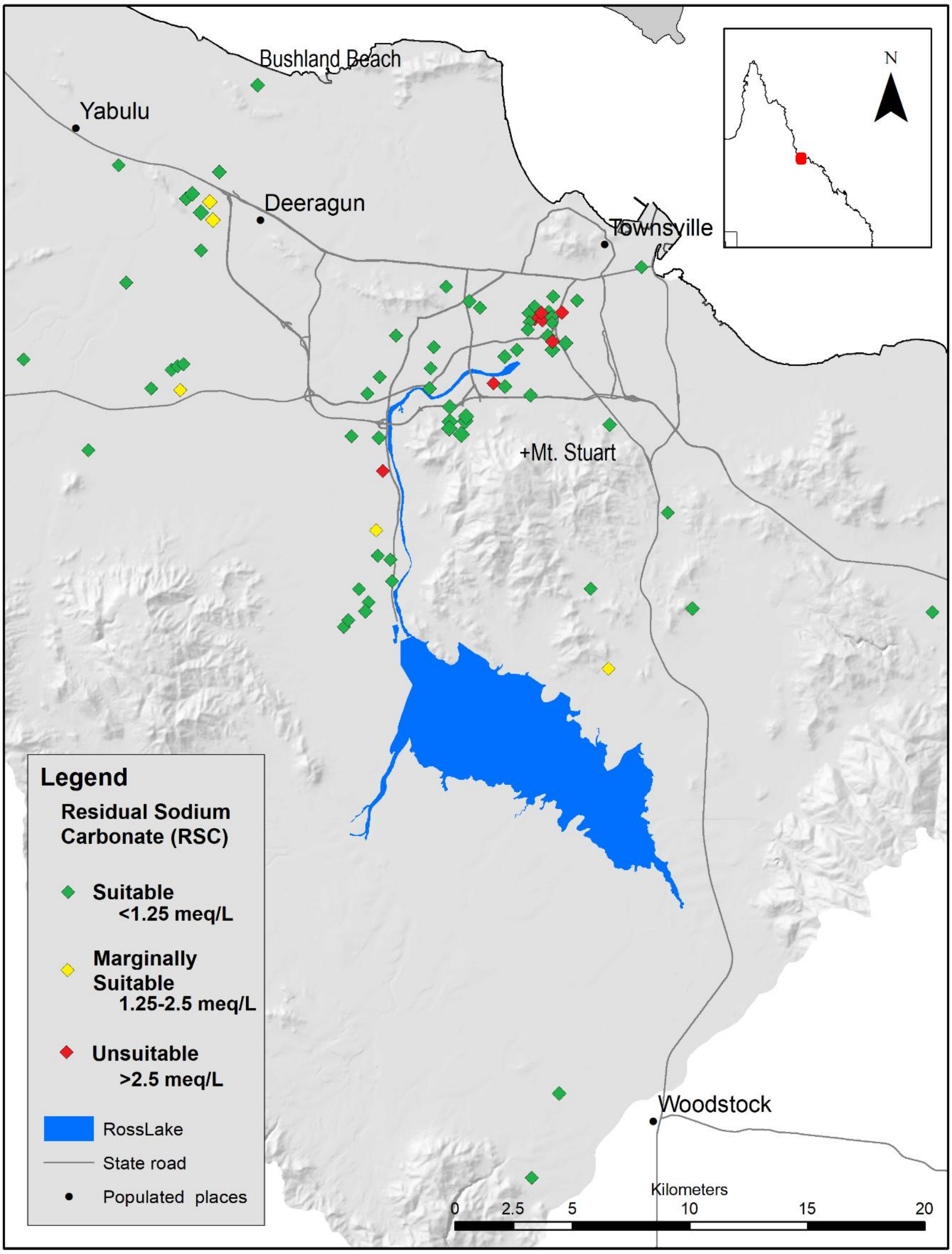

Figure 5.4.1: Map displaying results of RSC with samples shown as suitable (green diamond), marginally suitable (yellow diamond), and unsuitable (red diamond).

5.4.2 Sodium Adsorption Ratio (SAR)

SAR values were calculated for all samples (n=124) in the study area, with results ranging between 0.74 and 29.6 meq/L, indicating a range in values in the groundwater systems of the TCP. The samples showed 42.7% were classified as 'no problem', while the remaining 57.3% were categorized as 'slight to moderate'; no samples were classified as 'severe problem'.

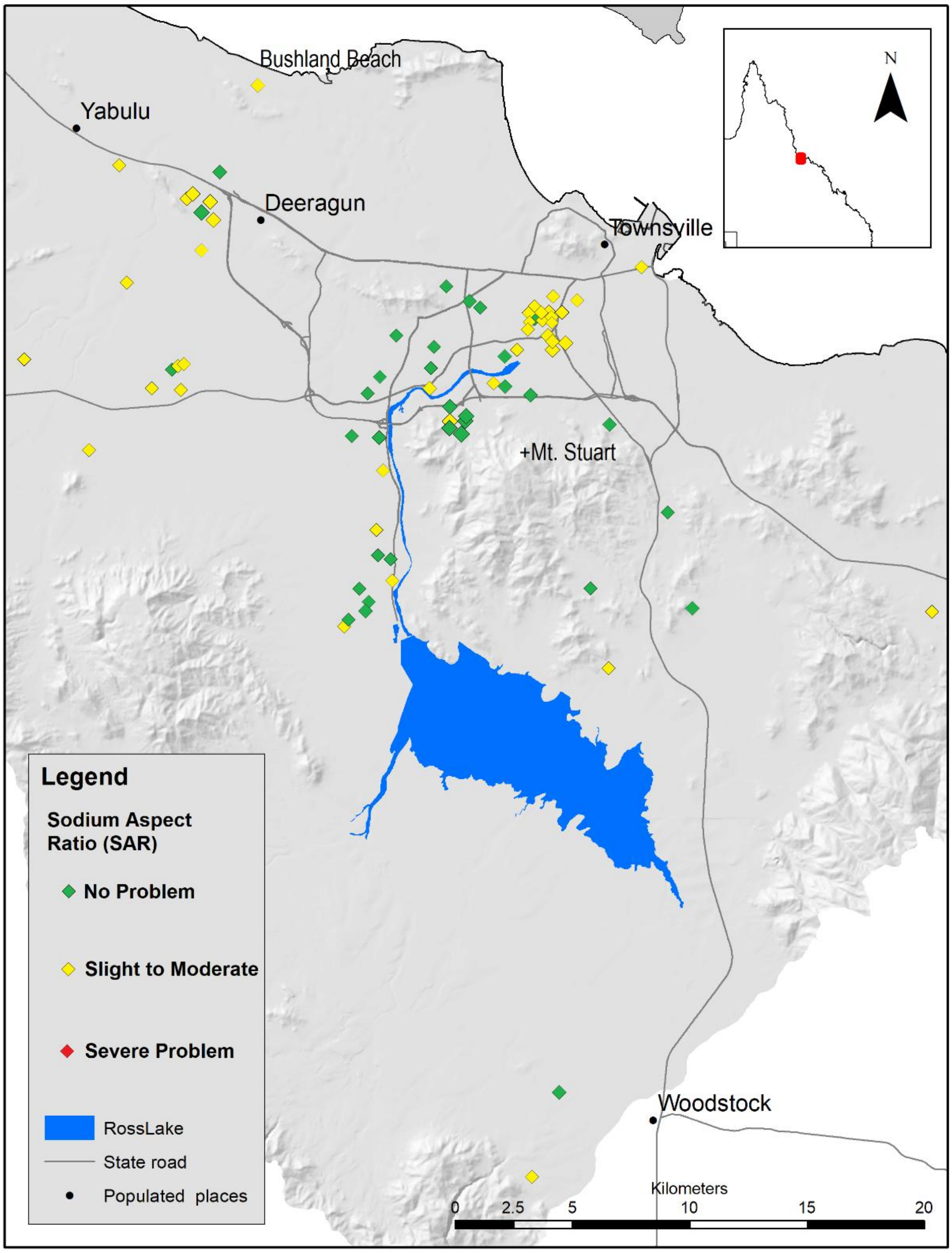

Figure 5.4.2: Map displaying results of SAR with samples shown as no problem (green diamond), slight to moderate (yellow diamond), and severe problem (red diamond).

Based on the findings from the HCA conducted in Chapter 4, an assessment was carried out to determine the suitability of the samples (n=86) for each water group (fig. 5.4.2). Within Group 1 waters, the majority fell under the category of 'slight to moderate', although one of the samples from subgroup A was classified as 'no problem'. In contrast, Group 2A waters showed 84% falling under 'slight to moderate', with the remaining 16% categorized as 'no problem', while Group 2B exhibited a different pattern, with 95% classified as 'no problem' and only 5% as 'slight to moderate'. The analysis indicated that Group 3 waters had the most significant concerns, with all of Group 3A classified as 'slight to moderate'. In Group 3B, 78% were categorized as 'slight to moderate', while the remaining 22% were deemed 'no problem'. Both subgroups within Group 4 were classified as 'no problem'.

5.4.3 Wilcox diagram

Based on the Wilcox (1955) diagram (fig. 5.4.3), Group 1 samples classify as C2S1, or medium salinity hazard and low sodium hazard, while Group 2 samples are mainly high salinity hazard and low sodium hazard, or C3S1, with few being better or worse.

Group 3 samples appear bimodal with Group 3A plotting mostly in C3S2 (high salinity/medium sodium hazard) or better, with a few exceptions and Group 3B (the more saline samples of the group) plotting in the S3/S4 range (high to very high salinity and sodium hazards). Group 4 waters are clearly the highest salinity, all classifying as C4 or very high salinity; these samples are spread across the sodium hazard rating S1-S4. In total, four samples plot in the C4S4 (very high salinity and sodium hazards), two from each Group 3B and Group 4B samples.

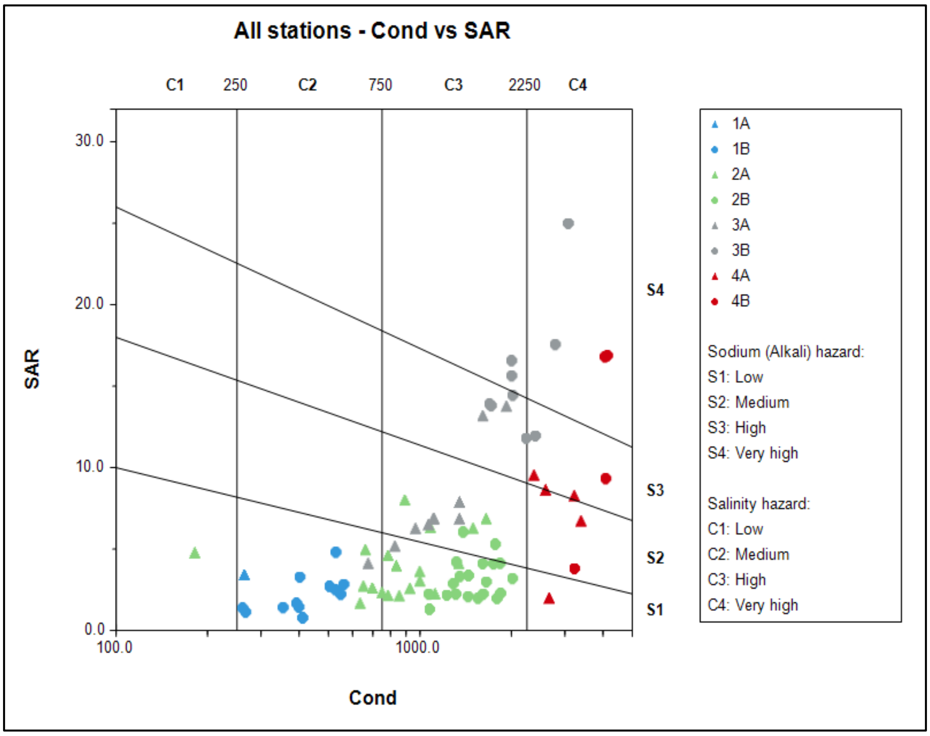

Figure 5.4.3: The Wilcox diagram classification of water groups. Noticeably, most samples fall within the low sodium hazard (S1) with high salinity hazard (C3).

5.5 Assessment of Seasonal Change

Paired sample t-tests (n=51) of seasonal repeats from the same bore resulted in non-significant p-values at 95% confidence for all Na^+, K^+, Ca^{2+}, Mg^{2+}, HCO_3^-, Cl^-, SO_4^{2-}, and EC tests, with values much less than significance ($p < 0.05$). Slight variability was detected in pH between the 2018 and 2019 Dry seasons and the 2018 Wet and 2019 Dry seasons (p-value <0.05 95% confidence). Temperature showed the greatest variability between the 2018 Wet and Dry season samples (p-value: 0.012), yet with only slight variability between the 2018 Wet and 2019 Dry season samples. No variability was detected between the 2018 Dry and 2019 Dry season samples. This indicates that groundwater temperatures may experience slight variations seasonally. Presumably, this would mostly affect shallower groundwater systems or those fed by quick surficial recharge pathways like creeks and streams, which are known in the area (Murtha 1975a pp. 6).

Paired sample correlations averaged 90% ($r^2 = 0.90$) between all variables and seasons, indicating that the ranked values of each individual season, across all variables, tends to be the same. This means that if the ranking of a sample site variable ranked lower in one season, it tended to rank lower in the comparative season.

Linear trends of stable isotope results (fig. 5.5.1) show nearly identical slopes between all three sampling sessions and near identical y-intercepts. The slopes for the 2018 Wet, 2018 Dry, and 2019 Dry seasons were 6.67, 6.58, and 6.55, respectively, and the y-intercepts were 2.04, 2.01, and 1.25, again respectively. All samples fall to the right of the Australian local meteoric water line (LMWL) and on or to the right of the global meteoric water line (GMWL), except for the three most depleted ^{18}O samples.

Groundwater hydrogeochemistry can fluctuate throughout the year as determined by many various local factors (Kumar *et al*. 2014). As previously noted, the number of repeated samples is limited, however, the available data shows that major ion values were consistent at each location during each sampling season.

These results can be explained by either 1) the groundwater chemistry remaining generally stable throughout the year, or 2) that each sample is the consistent end-member for the annual shift in hydrogeochemical signature, or 3) the sampling periodicity was insufficient to detect short-er term variations. Since the sampling sessions were 6-12 months apart, further research is required to determine hydrogeochemical variations on a shorter time scale. This sample set suggests that the annual hydrogeochemical signature of groundwaters in the area are consistent.

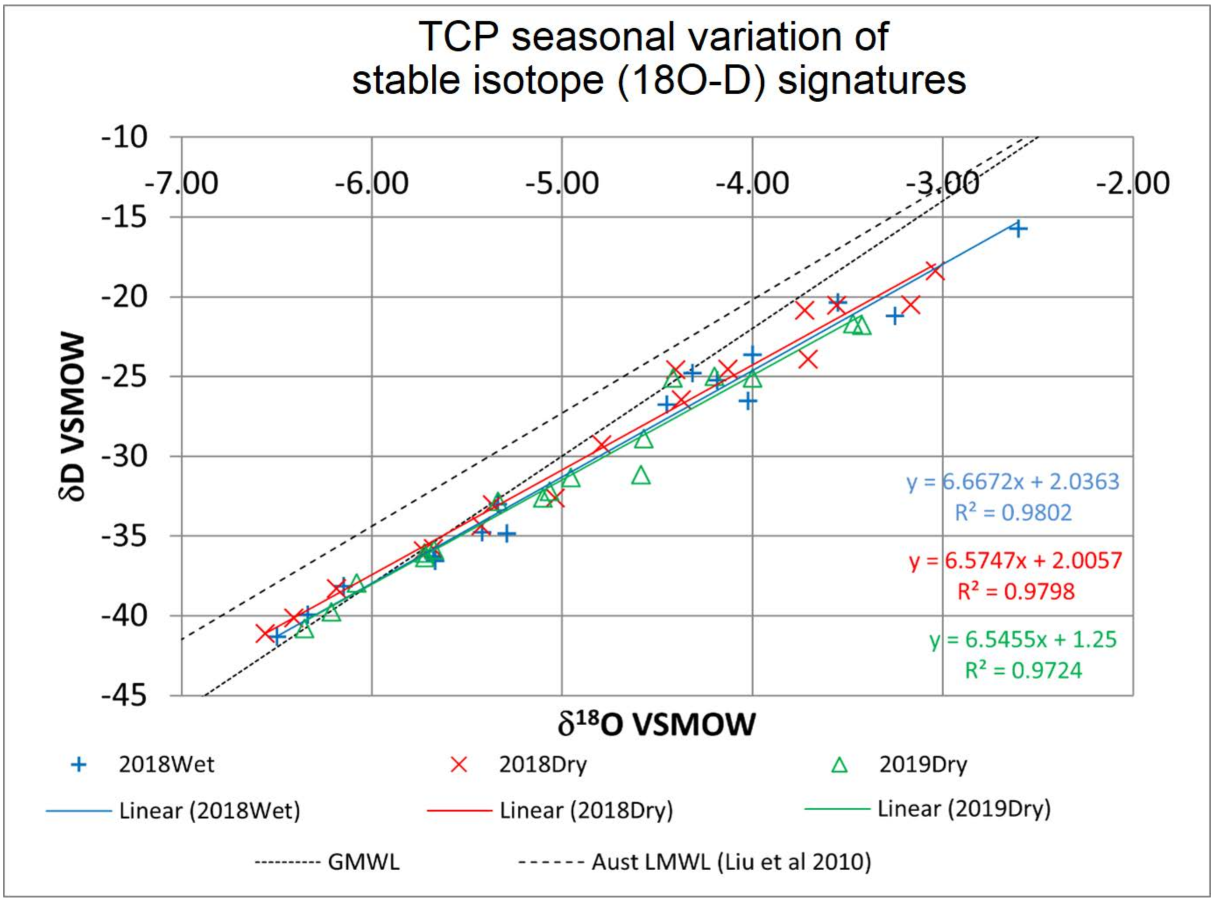

Figure 5.5.1: Water isotope results from the seasonal analysis of groundwater samples. Each season's samples (n=17) show near identical linear trends with r^2 values above 0.97, indicating consistency in ^{18}O and D values.

5.6 Discussion of Findings

Coastal plain aquifers worldwide have become the focus of extensive investigation due to concerns related to overextraction and degradation (Villholth and Conti 2018; Singh *et al.* 2017; Chucuya *et al.* 2022). These investigations encompass various water quality aspects, particularly those concerning drinking, irrigation, industrial, and agricultural uses. Coastal regions, in particular, face the added risk of saline intrusion. In the study area, water supply is drawn from a reticulated system managed by the local government, with the research aimed at assessing water quality standards beyond those applicable to drinking water.

Irrigation water quality has been assessed because domestic bores are used mainly for irrigation purposes, and the quality of groundwater can affect the soil being irrigated. Residual salts deposited in the soil from groundwater irrigation can resurface in drainage water or be leached by rainfall, entering the groundwater system as recharge (Hem 1985; Singh *et al.* 2017).

Elevated concentrations of carbonates can react with Na^{+} ions to form $NaHCO_3$, potentially impacting soil structure (Hem 1985). The RSC analysis revealed significant differences among the water groups. While most groundwaters exhibited suitable hydrogeochemistry for irrigation, exceptions were observed in Groups 2A and 3B. Group 2A was largely marginally suitable to unsuitable, whereas 70% of Group 3B was deemed unsuitable. Notably, Group 4B, with the highest average EC, demonstrated suitability for most samples. Hence, the precipitation of carbonate minerals remains a concern across fresher to moderately evolved groundwaters of the TCP.

Sodium concentration plays a pivotal role in assessing irrigation water quality, with SAR values indicating slight to moderate risks across all groundwaters except Groups 2B and 4. Groups 2B and 4A/B groundwaters, prevalent across the TCP, can be used without the potential to harm soil structure in areas with alkali soils.

The Wilcox diagram categorized the "sodium hazard" relationship based on salinity and excess sodium, resulting in medium to very high salinity levels across all water groups. Sodium hazards ranged from low to very high, with Group 4A slightly better than 4B. These findings indicate that not all groundwaters around the TCP are suitable for irrigation and should be contingent on the main soil type present in the area of use. Sodium emerges as the most critical factor in water quality, followed closely by alkalinity and concentrations of calcium and magnesium, all integral in influencing soil structure.

The estimated recharge rates for groundwater samples show significant and distinct differences between water groups. Group 1 demonstrates the highest recharge rates, averaging 75 mm/yr, while Group 4 exhibits the lowest, averaging only 3 mm/yr. Subgroups within each group reveal variations, with fresher groundwater signatures generally associated with higher recharge rates. Examination of recharge rates in relation to bore depth highlights variable patterns, with some subgroups exhibiting consistent trends and others showing variability. Overall, the study underscores the inverse relationship between recharge rates and EC concentrations across the water groups, with fresher groundwater having higher recharge rates.

In conclusion, the assessment of water quality in coastal plain aquifers in the TCP highlights the multifaceted nature of groundwater quality and its implications for various uses, particularly for irrigation. Significant variations in water quality parameters are present among distinct water groups, with sodium concentration identified as a critical factor affecting soil structure and permeability. The findings underscore the importance of considering the interplay between groundwater chemistry and soil characteristics in irrigation practices. The study provides insights into recharge rates, indicating higher rates for fresher groundwater.

5.7 References – Chapter 5

Chucuya, S, Vera, A, Pino-Vargas, E, Steenken, A, Mahlknecht, J, and Montalván, I, 2022, ‘Hydrogeochemical Characterization and Identification of Factors Influencing Groundwater Quality in Coastal Aquifers, Case: La Yarada, Tacna, Peru’, International Journal of Environmental Research and Public Health, vol. 19, 2815. https://doi.org/10.3390/ijerph19052815.

Clark, I 2015, *Groundwater Geochemistry and Isotopes*, CRC Press, Taylor and Francis Group, 428 p., DOI: 10.1201/b18347.

Clark, ID and Fritz, P 1997, *Environmental Isotopes in Hydrogeology*, CRC Press, Taylor & Francis Group, 328 p., ISBN 1-56670-249-6.

Crosbie, R, Morrow, D, Cresswell, R, Leaney, F, Lamontagne, S, and Lefournour, M, 2012, ‘New insights to the chemical and isotopic composition of rainfall across Australia’, CSIRO Water for a Healthy Country Flagship, Australia, CSIRO:EP125581, DOI: 10.5072/83/5849a0d6c685a.

Hem JD 1985, Study and Interpretation of Chemical Characteristics of Natural Water, 3 ed., U.S. Geological Survey (USGS) Water-Supply Paper 2254, Department of the Interior, United States Geological Survey.

Kumar, PJS, Elango, E, and James, EJ 2014, ‘Assessment of hydrochemistry and groundwater quality in the coastal area of South Chennai, India’, *Arabian Journal of Geosciences*, 7, pp. 2641-2653, DOI: 10.1007/s12517-013-0940-3.

Liu, J, Fu, G, Song, X, Charles, SP, Zhang, Y, Han, D, and Wang, S 2010, ‘Stable Isotopic Compositions in Australian Precipitation”, *Journal of Geophysical Research*, vol. 115(D23), 2010, DOI: 10.1029/2010JD014403.

Lowenstein, TK, Hardie, LA, Timofeeff, MN, and Demicco, RV 2003, ‘Secular variation in seawater chemistry and the origin of calcium chloride basinal brines’, *Geology*, vol. 31(10), pp. 857-860, DOI: 10.1130/G19728R.1.

Murtha, GG 1975a, ‘Soils and Land Use on the Northern Section of the Townsville Coastal Plain, North Queensland’, Soils and Land Use Series No. 55, CSIRO, viewed 15 April 2019, <https://publications.qld.gov.au/sl/dataset/soil-townsville-zed/resource/8b49d47d-889e-4632-9cd0-4f68d4c4652b>.

Singh, CH, Kumar, An, Shashtri, S, Kumar, Al, Kumar, P, and Mallick, J 2017, ‘Multivariate statistical analysis and geochemical modelling for geochemical assessment of groundwater of Delhi, India’, *Journal of Geochemical Exploration*, Elsevier, vol. 175, pp. 59-71, DOI: 10.1016/j.gexplo.2017.01.001.

Todd, D, and Mays, L 2005, *Groundwater Hydrology*, 3rd Edition, John Wiley and Sons, Inc., Hoboken, 652 p., ISBN: 978-1-118-00177-6.

Villholth, KG and Conti, KI 2018, ‘Groundwater governance: rationale, definition, current state and heuristic framework’, in Villholth, López_Gunn, Conti, Garrido & van der Gun (eds), *Advances in Groundwater Governance*, CRC Press, Taylor & Francis Group, pp. 3-31. Available from www.un-igrac.org.

Wilcox, LV 1955, ‘Irrigation Waters’, United States Salinity Laboratory, circular no. 969, United States Department of Agriculture, retrieved 01 July 2023 from <https://www.ars.usda.gov/arsuserfiles/20360500/pdf_pubs/P0192.pdf>.

Wood, WW 1999, ‘Use and misuse of the chloride-mass balance method in estimating ground water recharge’, *Ground Water*, Vol. 37(1), National Ground Water Association, pp. 1-2.

Wood, WW and Sanford, WE 1995, ‘Chemical and isotopic methods for quantifying ground-water recharge in a regional, semiarid environment’, *Ground Water*, Vol. 33(3), National Ground Water Association, pp. 458-468, DOI: . 10.1111/j.1745-6584.1995.tb00302.x.

Zaman, M, Shahid, SA, and Heng, L 2018 'Irrigation Water Quality', In: Guideline for Salinity Assessment, Mitigation and Adaptation Using Nuclear and Related Techniques, Springer, Cham, DOI: 10.1007/978-3-319-96190-3_5.

Chapter 6: Conclusion

6.1 Summary of Research Findings

This investigation aimed to address key research questions regarding the geological features, hydrogeochemical patterns, and their implications for effective groundwater resource management in the TCP. In this section, a comprehensive synthesis of the research findings concerning the hydrogeochemical characteristics, spatial distribution, and dominant factors influencing groundwater chemistry in the coastal plain aquifers of Townsville, Australia, is provided. The following are the key research questions and a synthesis of the results answering each of the questions:

Research Questions:

1. To what extent do geographic and geological features influence the hydrogeochemical characteristics of coastal plain groundwater systems in Townsville, Australia?

To investigate the extent to which geographic and geological features, such as fractured rock aquifers and limestone/dolomite areas, influence the hydrogeochemical characteristics, recharge patterns, and water quality parameters of coastal plain groundwater systems in Townsville, Australia, the hydro-chemical distinctions among the water groups delineated by HCA were analysed.

The HCA method categorized the dataset into four primary water groups, each exhibiting distinct hydrogeochemical patterns.

Group 1 symbolizes the least saline composition overall and represents freshwater characteristics. Group 1A, located near Woodstock and Bushland Beach is the freshest water composition in the dataset, sourced from local precipitation with limited influence from seawater due to distance from the coast and sufficient hydraulic gradient. Ten of the 14 samples (71.4%) in Group 1 had recorded depths and averaged 21.9m.

Group 2, characterized by a significant increase in EC compared to Group 1, displays notable variations between Group 2A and 2B, particularly in SO_4^{2-}, Ca^{2+}, and Mg^{2+} concentrations, reflecting differences in water chemistry influenced by different geological features and settings that most likely include carbonate dissolution. Group 2 waters are located across the TCP, from the suburb of Calcium, near Woodstock in the Upper Ross River basin, to the suburbs of Kelso, Rangewood and Deeragun on the western side of the TCP and surrounding the Mount Stuart complex. Also, Group 2 waters are not located near Group 3 waters or in the lower elevation levels of the coastal plain. Seventeen of the 19 samples (89.5%) had recorded depths and averaged 29.3m. Individually, Group 2A averaged 32.2m and Group 2B averaged 26.4m bore depth.

Both Group 3A and 3B exhibit parallel trends, with Group 3B displaying higher SO_4^{2-} and Na^+ concentrations. This group is localised in the suburbs of Pimlico, Mysterton, Hyde Park and South Townsville. Sixteen of the 20 samples for Group 3 had depths recorded and averaged 10.6m in depth. Individually, the bore depth for Group 3A and 3B was 10.4m and 10.8m, respectively.

Group 4, the most saline, demonstrates significant shifts in major ion concentrations between subgroups, suggesting complex interactions with geological features, probable flow rates, and potential seawater intrusion in current and former estuarine areas. Group 4 waters are mostly located near the centre of the TCP, in the suburbs of Douglas, Annandale, Mundingburra, Kirwan, Mount Louisa, Currajong, and Pimlico, with one sample located in Mount Low. Fourteen of the 19 samples (73.7%) had recorded bore depths and averaged 19.8m. Individually, the bore depth for Group 4 A and B groundwaters averaged 21.4m and 19m, respectively.

The hydro-chemical distinctions among the water groups delineated by HCA have revealed clear hydrogeochemical patterns within the groundwater system. These patterns highlight the influence of geological features in the hydrogeochemical characteristics and water quality parameters of the coastal plain. These parameters can be used to further update and inform water policy for areas of high growth or potential environmental detriments to the soil – which have carry-on effects in waterways leading to the GBR lagoon.

PCA further elucidates the hydro-chemical relationships within the dataset. PC1 primarily reflects Mg^{2+}, Ca^{2+}, and $CaCO_3$, indicating their significant influence on groundwater chemistry, which is interpreted to be dominated by carbonate dissolution. PC2, on the other hand, is mainly influenced by K^+ and SO_4^{2-} suggesting distinct hydro-chemical processes. SO_4^{2-} ions may originate from SO_4^{2-} minerals, such as gypsum ($CaSO_4{\cdot}2H_2O$) and anhydrite ($CaSO_4$). These minerals can dissolve into groundwater from geological formations containing evaporite deposits, such as sedimentary basins and coastal plains like Townsville. Other sources of SO_4^{2-} include the less-likely oxidation of sulphide minerals, to the more-likely seawater intrusion and biogeochemical processes. K^+ is commonly sourced from the weathering of potassium-bearing minerals in granitic and metamorphic rocks but also, more applicably, from evaporite deposits containing potassium salts. The co-occurrence of SO_4^{2-} and K^+ ions in groundwater suggests potential interactions between geological processes and hydrological conditions, including seawater intrusion and mineral weathering.

The distribution of water groups determined by HCA analysis on the PCA plot illustrates the influence of geological features on groundwater chemistry. Group 1 waters predominantly reside within the negative PC1 realm, indicating limited influence from major ions Mg^{2+} and Ca^{2+}. In contrast, Group 4B, housing the most saline samples, clusters within the positive domains of both PC1 and PC2, indicating complexity to the interactions and interconnectedness of the aquifer systems and geological formations.

In summary, the hydrogeochemical characteristics, recharge patterns, and water quality parameters of coastal plain groundwater systems in the TCP are significantly influenced by geological features, which include limestone/dolomite areas and most-likely former estuarine areas. Understanding these influences is crucial for effective groundwater resource management, facilitating the implementation of targeted strategies to ensure sustainability of the systems.

2. How does the hydrogeochemical composition, recharge dynamics, and water quality of coastal plain groundwater systems in Townsville, Australia, vary?

The hydrogeochemical composition of coastal plain groundwater systems in Townsville, Australia, is characterised by a wide array of parameters and variability in these parameters reflects the complex hydrological processes of the region. The pH values of the groundwater samples are neutral to slightly acidic, with an average of 6.8. The EC ranges from 137 to 7060 µS/cm, indicating variations in dissolved solids content across different areas, being generally lower in the upper parts of the catchments and increasing seaward. Na^+ is the dominant cation, with concentrations highest in coastal areas and decreasing inland. Ca^{2+} and Mg^{2+} are significant constituents that are influenced by mineral dissolution processes, with Ca^{2+} concentrations ranging from 17 to 674 mg/l and Mg^{2+} concentrations between 0 to 542 mg/l. The alkalinity of the groundwater primarily originates from carbon dioxide species dissolution and carbonate minerals, with HCO_3^- being the dominant anion. Cl^- and SO_4^{2-} concentrations vary widely, being influenced by sedimentary rock formations and dissolution processes. The water types are Na-Cl and Na-HCO_3 dominated, with variability reflecting the hydrogeochemical processes and mixing dynamics within the different aquifer systems; these processes include freshening, dissolution, evaporation, rock weathering, and potentially seawater intrusion.

HCA categorized the dataset into four primary water groups, each further divided into 'A' and 'B' subgroups, based on variations in salinity and chemical compositions. Group 1 represents the freshest water composition, while subsequent groups (Groups 2, 3, and 4) show increasing EC and distinct variations in major ion concentrations. The spatial distribution of water groups reveals certain patterns within the study area. Group 1 waters are predominantly located in the upper reaches of the catchment and near the coast. Group 2 waters are found along the sides of the Ross River and Mount Stuart complex, with exceptions in northern areas. These coincide with higher concentrations of ions in waters or groundwater systems with more heterogeneity, while Group 3 is clustered near the end of the Ross River in estuarine areas. Group 4 waters are located centrally and exhibit the highest salinity levels, and most likely represent highly concentrated waters from clay sediments, seawater incursion, or connate water trapped in topographical low areas of bedrock.

Recharge rates in TCP groundwater systems exhibit significant variability across different water groups, and the Mount Stuart complex is identified as a common recharge area for groundwater systems. The estimated recharge rates are higher for fresher groundwater signatures and all recharge rates are relatively low, reflecting the dry tropical climate of the area.

Water quality assessments underscore the importance of considering groundwater suitability for irrigation purposes. The RSC and SAR assessments suggest samples fall within the 'suitable' category. However, exceptions are observed in certain water groups, particularly Group 2A and Group 3B, indicating marginal to unsuitable groundwater quality for irrigation. The Wilcox diagram reveals medium to very high salinity levels across all water groups with sodium hazards ranging from low to very high and Group 4 exhibiting the highest salinity levels.

In summary, the hydrogeochemical composition, recharge dynamics, and water quality of coastal plain groundwater systems in Townsville exhibit complex spatial variations and interactions. While similarities exist in the dominance of certain ions and hydrogeochemical processes across different areas, significant differences are observed in recharge rates and water quality parameters among distinct water groups. Understanding these variations is crucial for sustainable groundwater management and the development of effective strategies to mitigate potential risks associated with groundwater extraction and irrigation practices.

3. How can an understanding of geographical and hydrogeological factors contribute to effective decision-making regarding water quality monitoring and sustainable use of groundwater resources?

This study addresses the third research question regarding the dominant factors that influence the distribution and variability of groundwater chemistry in the TCP and explores how this understanding can contribute to effective decision-making for water quality monitoring and sustainable groundwater use. The findings reveal that groundwater chemistry in the TCP is strongly influenced by geological processes such as carbonate dissolution, clay interactions, and evaporite processes. These factors play a significant role in controlling the distribution and chemical composition of groundwater, as well as contributing to major ion variability across distinct water groups within the region. Understanding these primary geological and hydrogeochemical drivers is needed for effective groundwater management, as it provides a foundation for monitoring programs, assessing risks to water quality, and implementing management strategies that consider the unique characteristics of each water group and its area of use.

Through PCA, this study identifies correlations among hydrogeochemical variables, showing the underlying processes that govern groundwater chemistry. These insights into the relationships between various ions help to understand the dominant processes that impact water quality and support decision-makers in prioritizing actions to mitigate contamination risks, adjust land-use plans, and protect groundwater resources. HCA further helps understanding by grouping groundwater samples into distinct water categories, each characterized by unique salinity and ion concentration profiles. This grouping provides practical guidance for water managers, allowing for the development of intervention strategies and monitoring frameworks tailored to specific hydrogeochemical characteristics and risk factors.

The assessment of groundwater quality for irrigation reveals additional complexities, as sodium concentrations, and other factors such as RSC and SAR, are found to vary significantly among the water groups. These variations have direct implications for soil health in particular areas, in terms of structure and permeability, as high sodium concentrations can degrade soil integrity over time. The use of the Wilcox diagram highlights these differences by categorizing groundwater samples based on their sodium hazard and salinity levels, revealing that some sources may not be suitable for irrigation without potentially compromising soil structure in areas of alkali soils. By identifying sodium as a critical factor, along with alkalinity, calcium, and magnesium concentrations, this analysis underscores the importance of incorporating water quality data into irrigation practices to prevent soil degradation in areas where alkali soils are prevalent.

The analysis of recharge rates using the CMB method highlights further differences between water groups, indicating variability in groundwater replenishment across the TCP. Recharge rates were generally low, with higher rates in fresher groundwater samples, while lower recharge was associated with more saline groundwater. This variation suggests an inverse relationship between recharge rates and EC, with fresher water groups exhibiting greater recharge. This understanding of recharge variability is needed for sustainable groundwater use, as it provides the data needed to anticipate risks associated with overextraction and to implement resource management practices that balance groundwater withdrawal with natural recharge rates. Protecting groundwater quality is essential for maintaining these recharge processes and sustaining the aquifer over the long term.

The hydrogeochemical tools used in this study, including Schoeller's chloro-alkaline indices and the Gibbs diagram, further enhance the understanding of groundwater chemistry by offering insights into specific chemical interactions. Schoeller's indices quantify ion exchange mechanisms, distinguishing between processes such as silicate weathering and evaporite dissolution, while the Gibbs diagram visually represents dominant hydrogeochemical processes that govern water chemistry across the TCP. These tools facilitate an understanding of groundwater dynamics, including potential seawater intrusion, which is vital for informed decision-making in regions where hydrogeochemistry may negatively impact soil and water quality. By understanding the interactions between groundwater chemistry and soil characteristics, decision-makers can develop proactive measures for land-use planning and risk mitigation that safeguard both water and soil health. The integration of these hydrogeochemical analyses, including HCA, PCA, and recharge rate estimation, provides an understanding of groundwater dynamics in the TCP, allowing for informed decisions that prioritize water security, ecological health, and resource sustainability.

In conclusion, this research provides a robust foundation for sustainable groundwater management in Townsville by clarifying the relationships between geological formations, recharge rates, and water chemistry. The study contributes to science by demonstrating the importance of combining empirical data and scientific analysis to inform evidence-based decision-making. The insights gained here are critical for the development of management frameworks that support the sustainable use of groundwater, enhance water quality monitoring, and preserve ecological balance in the TCP and similar coastal aquifer systems facing pressures from urbanization and increased demand.

6.2 Discussion and Implications

This study contributes critical insights into the understanding of groundwater dynamics in the TCP, a dry tropical region with groundwater resources highly susceptible to salinity and seawater intrusion risks. By analysing the hydrogeochemical and hydrogeological factors influencing groundwater quality and recharge rates, this research provides a scientific foundation for sustainable management of the environmental and climate challenges faced in the TCP. The implications of these findings resonate beyond the local context, offering broader insights relevant to similar coastal aquifers, including the Burdekin floodplain, the Pimpama Coastal Plain, and comparable systems worldwide.

Research on the Burdekin floodplain aquifer, a tropical groundwater system extensively used for agriculture, has revealed increased salinity over decades due to factors such as evapotranspiration of irrigation water, mixing with relict seawater, and seawater intrusion (Lenahan and Bristow 2010). Given the hydrogeological similarities between the TCP and Burdekin regions, such as the complex successions of Quaternary terrigenous and marine sediments and the presence of relict seawater, it is plausible that the TCP may experience comparable salinity dynamics. This is particularly relevant given the low recharge rates estimated through the CMB analysis in the TCP, which may be influenced by the presence of connate seawater, affecting chloride concentrations and potentially skewing recharge estimations. This aligns with findings in the Burdekin floodplain, where chloride concentrations vary significantly from <50 mg/l to >50,000 mg/l across different areas (Lenahan and Bristow 2010).

Further insights are available from the Pimpama Coastal Plain, situated in southern Moreton Bay. The Pimpama aquifer exhibits dual flow systems: a deeper system responsive to seasonal patterns and a shallower system influenced by individual rainfall events. The presence of elevated potentiometric heads in semi-confined aquifers in the Pimpama region results in upward movement of saline to hypersaline groundwater (Harbison and Cox 2002). The TCP, which also contains semi-confined aquifers as evidenced by observed rises in water levels within bore casings, may similarly experience upward groundwater movement. However, in the TCP, the deeper groundwater system (Group 2) generally exhibits fresher water, which implies that, unlike the Pimpama system, this upward movement could result in a “freshening” effect on overlying, more saline waters (Group 4). Personal correspondence with local residents has also indicated the historical presence of springs around Townsville, suggesting that some groundwater systems were previously under artesian pressure, a condition consistent with the semi-confined aquifers observed today.

The TCP also shares characteristics with other coastal aquifers along the GBR coastline in terms of submarine groundwater discharge (SGD) processes. In coastal regions along the GBR, SGD includes both freshwater discharge from land as well as seawater circulation through sediments. In the context of the TCP, SGD is exemplified by known "wonky holes," or submarine springs discharging freshwater into the ocean. These springs are driven by potentiometric pressure within coastal aquifers, allowing freshwater to discharge under the ocean floor. However, excessive groundwater extraction in the TCP could reduce this potentiometric pressure, potentially allowing seawater to be “pulled” into the aquifer system or accelerating the rate of seawater intrusion. This underscores the importance of managing extraction rates to preserve the natural balance of SGD and prevent the encroachment of seawater into freshwater aquifers, which are critical to the ecological health of near-shore reef environments (Stieglitz 2005; Harbison and Cox 2002).

The study’s findings not only contribute to advancing scientific understanding but also inform evidence-based decision-making for sustainable water resource management. The data generated through this research directly supports risk management efforts by expanding the knowledge base needed for informed groundwater management decisions. Effective risk management in groundwater systems necessitates addressing inherent uncertainties in hydrogeological properties and recharge processes. In clay-rich soils, such as those prevalent in the TCP, the impact of total annual rainfall on recharge rates is lower compared to other climate characteristics, due to the low hydraulic conductivity typical of clay soils. This pattern is consistent in climate types like Aw, characteristic of the TCP, where climate conditions beyond annual rainfall, such as evaporation and temperature, can have a more substantial influence on recharge (Barron *et al.* 2010). Understanding these subtleties is crucial for effective planning in the TCP, where climate projections indicate potential rapid changes, including shifts that could influence groundwater availability (CSIRO 2020).

In addition to climate-related uncertainties, sustainable groundwater management depends on data to establish baseline resource conditions and to measure the effects of management interventions over time. Groundwater Information Systems (GWIS) provide a “bookkeeping” framework, essential for tracking extraction and recharge, which are necessary for responsible aquifer management. Shallow or unconfined aquifers, high-extraction regions, and systems influenced by climate factors require more frequent monitoring. In the TCP, a GWIS could enable tracking of critical metrics, facilitating informed decision-making aimed at maintaining the balance between extraction and recharge (Staples *et al.* 2020).

In addition to supporting risk assessment frameworks, the findings from this research lay the groundwork for enhanced resource management in similar coastal systems. Comparative analysis with the Burdekin floodplain and the Pimpama Coastal Plain underscores the stratification, variability, and recharge complexities characteristic of these aquifers. For instance, salinity levels in the Burdekin aquifer have been observed to increase due to processes such as evapotranspiration, seawater intrusion, and mixing with relict seawater—processes that may also impact the TCP due to shared geological and climatic characteristics (Lenahan and Bristow 2010). Additionally, in both the TCP and Pimpama systems, groundwater flows respond variably to climate and extraction pressures, indicating a need for adaptive management that accounts for these dynamic and interconnected processes.

The TCP's stratified and heterogeneous groundwater system aligns with findings from both the Burdekin and Pimpama studies, reinforcing the understanding that coastal aquifers along Australia's eastern coastline often exhibit significant variability in water quality, stratification, and recharge mechanisms. For example, in both the Pimpama and Burdekin systems, groundwater quality varies across depth, with salinity levels influenced by complex mixing processes rather than simple freshwater recharge or seawater encroachment alone. In the TCP, similar hydrogeochemical analyses, including salinity measurements, ionic ratios, and stable isotope assessments, allowed for the identification of distinct groundwater groups with varying salinity and ionic composition. This supports the findings from the Pimpama study, where discrimination between groundwater bodies was achieved through these same parameters, underscoring the effectiveness of these methodologies in characterizing groundwater systems within complex coastal aquifers (Harbison and Cox 2002).

Additionally, like the Pimpama region, the TCP is predominantly a domestic groundwater resource, with extraction primarily for lawn and garden irrigation rather than large-scale agricultural use. Despite differences in usage, the fundamental processes remain comparable. Groundwater extracted for irrigation undergoes soil infiltration and evapotranspiration, potentially concentrating solutes in the soil. In semi-arid coastal regions, this can lead to an accumulation of salts in the unsaturated zone, impacting both groundwater quality and soil health over time.

Recharge mechanisms in the TCP are also comparable to those observed in the Pimpama Coastal Plain. While shallow groundwater recharge in the TCP occurs primarily through direct infiltration, deeper groundwater recharge likely includes contributions from landward ranges, such as the Mount Stuart complex, which has been identified as a recharge source for at least two groundwater systems within the plain. Given that the TCP's geological history includes the same ocean level fluctuations as regions like Moreton Bay, its sediment composition (Quaternary-age marine, estuarine, fluvial, and alluvial deposits) further supports the notion of complex recharge and mixing dynamics. The existence of paleochannels within the TCP is also indicative of fluvial incision processes that shaped the coastal plain around 18,000 years ago, providing conduits for groundwater flow and storage, similar to those observed in Moreton Bay (Harbison and Cox, 2002).

The study's implications extend to broader environmental and climate considerations. Projected climate impacts, such as sea level rise and decreased seasonal rainfall, may exacerbate extraction-induced risks of seawater intrusion in the TCP. Reduced rainfall and increased evapotranspiration may further concentrate solutes in the soil, particularly in areas where groundwater is used for domestic irrigation. Given the fragile balance of these coastal aquifers, management practices should focus on preserving the natural recharge-discharge dynamics, mitigating the risk of accelerated seawater intrusion, and ensuring that extraction rates do not compromise groundwater quality (CSIRO 2020, Hennessy *et al*. 2008, Harbison and Cox 2002, Stieglitz 2005).

In conclusion, this research offers a detailed examination of groundwater dynamics within the TCP, contributing valuable insights to the broader understanding of coastal aquifers along Australia's eastern coastline. Through comparative analysis with similar systems, such as the Burdekin and Pimpama coastal plains, this study highlights the stratification, variability, and complex recharge mechanisms characteristic of these regions. The findings provide a scientific basis for the development of targeted groundwater management strategies to protect water quality and sustain groundwater resources in the TCP under changing climate conditions. By enhancing the scientific knowledge base, this research supports informed decision-making and the establishment of effective monitoring networks, aiding in the development of adaptive, evidence-based strategies for sustainable groundwater management (Arroyo-Figueroa *et al*. 2024).

6.3 Recommendations for Future Research

In certain contexts, the presence of iodide, boron, bromide and barium tracers can offer valuable insights for differentiating whether an aquifer has been impacted by seawater or other saline sources. To distinguish between seawater intrusion and contamination from connate brine, successful methodologies have encompassed the comparative analysis of iodide, boron, and barium concentrations in groundwater samples (Hem 1985 pp. 98). As future research advances our understanding of the Townsville region's groundwater systems, incorporating these analytes in initial assessments could help identify aquifer systems influenced by seawater intrusion. Furthermore, periodic monitoring of these elements may facilitate the ongoing delineation and tracking of intrusion boundaries.

Creek to Coral (2007 pp. 10) notes that preserving recharge areas in the upper catchment is crucial for maintaining water quantity in aquifers, as well as ensuring water quality and quantity upon discharge into marine ecosystems and that monitoring of coastal groundwater extraction is essential to avert rising salinity in aquifers and mitigate the potential strain on coastal vegetation and riparian zones. The key issues identified in this report are arguably still present today. Recommendations are consistent within the literature and can be summarized in recharge areas needing to be protected and groundwater extraction should be carefully monitored (Creek to Coral 2007 pp. 10). Creek to Coral (2007 pp. 3) notes that the hydrogeochemical maps produced by Reid (1975) were not available. The maps were located and are included in Appendix 4.

Water quality results from subsequent reports (Creek to Coral 2008 pp. i) indicate that the water quality in the Ross River basin were indicated as 'disturbed'. The water quality will continue to deteriorate without increased monitoring and policy intervention to regulate groundwater use and bore installations. Initial monitoring and sampling are recommended to commence in areas where there is the highest bore density for existing (EX) domestic bores (fig. 6.3.1). This includes the suburbs of Rasmussen and Kelso, which have a bore density of 15-22 bores per square kilometre (sq/Km). Additional areas recommended for the start of monitoring include the suburbs of Pimlico, Currajong, Mysterton, and Hermit Park as these suburbs generally show Group 3 waters, which pose the greatest risk to alkali soils. These soils are prevalent across the TCP and special consideration needs to be given to qualifying and quantifying soil loss, sediment loads in run-off and creeks and streams that drain to the GBR lagoon.

Future research should examine submarine groundwater discharge (SGD) off the coast of Townsville, which are known to exist (Stieglitz 2005). This research should identify SGD aquifer systems in the TCP and examine consequences and effects of over-extraction in these aquifers and the impacts on marine ecosystems in the GBR.

Lastly, results from groundwater age-dating (14-carbon and tritium) performed on three samples was completed but was deemed beyond the scope of this study. These results are included in Appendix 3, and each sample location is denoted by the Queensland bore registration number (RN).

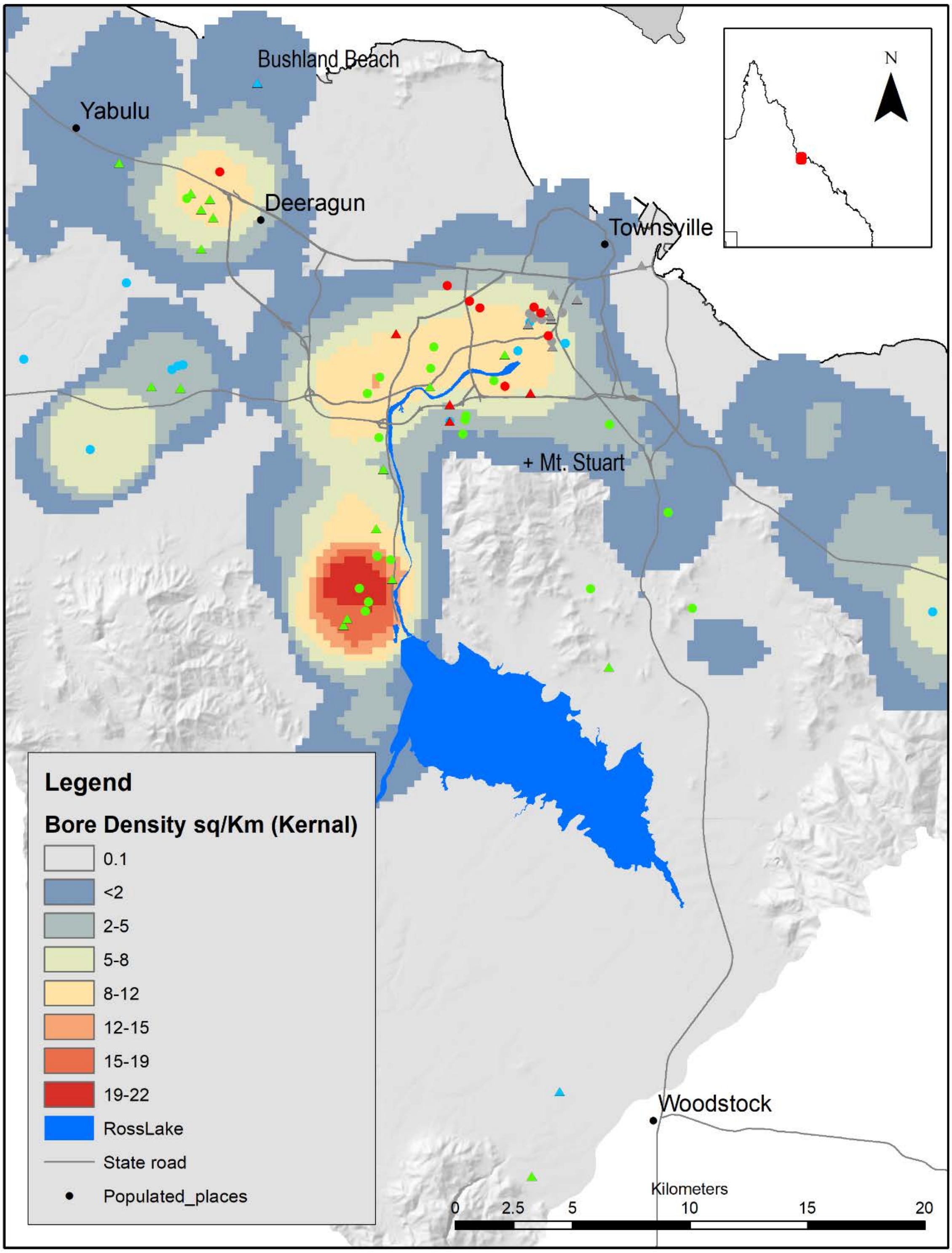

Figure 6.3.1: Kernal density of registered, domestic bores in the study area, with the current status of 'existing' (EX). The suburbs of Kelso and Rasmussen have the highest density at 15-22 bores per sq/Km.

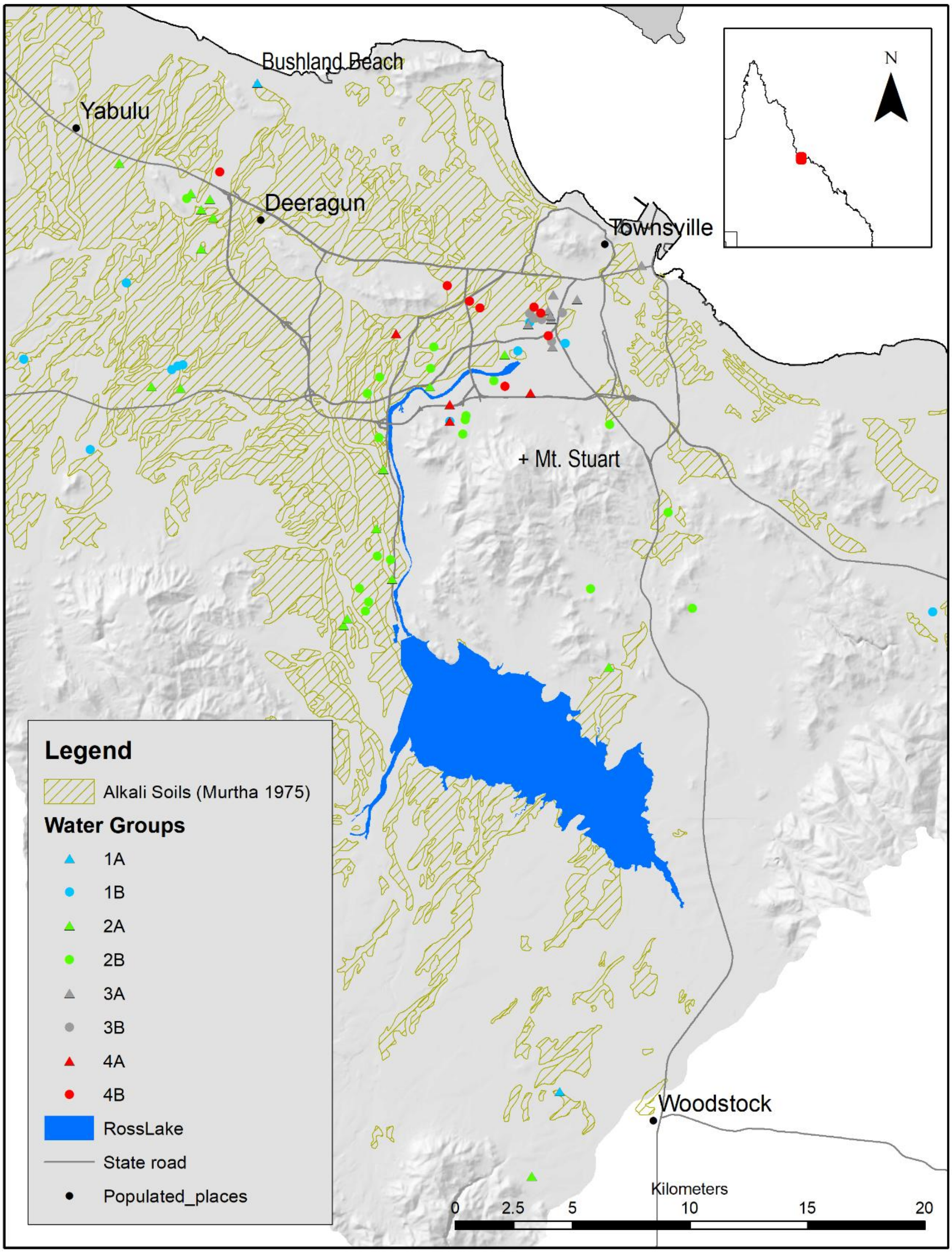

Figure 6.3.2: Regional map of the study area showing sample locations and the prevalence of alkali soils (modified from Murtha 1975 a and b). Use of high SAR value groundwater for irrigation on alkali soils can lead to decrease soil permeability and loss of soil structure, resulting in increased sediment loads in run-off waters emptying into the GBR lagoon.

References - Master

Appelo, CAJ and Postma, D 2005, *Geochemistry, groundwater and pollution*, 2 ed., Taylor and Francis, A.A. Balkema Publishers, Great Britain.

An, G, Kang, H, Fu, R, Xu, D and Li, J 2023, ‘Investigation on the Hydrogeochemical Characteristics and Controlling Mechanisms of Groundwater in the Coastal Aquifer’, *Water*, MDPI, vol. 15(9), DOI: 10.3390/w15091710.

Ansari, AA and Umar R 2019, ‘Evaluation of hydrogeochemical characteristics and groundwater quality in the quaternary aquifers of Unnao District, Uttar Pradesh, India’, *HydroResearch*, vol. 1, pp. 36-47, DOI: 10.1016/j.hydres.2019.01.001.

Arroyo-Figueroa C, Chalá DC, Gutiérrez-Ribon G, Quiñones-Bolaños E 2024, ‘A Framework to Evaluate Groundwater Quality and the Relationship between Rock Weathering and Groundwater Hydrogeochemistry in the Tropical Zone: A Case Study of Coastal Aquifer Arroyo Grande, in the Caribbean Region of Colombia’, Water, vol. 16(12), pp. 1650, DOI: 10.3390/w16121650.

Barron, O, Pollock, D, Crosbie, R, Dawes, W, Charles, S, Mpelasoka, F, Aryal, S, Donn, M, and Wurcker, B 2010, *The impact of climate change on groundwater resources: The climate sensitivity of groundwater recharge in Australia*, CSIRO: Water for a Healthy Country Report to National Water Commission. Retrieved 7 November 2024 from <https://www.academia.edu/download/43535713/The_impact_of_climate_change_on_groundwa20160309-24861-1up5wti.pdf>.

Bartos, TT and Ogle KM 2002, ‘Water Quality and Environmental Isotopic Analyses of Ground-Water Samples Collected from the Wasatch and Fort Union Formations in Areas of Coalbed Methane Development – Implications to Recharge and Ground-Water Flow, Eastern Powder River Basin, Wyoming’, Water-Resources Investigations Report 02-4045, United States Geological Survey (USGS), pp. 1-96, U.S. Department of the Interior. Retrieved 06 August 2023 from <https://pubs.usgs.gov/wri/wri024045/>.

Belkhiri, L, Boudoukha, A, and Mouni, L 2011, ‘A multivariate Statistical Analysis of Groundwater Chemistry Data’, *International Journal of Environmental Research*, vol. 5(2), pp. 537-544, < https://www.researchgate.net/publication/236612300_A_multivariate_Statistical_Analysis_of_Groundwater_Chemistry_Data>.

Boggs, S 2014, *Principles of sedimentology and stratigraphy*, 5th edn, Pearson, St. Ives, England.

Boyd, CE 2000, *Water quality: an introduction*, Kluwer Academic, Springer New York, NY, DOI: 10.1007/978-1-4615-4485-2.

Brashears, ML 1971, ‘Review of Ground-Water Investigations made by the Australian Groundwater Consultants PTY. Limited in the Townsville Region, Queensland, Australia’, Leggette, Brashears & Graham Consulting Ground-Water Geologists (New York), Irrigation & Water Supply Commission, QLD DNR Library I29952.

Business Queensland 2020, *Developing Water Plans*, Business Queensland, Queensland Government viewed 09 January 2024, <https://www.business.qld.gov.au/industries/mining-energy-water/water/catchments-planning/planning>.

Business Queensland 2024, *Water plan areas*, Business Queensland, Queensland Government, viewed 09 January 2024 from

<https://www.business.qld.gov.au/industries/mining-energy-water/water/catchments-planning/water-plan-areas>.

Cary, Lise, *et al.* 2015 “Origins and Processes of Groundwater Salinization in the Urban Coastal Aquifers of Recife (Pernambuco, Brazil): A Multi-Isotope Approach”, *The Science of the Total Environment*, vol. 530–531, pp. 411–29, DOI: 10.1016/j.scitotenv.2015.05.015.

Carucci, V, Petitta, M, and Aravena, R 2012 “Interaction between Shallow and Deep Aquifers in the Tivoli Plain (Central Italy) Enhanced by Groundwater Extraction: A Multi-Isotope Approach and Geochemical Modelling”, *Applied Geochemistry*, vol. 27(1), pp. 266–80, DOI: 10.1016/j.apgeochem.2011.11.007.

Chander, KS, Kumar, An, Shashtri, S, Kumar, Al, Kumar, P, and Mallick, J 2017, ‘Multivariate statistical analysis and geochemical modelling for geochemical assessment of groundwater of Delhi, India’, *Journal of Geochemical Exploration*, vol. 175, pp. 59-71, DOI: 10.1016/j.gexplo.2017.01.001.

Chowdhury, P, Mukhopadhyay, BP, Nayak, S, and Bera, A 2022, ‘Hydro-chemical characterization of groundwater and evaluation of health risk-assessment for fluoride contamination areas in the eastern blocks of Purulia district, India’, *Environment, Development and Sustainability*, vol. 24(9), pp. 11320-11347, DOI: 10.1007/s10668-021-01911-1.

Chucuya, S, Vera, A, Pino-Vargas, E, Steenken, A, Mahlknecht, J, and Montalván, I, 2022, ‘Hydrogeochemical Characterization and Identification of Factors Influencing Groundwater Quality in Coastal Aquifers, Case: La Yarada, Tacna, Peru’, International Journal of Environmental Research and Public Health, vol. 19, 2815. https://doi.org/10.3390/ijerph19052815.

Clark, I 2015, *Groundwater Geochemistry and Isotopes*, CRC Press, Taylor and Francis Group, 428 p., DOI: 10.1201/b18347.

Clark, ID and Fritz, P 1997, *Environmental Isotopes in Hydrogeology*, CRC Press, Taylor & Francis Group, 328 p., ISBN 1-56670-249-6.

Cooper, CA, Hershey, RL, Healey, JM, and Lyles, BF 2013, ‘Estimation of Groundwater Recharge at Pahute Mesa using the Chloride Mass-Balance Method’, Publication No. 45251, National Nuclear Security Administration, US Department of Energy, Las Vegas, Nevada.

Creek to Coral 2007, *A Summary Review of Groundwater Research and Knowledge for the Black River and Ross River Basins*, Townsville City Council – Creek to Coral, Townsville. Retrieved from <http://www.creektocoral.org/draftwqip/backround/CCIbackground/>.

Creek to Coral 2008, ‘Water Quality Condition of the Black and Ross River Basins’, Townsville City Council, viewed 10 April 2019, <http://www.creektocoral.org/draftwqip/backround/wqcon/WQconditionreportfinal.pdf>.

Crosbie, R, Morrow, D, Cresswell, R, Leaney, F, Lamontagne, S, and Lefournour, M, 2012, ‘New insights to the chemical and isotopic composition of rainfall across Australia’, CSIRO Water for a Healthy Country Flagship, Australia, CSIRO:EP125581, DOI: 10.5072/83/5849a0d6c685a.

CSIRO (Commonwealth Scientific and Industrial Research Organisation) 2020, *State of the Climate 2020*, Bureau of Meteorology, Australian Government, viewed 04 July 2021, <https://www.csiro.au/en/research/environmental-impacts/climate-change>.

Department of Environment and Science 2020, *Groundwater Ambient Network (GWAN) – Water quality*, WetlandInfo, Queensland Government, viewed 21 January 2020, <https://wetlandinfo.des.qld.gov.au/wetlands/assessment/monitoring/current-and-future-monitoring/groundwater-ambient-network.html>.

Eaton, FM 1950, 'Significance of carbonates in irrigation waters', Soil Science, *69*(2), pp. 123–134, DOI: 10.1097/00010694-195002000-00004.

Eriksson, E and Khunakasem, V 1969, Chloride Concentration in Groundwater, Recharge Rate and Rate of Deposition of Chloride in the Israel Coastal Plain. Journal of Hydrology, vol. 7(2), pp. 178-197, DOI: 10.1016/0022-1694(69)90055-9.

Farnham, IM, Singh, AK, Stetzenbach, KJ and Johannesson, KH 2002, 'Treatment of nondetects in multivariate analysis of groundwater geochemistry data', *Chemometrics and Intelligent Laboratory Systems*, vol. 60(1-2), DOI: 10.1016/S0169-7439(01)00201-5.

Fernbach, N 2016, *Townsville residents turn to bores as water restrictions and dry spell continue*, ABC News North Queensland, viewed 19 April 2019, <https://www.abc.net.au/news/2016-12-07/boring-solution-to-drought-in-townsville/8096130>.

Freeze, RA, and Cheery, JA 1979, Groundwater: Englewood Cliffs, NJ, Prentice-Hall, pp. 604.

Gibbs, RJ 1970 'Mechanisms Controlling World Water Chemistry.', *Science*, vol. 170, no. 3962, pp. 1088–90, https://doi.org/10.1126/science.170.3962.1088.

Gosselin, DC, Harvey, FE, and Frost, CD 2001, 'Geochemical Evolution of Ground Water in the Great Plains (Dakota) Aquifer of Nebraska: Implications for the Management of a Regional Aquifer System', Groundwater, vol. 39(1), pp. 98-108. DOI: 10.1111/j.1745-6584.2001.tb00355.x.

Gugulothu, S, Subbarao, N, Das, R and Dhakate, R 2022, 'Geochemical evaluation of groundwater and suitability of groundwater quality for irrigation purpose in an agricultural region of South India', *Applied Water Science*, vol. 12(142), pp. 1-13, DOI: 10.1007/s13201-022-01583-w.

Güler, C, Thyne, GD, McCray, JE, and Turner, KA 2002, 'Evaluation of graphical and multivariate statistical methods for classification of water chemistry data', *Hydrogeology Journal*, vol. 10, pp. 455–474, DOI: 10.1007/s10040-002-0196-6.

Güler, C, Kurt, MA, Alpaslan, M, and Akbulut, C 2012, 'Assessment of the impact of anthropogenic activities on the groundwater hydrology and chemistry in Tarsus coastal plain (Mersin, SE Turkey) using fuzzy clustering, multivariate statistics and GIS techniques', *Journal of Hydrology*, vol. 414, pp. 435-451, DOI: 10.1016/j.jhydrol.2011.11.021.

Gunn, J, Manning, C, and Connolly, N 2009, *Basins, Catchments and Receiving Waters of the Black and Ross River Basins Water Quality Improvement Plan Area*, Townsville City Council – Creek to Coral, Townsville.

Gunn, J. and Manning, C. 2010, Black Ross (Townsville) Water Quality Improvement Plan: Improving Water Quality from Creek to Coral, Townsville City Council - Creek to Coral, Townsville, viewed 19 April 2019, <http://www.creektocoral.org/wqip/plandocs_final.html>.

Halliwell, DJ, Barlow, KM and Nash, DM 2001, 'A review of the effects of wastewater sodium on soil physical properties and their implications for irrigation systems', *Australian Journal of Soil Research*, vol. 39, pp. 1259-1267, DOI: 10.1071/SR00047.

Han, DM, Song, XF, Currell, MJ, Yang, JL, and Xiao, GQ 2014, ‘Chemical and isotopic constraints on the evolution of groundwater salinization in the coastal plain aquifer of Laizhou Bay, China’, *Journal of Hydrology*, vol. 508, pp. 12-27, DOI: 10.1016/j.jhydrol.2013.10.040.

Harbison, J and Cox, M 2002, ‘Hydrological characteristics of groundwater in a subtropical coastal plain with large variations in salinity: Pimpama, Queensland, Australia”, *Hydrological Sciences Journal*, vol. 47(4), pp. 651-665, DOI: 10.1080/02626660209492966.

Havril T, Toth T, Molson JW, Galsa A, Mádl-Szőnyi J 2018, ‘Impacts of predicted climate change on groundwater flow systems: Can wetlands disappear due to recharge reduction?’, Journal of Hydrology, 563, pp. 1169-1180, DOI: 10.1016/j.jhydrol.2017.09.020 Hopley, D (ed) 1978, *Geographical studies of the Townsville Area*, Monograph Series Occasional Paper No. 2, Department of Geography, James Cook University, ISBN: 909701 13 X.

Helena, B, Pardo, R, Vega, M, Barrado, E, Fernandez, JM, and Fernandez L 2000, ‘Temporal evolution of groundwater composition in an alluvial aquifer (Pisuerga River, Spain) by principal component analysis’, *Water Resources*, Elsevier, Pergamon, vol.34(3), pp. 807-816, DOI: 10.1016/S0043-1354(99)00225-0.

Hem JD 1985, Study and Interpretation of Chemical Characteristics of Natural Water, 3 ed., U.S. Geological Survey (USGS) Water-Supply Paper 2254, Department of the Interior, United States Geological Survey.

Hennessy K, Webb L, Ricketts J, Macadam I 2008, ‘Climate Change Projections for the Townsville Region’, CSIRO, Townsville City Council, viewed 19 April 2019, <http://www.creektocoral.org/draftwqip/climatechange/csiro/>.

Kaiser, HF 1960 ‘The Application of Electronic Computers to Factor Analysis’, *Educational and Psychological Measurement*, Vol. 20(1), pp. 141-151, DOI: 10.1177/001316446002000116.

Kaur, L, Rishi, MS, Sharma, S, Sharma, B, Lata, R, and Singh, Gagandeep 2019, “Hydrogeochemical characterization of groundwater in alluvial plains of river Yamuna in northern India: An insight of controlling processes’, *Journal of King Saud University – Science*, vol. 31(4), ScienceDirect, DOI: 10.1016/j.jksus.2019.01.005.

Kearey P 2001, *The New Penguin Dictionary of Geology*, 2nd ed., Penguin Group, England.

Klassen J, Allen, DM 2017, ‘Assessing the risk of saltwater intrusion in coastal aquifers’, Journal of Hydrology, 551, pp. 730-735, DOI: 10.1016/j.jhydrol.2017.02.044.

Kovalevsky, VS, Kruseman, GP, and Rushton KR 2004, *Groundwater studies: an international guide for hydrogeological investigations*, IHP-VI Series on Groundwater No. 3, UNESCO, United Nations, 430 p., ISBN 92-9220-005-4. Retrieved 10 August 2023 from <https://unesdoc.unesco.org/ark:/48223/pf0000134432>.

Kumar, PJS, Elango, E, and James, EJ 2014, ‘Assessment of hydrochemistry and groundwater quality in the coastal area of South Chennai, India’, *Arabian Journal of Geosciences*, 7, pp. 2641-2653, DOI: 10.1007/s12517-013-0940-3.

Lenahan, MJ and Bristow, KL 2010, ‘Understanding sub-surface solute distributions and salinization mechanisms in a tropical coastal floodplain groundwater system’, *Journal of Hydrology*, vol. 390(3-4), pp. 131-142, DOI: 10.1016/j.jhydrol.2010.06.009.

Li, P, He, Xiaodong, and Guo, W 2019, ‘Spatial groundwater quality and potential health risks due to nitrate ingestion through drinking water: A case study in Yan’an City on the

Loess Plateau of northwest China', *Human and Ecological Risk Assessment: An International Journal*, vol. 25(1-2), pp. 11-31, DOI: 10.1080/10807039.2018.1553612.

Liu, J, Fu, G, Song, X, Charles, SP, Zhang, Y, Han, D, and Wang, S 2010, 'Stable Isotopic Compositions in Australian Precipitation", Journal of Geophysical Research, vol. 115(D23), 2010, DOI: 10.1029/2010JD014403.

Llyod, JW and Heathcote JA 1985, *Natural inorganic hydrochemistry in relation to groundwater: An introduction*, Clarendon Press, Oxford, United Kingdom.

Lowenstein, TK, Hardie, LA, Timofeeff, MN, and Demicco, RV 2003, 'Secular variation in seawater chemistry and the origin of calcium chloride basinal brines', *Geology*, vol. 31(10), pp. 857-860, DOI: 10.1130/G19728R.1.

Marei, A, Khayat, S, Weise, S, Ghannam, S, Sbaih, M, and Geyer, S 2010, 'Estimating groundwater recharge using chloride mass-balance method in the West Bank, Palestine', *Hydrological Sciences Journal*, vol. 55(5), Taylor and Francis, pp. 780-791, DOI: 10.1080/02626667.2010.491987.

Mazor, E 2004, *Chemical and Isotopic Groundwater Hydrology*, 3 ed., Marcel Dekker Inc., Halsted Press (John Wiley & Sons), United States of America, ISBN: 0-8247-4704-6.

Menció, A and Mas-Pla, J 2008, 'Assessment by multivariate analysis of groundwater-surface water interactions in urbanized Mediterranean streams', *Journal of Hydrology*, Elsevier, vol. 352, pp. 355-356, DOI: 10.1016/j.jhydrol.2008.01.014.

Mensah, FO, Alo, C, and Yidana, SM 2014, 'Evaluation of Groundwater Recharge Estimates in a Partially Metamorphosed Sedimentary Basin in a Tropical Environment: Application of Natural Tracers', *The Scientific World Journal*, Article ID 419508, DOI: doi.org/10.1155/2014/419508.

Mook, WG 2006, *Introduction to Isotope Hydrology: Stable and Radioactive Isotopes of Hydrogen, Oxygen and Carbon*, International Association of Hydrogeologists, Taylor & Francis/Balkema, Great Britain, ISBN 100-415-38197-5.

Morton, WH 1973 "Groundwater in the Bohle-Ross Rivers Area, Townsville, QLD", Australian Groundwater Consultants PTY. LTD, Department of Environment & Resource Management, catalogue 551.49 GRO 1973, QLD DNR Library: I42148, available from <https://trove.nla.gov.au/version/192977949>.

Munksgaard, NC, Wurster, CM, Bird, MI 2011, 'Continuous analysis of δ18O and δ18D values of water by diffusion sampling cavity ring-down spectrometry: a novel sampling device for unattended field monitoring of precipitation, ground and surface waters', *Rapid Communications in Mass Spectrometry*, vol. 25, pp. 3706-3712, DOI:10.1002/rcm.5282.

Murtha, GG 1975a, 'Soils and Land Use on the Northern Section of the Townsville Coastal Plain, North Queensland', Soils and Land Use Series No. 55, CSIRO, viewed 15 April 2019, <https://publications.qld.gov.au/sl/dataset/soil-townsville-zed/resource/8b49d47d-889e-4632-9cd0-4f68d4c4652b>.

Murtha, GG 1975b, 'Soils and Land Use on the Southern Section of the Townsville Coastal Plain, North Queensland', Soils and Land Use Series No. 55, CSIRO, viewed 15 April 2019, <https://publications.qld.gov.au/sl/dataset/soil-townsville-zed/resource/963b3843-d6db-4866-b1a5-868639986754>.

Piper, AM 1944 '*A Graphical Procedure in the Geochemical Interpretation of Water Analysis*', U S Geological Survey (USGS), Groundwater Note 12. DOI: 10.1029/TR025i006p00914.

Queensland Government 2017, *Water Plan (Burnett Basin) 2014*, Office of the Queensland Parliamentary Counsel, Queensland Government, Brisbane, <https://www.legislation.qld.gov.au/view/html/inforce/current/sl-2014-0184>.

Queensland Government 2020, *Water Plan (Moreton) 2020*, Office of the Queensland Parliamentary Counsel, Queensland Government, Brisbane, <https://www.legislation.qld.gov.au/view/html/inforce/current/sl-2007-0031>.

Queensland Government 2024, 'Black Catchment Story', Department of Environment, Science and Innovation, Brisbane, <https://wetlandinfo.des.qld.gov.au/wetlands/ecology/processes-systems/water/catchment-stories/transcript-black.html>.

Raymond, MAA, McNeil, VH 2013, 'Queensland wet tropics and Black and Ross catchments: Regional chemistry of the groundwater', Department of Science, Information Technology, Innovation and the Arts, Brisbane, v. 2, Libraries Australia ID 50859873, viewed March 23, 2021, <http://hdl.handle.net/10462/pdf/833>.

Reid, P 1975, 'Hydrogeology of the Lower Ross and Bohle River', James Cook University Honours Thesis, JCU Library.

SEAO2 2008, *Climate change in Townsville and potential impacts on water quality*, Townsville City Council – Creek to Coral, Townsville.

Schoeller, H 1977, Geochemistry of Groundwater. In: Groundwater Studies—An International Guide for Research and Practice, UNESCO, Paris, Ch. 15, pp.1-18.

Singh, CH, Kumar, An, Shashtri, S, Kumar, Al, Kumar, P, and Mallick, J 2017, 'Multivariate statistical analysis and geochemical modelling for geochemical assessment of groundwater of Delhi, India', *Journal of Geochemical Exploration*, Elsevier, vol. 175, pp. 59-71, DOI: 10.1016/j.gexplo.2017.01.001.

State of Queensland 2013, *Environmental Protection (Water) Policy 2009: Black River Basin Environmental Values and Water Quality Objectives, Basin No. 117, including all waters of the Black River Basin and adjacent coastal waters*, Department of Environment and Heritage Protection, Queensland Government, Brisbane, <https://environment.des.qld.gov.au/__data/assets/pdf_file/0023/88106/black-river-basin-ev-wqo.pdf>.

State of Queensland 2018, Water Act 2000, Department of Natural Resources, Mines, and Energy viewed 20 April 2019, <https://www.legislation.qld.gov.au/view/pdf/inforce/current/act-2000-034>.

***The State of Queensland 2019, Queensland Spatial Catalogue – Qspatial, Department of Natural Resources, Mines and Energy, viewed 05 May 2019, <http://qldspatial.information.qld.gov.au/catalogue/custom/index.page>.

Stieglitz, T 2005, 'Submarine groundwater discharge into the near-shore zone of the Great Barrier Reef, Australia', *Marine Pollution Bulletin*, vol. 51, pp. 51-59, DOI: 10.1016/j.marpolbul.2004.10.055.

Subba Rao, N, Surya Rao, P, Venktram Reddy, G, Nagamani, M, Vidyasagar, G, Satyanarayana, NIVV 2012, 'Chemical characteristics of groundwater and assessment of groundwater quality in Varaha River Basin, Visakhapatnam District, Andhra Pradesh, India", *Environmental Monitoring Assessment*, vol. 184, pp. 5189-5214, DOI: 10.1007/s10661-011-2333-y.

Ting, CS, Kerh, T, and Liao, CJ 1998, ‘Estimation of groundwater recharge using the chloride mass-balance method, Pingtung Plain, Taiwan’, *Hydrogeology Journal*, vol. 6, no. 2, pp. 282-292, DOI: 10.1007/s100400050151.

Todd, D, and Mays, L 2005, *Groundwater Hydrology*, 3rd Edition, John Wiley and Sons, Inc., Hoboken, 652 p., ISBN: 978-1-118-00177-6.

Townsville Regional Council 2016, ‘Townsville Regional Stormwater Strategy’, Bligh Tanner Pty Ltd Job No. 2015.025.600, Townsville Regional Council, retrieved 20 March 2022 from: < https://www.townsville.qld.gov.au/__data/assets/pdf_file/0015/30048/2016-06-28-Regional-Stormwater-Strategy-Part-2-Analysis-Report.pdf>.

Townsville State of Environment Report 2003, Inland Waters, Townsville City Council, viewed 17 April 2019, <http://www.soe-townsville.org/inlandwaters.html>.

Trezise, DL and Stephenson, PJ 1990, *Rocks and Landscapes of the Townsville District*, Department of Resource Industries, Queensland Government, ISBN 0 7242 33 81.

USSL Salinity Laboratory (1954) Diagnosis and Improvement of Saline and Alkaline Soils. US Department of Agriculture Handbook, No. 60, 160 p.

van der Gun, J 2018, ‘Data, information, knowledge and diagnostics on groundwater’, in Villholth, López_Gunn, Conti, Garrido & van der Gun (eds), *Advances in Groundwater Governance*, CRC Press, Taylor & Francis Group, pp. 193-213. Available from www.un-igrac.org.

van Engelenburg, J, Hueting, R, Rijpkema, S, Teuling, AJ, Uijlenhoet, R, and Ludwig, F 2018, ‘Impact of Changes in Groundwater Extractions and Climate Change on Groundwater-Dependent Ecosystems in a Complex Hydrogeological Setting’, *Water Resource Management*, vol. 32, pp. 259-272, DOI: 10.1007/s11269-017-1808-1.

Villholth, KG and Conti, KI 2018, ‘Groundwater governance: rationale, definition, current state and heuristic framework’, in Villholth, López_Gunn, Conti, Garrido & van der Gun (eds), *Advances in Groundwater Governance*, CRC Press, Taylor & Francis Group, pp. 3-31. Available from www.un-igrac.org.

Wells, RC 1923, ‘Sodium Sulphate: Its sources and uses’, Department of the Interior, United States Geological Survey, Bulletin 717, pp. 1-43, DOI: 10.3133/b717.

Werner, AD 2010, ‘A review of seawater intrusion and its management in Australia’, Hydrogeology Journal, vol. 18(1), viewed 15 February 2018, DOI: 10.1007/s10040-009-0465-8.

Wilcox, LV 1955, ‘Irrigation Waters’, United States Salinity Laboratory, circular no. 969, United States Department of Agriculture, retrieved 01 July 2023 from <https://www.ars.usda.gov/arsuserfiles/20360500/pdf_pubs/P0192.pdf>.

Wood, WW 1999, ‘Use and misuse of the chloride-mass balance method in estimating ground water recharge’, Ground Water, Vol. 37(1), National Ground Water Association, pp. 1-2, DOI: 10.1111/j.1745-6584.1999.tb00949.x.

Xian, X, Pang, M, Zhang, J, Zhu, M, Kong, F, Xi, M 2019, ‘Assessing the effect of potential water and salt intrusion on coastal wetland soil quality: simulation study’, Journal of Soils and Sediments, Preprint, viewed 31 March 2019, DOI: 0.1007/s11368-018-02225-y.

Zaman, M, Shahid, SA, and Heng, L 2018 ‘Irrigation Water Quality’, In: Guideline for Salinity Assessment, Mitigation and Adaptation Using Nuclear and Related Techniques, Springer, Cham, DOI: 10.1007/978-3-319-96190-3_5.

Zaidi, FK, Nazzal Y, Jafri, MK, Naeem, M, and Ahmed, I 2015 “Reverse Ion Exchange as a Major Process Controlling the Groundwater Chemistry in an Arid Environment: A Case Study from Northwestern Saudi Arabia”, *Environmental Monitoring and Assessment*, vol. 187(10), pp. 607–618, DOI: 10.1007/s10661-015-4828-4.

Appendices

7.1 Appendix 1: N=19 Seasonal Analysis Detailed Hydroeochemical Results

This file contains detailed hydrogeochemical results for the 19 sampling sites used in the paired t-testing for seasonal analysis. Subsequently, the 3 data points from each site were averaged, creating the N=86 dataset. This is available as a supplementary data file.

7.2 Appendix 2: N=86 Detailed Hydroeochemical Analyses Results

This file is the N=86 dataset with detailed hydrogeochemical results and is available in supplementary data file.

7.3 Appendix 3: Hydrogeochemical Results for 14-Carbon and Tritium

Includes groundwater age-dating data not included in master's thesis (3 samples) and is available in supplementary data file.

7.4 Appendix 4: Historic Geochemical Maps (Reid 1975)

This file contains digitised .pdf versions of hydrogeochemical maps from James Cook University Honours Thesis by Peter Reid (1975) 'Hydrogeology of the Lower Ross and Bohle River' and is available in supplementary data file.